2008

Ferrocenylmethylchalcogenolate reagents for THE PREPARATION OF NOVEL GROUP 11/16 POLYNUCLEAR CLUSTERS

Siawash Ahmar

FERROCENYLMETHYLCHALCOGENOLATE REAGENTS FOR THE PREPARATION OF NOVEL GROUP 11/16 POLYNUCLEAR CLUSTERS

(Spine title: Ferrocenylmethylchalcogenolate Group 11 Clusters)

(Thesis format: Monograph)

by

Siawash Ahmar

Graduate Program in Chemistry

A thesis submitted in partial fulfillment
of the requirements for the degree of
Master of Science

Faculty of Graduate Studies
The University *of* Western Ontario
London, Ontario, Canada
June 3, 2008

The University Of Western Ontario

Faculty of Graduate Studies

CERTIFICATE OF EXAMINATION

Supervisor	Examiners
Dr. John F. Corrigan	Dr. Nicholas C. Payne
Supervisory Committee	Dr. Yining Huang
_____	Dr. Mahi R. Singh
_____	

The thesis by

Siawash Ahmar

entitled:

FERROCENYLMETHYLCHALCOGENOLATE REAGENTS FOR THE PREPARATION OF NOVEL GROUP 11/16 POLYNUCLEAR CLUSTERS

is accepted in partial fulfilment of the
requirements for the degree of
Master of Science

Date _____

_____
Chair of the Thesis Examination Board

ABSTRACT

The preparation of silylated ferrocenylmethyl chalcogen reagents $CpFe(\eta^5\text{-}C_5H_4CH_2ESiMe_3$ [E = S (**1**), Se (**2**)] in good yield is presented. These ligands were designed to have an alkyl spacer between the cyclopentadienyl group of ferrocene and the chalcogen atom that would act as an insulating bridge. Reactions of (**1**) or (**2**) with group 11 metal salts afforded single crystals of $[Cu_3(SCH_2Fc)_3(PPh_3)_3]$ (**3**), $[Ag_{48}S_6(SCH_2Fc)_{36}]$ (**4**), $[Ag_{10}(SCH_2Fc)_{10}(PPh_3)_4]$ (**5**) and $[Ag_8(SeCH_2Fc)_8(PPh_3)_4]$ (**6**) that were suitable for X-ray analysis.

Cyclic voltammetry experiments were conducted on (**3**) and (**4**) where single pseudo-reversible oxidation waves were observed at all scan rates and after repetitive cycles. No evidence of bond cleavage or communication between iron centres and chalcogen atoms was observed suggesting that the alkyl spacer acts as an insulating bridge.

KEYWORDS:

Nanocluster, semiconductor, ferrocene, group 11, chalcogen, silylchalcogenolate, cyclic voltammetry, X-ray crystallography.

ACKNOWLEDGEMENTS

I would like to start off by thanking my supervisor Dr. John F. Corrigan for all of his guidance, support and patience. It wasn't until after my undergraduate 490 experience in this lab that I wanted to pursue a graduate degree. I must admit that at first I had some regrets, mainly due to the lack of success in obtaining any results. These past two and half years have been some of the most frustrating and difficult years since I started my studies here at the University of Western Ontario. However, with his (Dr. Corrigan) encouragement and confidence in my abilities, I am now finally completing my Masters degree. I am very grateful to have had a supervisor like Dr. Corrigan because I don't know how many other supervisors could have put up with my antics, in and outside of the lab. I would also like to thank John for solving and refining the structure of my $Ag_{48}S_6(SCH_2Fc)_{36}$ cluster.

I would also like to thank members of the chemistry staff for their help and support. Firstly, I would like to thank Yves Rambour, since the first day he started here I made sure to keep him busy. If it wasn't for his promptness in repairing my Schlenk line, several times, and our broken glassware, I would still be in the lab. Chris Kirby and Nadine Merkley for their assistance in running NMR spectroscopy, and Doug Hairsine for running mass spectra for me. Mike Jennings for running my $Cu_3(SCH_2Fc)_3$ crystals and allowing us to use the instrument on his days off. The helpful staff at Chem Stores, Marylou Hart, Sherri McPhee and Marty Scheiring, for their assistance in meeting my chemical and supply needs.

This journey has been made more memorable because I have been privileged to have terrific lab mates. They have made the rough days easier to get through and the good days that much better. In alphabetical order I would like to thank Aneta Borecki, Marty Degroot, Diane Kanas, Chhatra (strongman) Khadka, Collin Kowalchuk, Dan (G-diddy) MacDonald, and "Drill Sergeant" Elizabeth Turner. I owe a special thanks to my boys Chhatra and Dan. Dan has come in on weekends to run my crystals (all my silver clusters) and solved and refined the structures of my $Ag_{10}(SCH_2Fc)_{10}$ and $Ag_8(SeCH_2Fc)_8$ clusters. Chhatra has not only been an amazing lab mate but also a great friend, he is the reason why I haven't been sleeping on the streets of London.

Finally, I would like to extend my greatest thanks to my family for all their love and support throughout this whole experience. Without them I know that I would not have been able to accomplish what I have. My parents have sacrificed everything to ensure that my brothers and I have all the opportunities to better ourselves and have always encouraged us to do so. I am forever in their debt, and hope that I have made them proud. I am also thankful for having two younger brothers that have always been there when I've needed them to be. I can't forget to thank my girlfriend Nikki Khetani for her love and encouragement. Although she is not too fond of chemistry, she always pretends to be interested and keeps me on track.

My experiences here at Western, both as an undergraduate and graduate student have been the best ones of my life and I am very fortunate to have had great friends, classmates, and colleagues.

TABLE OF CONTENTS

LIST OF TABLES

LIST OF FIGURES

CHAPTER 1

CHAPTER 2

CHAPTER 3

LIST OF SCHEMES

CHAPTER 1

CHAPTER 2

CHAPTER 3

LIST OF ABBREVIATIONS

Å.....Angstrom

br.....broad

^{n}Bu.....*n*-butyl

^{t}Bu..... *tert*-butyl

Cp..... cyclopentadienyl

CV..... cyclic voltammetry

E.....chalcogen atom

Et..... ethyl

eV..... electron volts

Fc..... CpFe(η^5-C_5H_4)

g.....gram

h..... hours

HOMO.....highest occupied molecular orbital

K.....Kelvin

kJ.....kilojoule

LUMO.....lowest unoccupied molecular orbital

M.....any metal atom

Me.....methyl

MHz..... MegaHertz

mL..... milliliter

mm..... millimeter

mmol..... millimole

nm..... nanometer

NMR..... nuclear magnetic spectroscopy

OAc..... acetate

Ph..... phenyl

ppm..... parts per million

^{i}Pr..... *iso*-propyl

^{n}Pr.....*n*-propyl

QD..... quantum dot

R.....organic side group

s..... singlet (NMR)

THF..... tetrahydrofuran

TMEDA..... tetramethylethyl-enediamine

TOP..... trioctylphosphine

TOPO..... trioctylphosphine oxide

UV.....ultraviolet

CHAPTER 1

INTRODUCTION: Ferrocene and Ferrocenyl Derivatives: A Brief History and Recent Advances Into the Realm of Semiconductor Nanomaterials

1.1. Semiconductor Nanomaterials

In the past 30 years cluster chemistry has extended greatly in the fields of both inorganic and organometallic chemistry and is now at the heart of the emerging field of 'nano-science'. Nanoclusters of semiconducting materials have been intensively studied to determine how the characteristic properties of the bulk solid-state develop with size. The physical properties of these materials resemble intermediates between those of a molecular complex and the bulk solid-state.[1-3] The synthesis of these materials has been difficult because of the requirements of monodispersity in both shape and size, and perfect crystallinity. In most instances nanocrystals have been made by using some form of arrested precipitation reaction from organometallic precursors.[4-6] Although many synthetic approaches have been reported, one of the more common synthetic methods involve the pyrolysis of organometallic reagents by injection into a hot coordinating solvent which provides temporally discrete nucleation and allows for controlled growth of larger nanocrystallites.[5] Size selective precipitation of aliquots from the growth solution permits isolation of crystallites with narrow size distributions, and this process can then be monitored by optical techniques. A narrow size distribution in samples results in sharp absorption features and strong "band-edge" emission which is tunable with particle size and composition.[4-5] Transition Electron Microscopy (TEM) and X-ray powder

diffraction in combination with computer simulations are used to characterize structural features. While very effective and simple, this approach has limited scope because the exact molecular formulae and structural frameworks cannot be determined using these techniques, and therefore there is great incentive to find new and general synthesis routes to these materials.

Although there has been considerable progress in the controlled synthesis of group 12–16 semiconductor crystallites, complete structural characterization and interpretation of sophisticated optical experiments often remain difficult due to polydispersity in size and shape, surface electronic defects due to uneven surface derivatization and poor crystallinity. Therefore it is essential to have an appropriate high quality model system to characterize and distinguish the properties truly inherent to the nanometer size regime from those associated with variations in sample quality. Recent progress in the synthesis of single-crystal metal-chalcogen (ME, M = Zn, Cd; E = S, Se, Te) clusters has led to the development of a homologous series of compounds with the largest cluster molecule in the series overlapping in size with the smallest CdSe nanocrystals.[7] Optical studies of CdSe series manifest the quantum-confinement effect seen for larger CdSe nanocrystals. Furthermore, in these systems surface ligands appear to play a crucial role with respect to their emission properties.[7] For all cluster molecules in the series, the photoluminescence spectra are broad, considerably red shifted from the absorption onset, and no emission is detected at room temperature.[7] These properties resemble the characteristics of the "deep trapped emission" in larger nanocrystals, which arises from forbidden transitions of

surface states. Therefore there is further incentive to design general synthetic methodologies to explore the tunability of these semiconducting clusters by altering the nature of their surface ligands, and potentially introducing new functionalities.

1.2. General Introduction to Nanomaterials and the Quantum Confinement Effect

In the expanding world of nanotechnology, the term nano describes structural features of a compound or material that have at least one dimension in the nanometer range, typically 1–100 nm (1 nm = 10^{-9} m). These materials can be subdivided into different subclasses depending on their physical features, which include, among many others, nanoparticles, quantum dots, nanowires, nanotubes and thin films. The physical properties of these materials often differ significantly with respect to their bulk or solid state properties.

Illustrated in Figure 1.1 is a schematic energy diagram for a given bulk metal (left), semiconductor (centre) and a molecule (right).[8] The lower energy region is referred to as the valence band (VB) and energy states are typically filled in bulk metals and semiconductors. The upper region is called the conduction band (CB) and is normally unoccupied.[9] For bulk solid-state materials, an overlapping of energy levels or atomic orbitals of several hundred thousand to millions of atoms results in a valence band that can be approximated as a continuum. In contrast, for molecular compounds and semiconductor nanoparticles the electronic properties are made up the sum of individual molecular orbital contributions, where quantization of energy levels within the

valence and conduction bands is observed in addition to the separation by a 'forbidden' band gap.[8,9] The lowest energy transition that can take place is between the band gap of the highest occupied molecular orbital (HOMO) of the valence band and the lowest unoccupied molecular orbital (LUMO) of the conduction band.[8] Therefore, electrons are easily promoted into the conduction band in metals because of negligible energy barrier between the two bands giving rise to metals being good electrical conductors. In contrast, the molecular or atomic units have a much larger band gap giving rise to properties characteristic of insulators.[9] Semiconductors on the other hand, are defined as solids whose electrical conductivity is in between that of a metal and that of an insulator.[9] These materials are of great interest in electronic applications because they require a certain energy input to overcome the energy barrier which allow for selective conductivity. Nanoparticles of metals and semiconductors exhibit these properties resulting in to a systematic blue-shift in their absorption spectra with decreasing size. [8] This phenomenon is referred to as the quantum confinement effect and is explained in the following section.

As already alluded to, an electron can be excited into the conduction band leaving behind a hole in the valence band. This electron-hole pair is referred to as the Mott-Wannier exciton and exhibits a Coulombic attraction that can be considered an 'atomic-species' with its own Bohr radius confined within the boundaries of the particle.[1-3] A unique situation arises when the size of the semiconductor crystal decreases and becomes smaller than that of the exciton Bohr radius. As a consequence, the electrons acquire a higher state of kinetic

energy (shorter wavelength) to 'fit' into the crystal, and results in the quantum confinement effect explaining the shift to higher energy with decreasing particle size.[1-3]

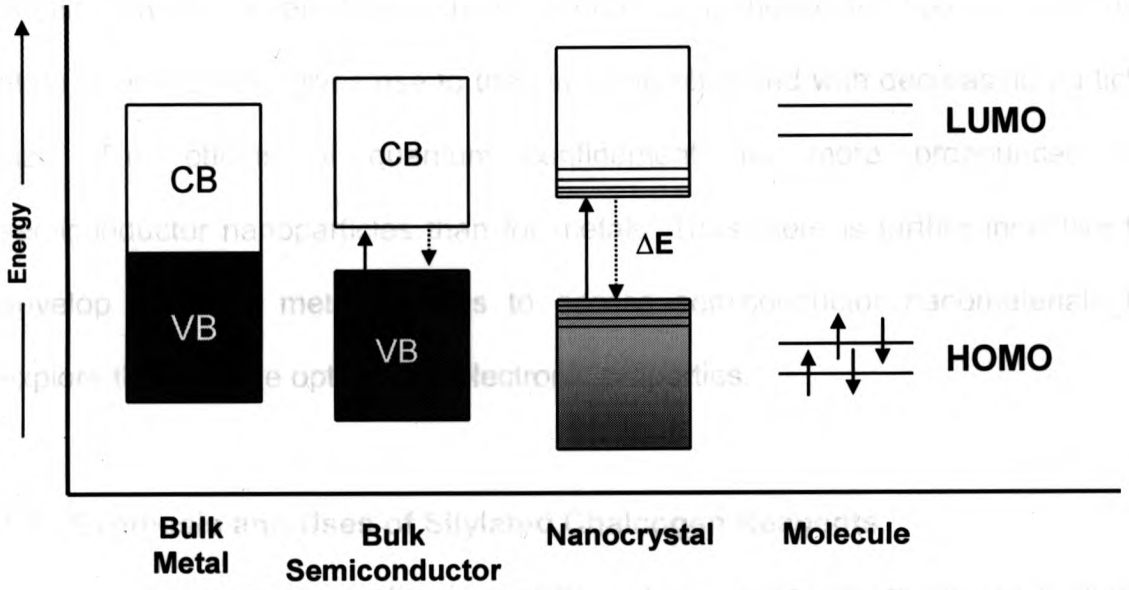

Figure 1.1 Schematic energy band diagram for bulk metal/semiconductor, naocrystal and molecule.[8]

A simplified example of quantum confinement is given by Denison[10]: one can envision a spherical crystal with a diameter **D**, where **D** must be smaller than the de Broglie wavelength, **λ**:

$$\lambda = h / p \qquad (1.1)$$

where h is Planck's constant and p is the particle momentum. If **E** is the kinetic energy:

$$E = (3/2)kT = p^2 / 2m \qquad (1.2)$$

where k Boltzmann's constant and m the mass of the electron/exciton, then at room temperature (~300 K) λ is found to be ~6 nm. Therefore, for a spherical crystal of **D** < 6 nm results in the electrons or exciton confined into a space smaller than it normally likes to have. In order to fit, the exciton takes on a higher state of energy and gives rise to the blue-shift observed with decreasing particle size. The effects of quantum confinement are more pronounced for semiconductor nanoparticles than for metals. Thus there is further incentive to develop synthetic methodologies to access semiconductor nanomaterials to explore their unique optical and electronic properties.

1.3. Synthesis and Uses of Silylated Chalcogen Reagents

One route to the synthesis of semiconductor metal-chalcogen compounds, M–E (E = S, Se, and Te) is the use of silylated chalcogen reagents which offer a soluble source of the chalcogen at mild reaction conditions. Both cyclic and acyclic silylated reagents have been used in the synthesis of metal-chalcogenolate complexes and clusters. Schemes 1.1 and 1.2 outline some reaction schemes used in the preparation ME complexes using silylated reagents.

Fenske and coworkers have utilized silylated reagents, $RESiMe_3$ (R = alkyl, aryl or $SiMe_3$; E = S, Se, Te), to synthesize a wide range of structurally unique, monodisperse, high-nuclearity clusters.[13] Another attractive feature of silylated chalcogen reagents is their solubility in common organic solvents that allow for a wider range of reactivity with metal salts. The overall reaction of these

reagents is driven by the formation of thermodynamically favorable byproduct, $XSiMe_3$ (X = halide, acetate) as outlined in scheme 1.3.

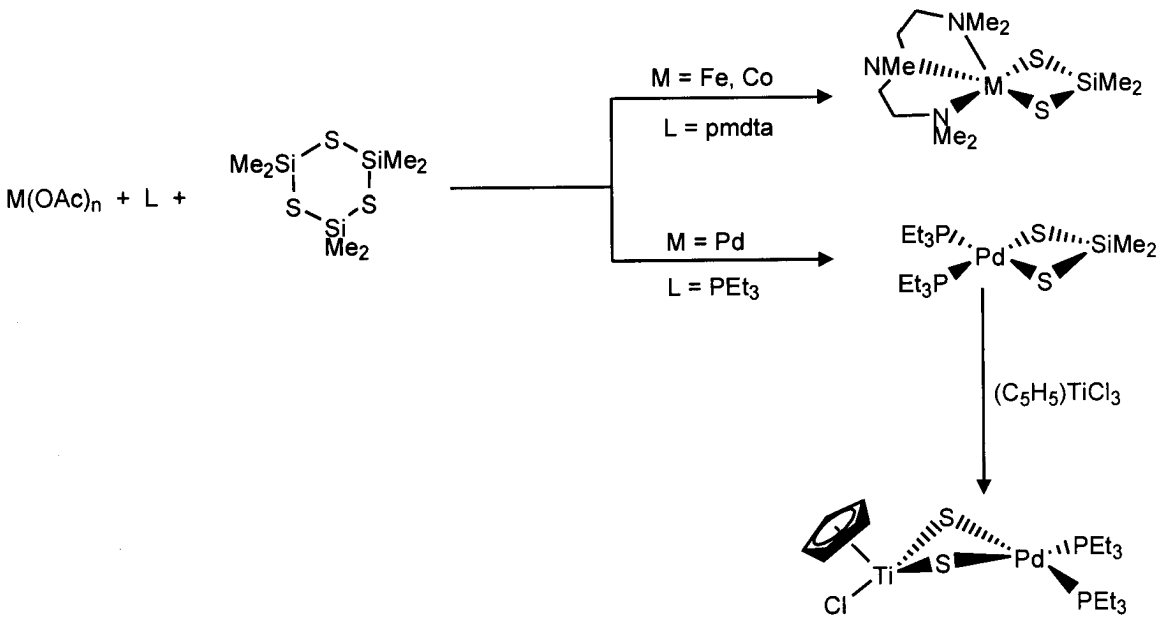

Scheme 1.1 Reaction scheme of cyclotrisilathiane with metal acetate salts in the synthesis of metal silanedithiolato complexes. [11]

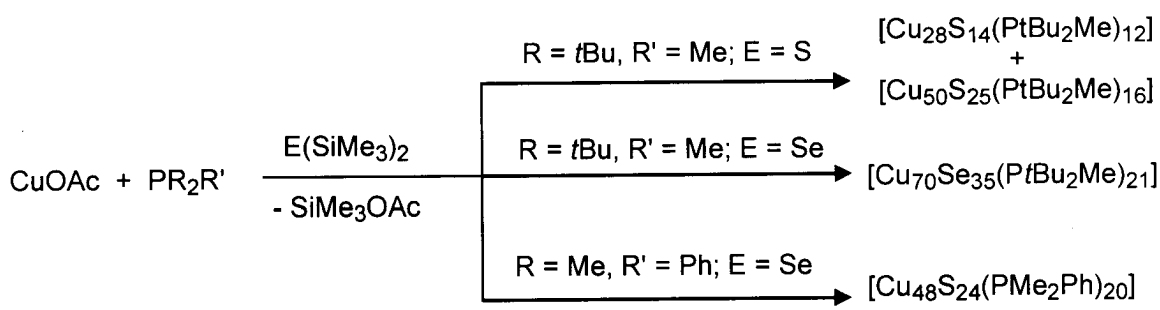

Scheme 1.2 Reaction scheme of bis(trimethylsilyl)chalcogenide with copper acetate in the synthesis of copper-chalcogenide clusters varying in size. [12]

$$M\text{-}X_n + n\ RESiMe_3 \rightarrow [M(ER)_n]_m + XSiMe_3 \quad \textbf{Eq. (1)}$$

$$M\text{-}X_n + n/2\ E(SiMe_3)_2 \rightarrow (ME_{n/2})_m + XSiMe_3 \quad \textbf{Eq. (2)}$$

$$M\text{-}X_n + n/2\ RESiMe_3 + n/4\ E(SiMe_3)_2 \rightarrow [M(ER)_{n/2}E_{n/4}]_m + XSiMe_3 \quad \textbf{Eq. (3)}$$

X = halide, acetate; E = S, Se, Te

Scheme 1.3 General reaction equations for the synthesis of ME complexes using acyclic silylated chalcogen reagents.[11]

The inherent strength of the E–Si bond (bond energy = 293 kJ/mol for E = S)[14] allows for selective cleavage of this bond to make a M–E bond that is driven by formation of X–Si bond (bond energies = 381 kJ/mol for X = Cl; 452 kJ/mol for X = O).[14] The silane by-product is soluble and volatile, therefore it can be easily removed from the reaction solution as required, but does not typically interfere with the crystallization of the metal-chalcogen species.[11] Furthermore, the progress of these reactions can be easily monitored by identification of $XSiMe_3$ using NMR spectroscopy.

The nature of the final M–E product is highly dependent on the reaction conditions. The general synthetic strategy employed with these reagents requires a transition metal salt, MX (X = halide, acetate), solubilized by a coordinating ligand, either a tertiary phosphine or an amine, to which the silylated chalcogen reagent is added at a low temperature, usually below 0 °C.[10-13] The solvent system, temperature, and steric effects of the solubilizing ligand all contribute to the control of the nuclearity and structure of the final product. Structural diversity is also observed due to the flexibility of chalcogenide (E^{2-}) and chalcogenolate (RE^-) ligands and their ability to adopt several stable bridging

coordination modes with transition metals.[15] For example in scheme 1.3 equation 3, the use of both chalcogenide and chalcogenolate ligands leads to the formation of both surface and interstitial M–E bonds. Chalcogenolate ligands of the type $RESiMe_3$ (R = organic moiety) offer an additional mode of transport for introducing various functional groups to metal centres and surfaces. Depending on the steric requirements of the R group and ancillary ligands used, both terminal and bridging coordination modes are observed for these ligands, although the latter is more common for the larger chalcogens Se and Te.[15]

There are several approaches to the synthesis of silylated chalcogen reagents, however the synthetic strategies employed by our group for $E(SiMe_3)_2$ and $RESiMe_3$ will be presented. These reagents are relatively easily prepared. Bissilylated chalcogenides, $E(SiMe_3)_2$ (E = S, Se, Te), are made by silylating the reduced elemental chalcogen, Na_2E, with chlorotrimethylsilane, $ClSiMe_3$.[16] Organo(trimethylsilyl) chalcogen reagents, $RESiMe_3$ (R = organic group; E = S, Se, Te), are typically synthesized by adding elemental chalcogens to a Grignard reagent, R-MgX (R = organic; X = halide), with the desired R functionality in dietyhyl ether.[17] The chalcogen elements S, Se and Te insert readily into the R–Mg bond of Grignard reagents, and can then be silylated with cholorotrimethylsilane generating $RESiMe_3$ and MgX_2.[17] An alternate route for the synthesis of organo(trimethylsilyl) chalcogenides involves the reductive cleavage of a diorganyldichalcogenide, R_2E_2 (R = organic group; E = S, Se, Te), with either a metal hydride or alkyllithium reagent to generate $M^+(^-ER)$.[16] Silylation then generates $RESiMe_3$ and MCl. From a synthetic standpoint, these

reagents are ideal precursors since they allow for the controlled synthesis of metal-chalcogen complexes, $(ME)_n$, at lower temperatures compared to ME complexes obtained by the pyrolysis of phosphine chalcogenide precursors, TOPE/TOPO (tri-*n*-octylphosphine chalcogenide/tri-*n*-octylphosphine oxide) that require temperatures of up to several hundred degrees Celsius.[4,5] Furthermore, these reagents open the possibility for the synthesis of new precursors to generate ME clusters with new functionalities as well as the opportunity to synthesize heterometallic complexes MM'E.[18] Both of these areas are currently being investigated by our group and several others.

1.4. Ferrocene: A Brief History and Recent Advances

The compound bis(η^5-cyclopentadienyl)iron(II) or better known as ferrocene was first prepared unintentionally in 1951 by Pauson and Kealy by the reaction of cyclopentadienyl (abbreviated as Cp) magnesium bromide and ferric chloride with the goal of oxidatively coupling the diene to prepare fulvalene.[19] It was not until 1952 when Robert Burns Woodward and Geoffrey Wilkinson proposed a structure based on its reactivity.[20] The structure was later confirmed by X-ray crystallography clearly showing the sandwich type structure that was proposed earlier.[21] The work of Ernst Fischer and Geoffrey Wilkinson on ferrocene and other metallocenes earned them a Nobel Prize in chemistry in 1973, and helped recognize organometallic chemistry as a distinct subfield.

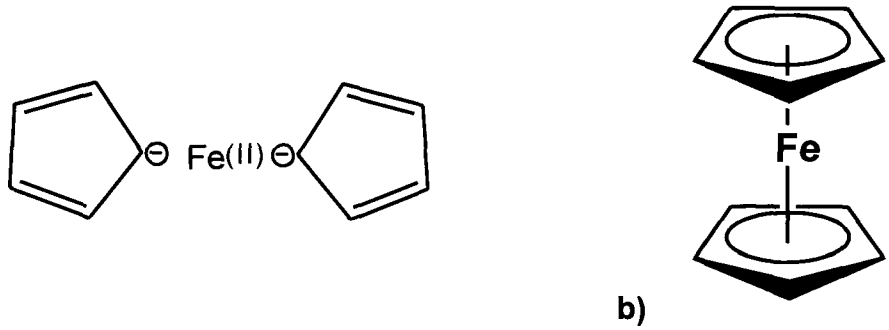

a) b)

Figure 1.2 (a) Structure proposed by Pauson and Kealy (b) Structure solved by Dunitz, Orgel and Rich.[20]

Ferrocene is now prepared more efficiently by the reaction of sodium Cp with anhydrous ferrous chloride in ethereal solvents. As illustrated in figure 1.2b, the structure of ferrocene is described as a "sandwich" complex where the iron atom is sandwiched between two parallel Cp rings. There is a small energy barrier separating the staggered and the eclipsed rotational orientations of the parallel Cp rings.[22] The term 'sandwich compound' has since been extended in organometallic nomenclature to describe any chemical compound containing a metal atom sandwiched between two aromatic groups. The best known members with the sandwich motifs are the metallocenes, $M(C_5H_5)_2$ where M = Cr, Fe, Co, Ni, Zr, Ti, V, Mo, W, Zn. These species are also called bis(cyclopentadienyl)metal complexes. The properties of these compounds vary greatly, especially with respect to their stability. Metallocene MCp_2 where M = V, Cr, Mn, Co are all very air-sensitive making them difficult to work with.[23]

The chemistry of ferrocene has dominated that of other metallocenes, mainly because of its stability and its inexpensive commercial availability which has allowed for the preparation of many ferrocene derivatives and ferrocene containing compounds. The stability of ferrocene can be accounted for by

examining the metal-ligand interactions in these species which involve a complicated covalent bonding situation resulting from a combination of donation of electron density from the ligand to the metal and 'back-donation' from the metal to the ligand.[24] This type of bonding pattern is similar to that seen in transition metal carbonyl compounds, such as $[Fe(CO)_5]$. The importance of this type of covalent bonding and the involvement of the metal d orbitals results in nine bonding molecular orbitals that are filled, meeting the electronic requirements for a stable 18 electron species.[23-24]

Furthermore, the aromatic groups of metallocene compounds can be easily functionalized which has allowed for a series of various metallocene derivatives to have been prepared. For example, Beer and coworkers have prepared a series of cobaltocenium[25-27] and ferrocene[26,27] derivatives used to selectively detect ions and neutral species.

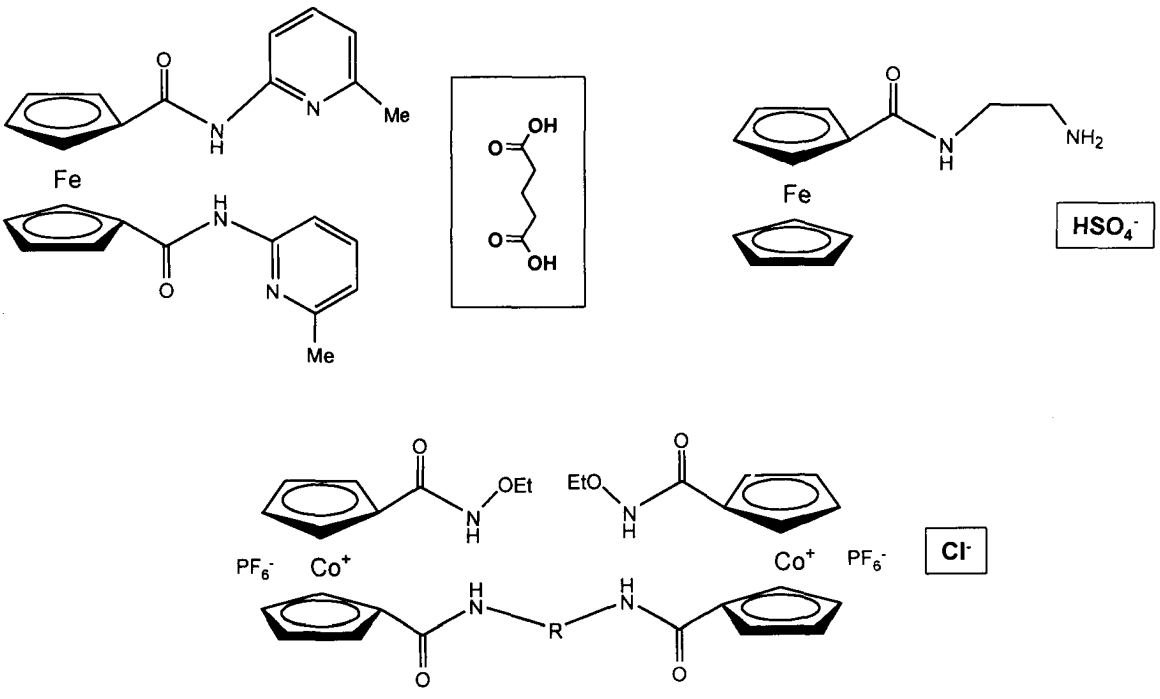

Figure 1.3 Metallocene receptors and their respective ion or molecule detected (boxed).[25-27]

Figure 1.3 shows some of these metallocene receptors and the molecules they selectively detect. These receptors detect specific molecules by H-bonding interactions between the amide group on the receptor and anion or neutral molecules, similar to the mode of binding seen in enzyme binding sites.[25-27] As a result these receptor-ion interactions form a stable complex that can be detected electrochemically. Cyclic voltammetric experiments showed significant shifts with respect to free receptor.[27] The addition of specific anions or neutral molecules resulted in significant cathodic shifts of the reversible Cp_2Co^+/Cp_2Co or Cp_2Fe/Cp_2Fe^+. This suggests that the receptor is stabilized in the presence of the anion and therefore more difficult to reduce. These receptors have also been shown to be selective depending on the environment of the binding cleft and anion of interest. Receptor molecules designed to non-covalently bind anionic or neutral molecular species have a wide range of applicability in biological systems and chemical processes.

A relatively new class of macromolecules, known as dendrimers, offers a unique framework for the incorporation of ferrocenyl units. Dendrimers are nano-sized, highly branched molecules which stem from a central core to a periphery that becomes denser with increasing number of branches. Current emphasis of these macromolecules is on the modification of the properties of dendritic molecules ('branches') by either the introduction of internal functionalities into the dendrimer structure or the fictionalization of dendritic surfaces.[28-30] Various ferrocenyl dendrimers have been prepared and have the potential to function as electrochemical sensors, in the same manner described above, when all

ferrocenyl units are equivalent, that is there is no communication between ferrocene units. The redox potentials of the ferrocene units are measured by cyclic voltammetry (CV) and show a single wave for equivalent units indicating that all redox centres are reduced at the same potential. A single wave would not be observed if ferrocene units were able to interact or 'sense' the presence of another unit. Rather, the oxidation of the subsequent unit would be more difficult and seen as a second wave at a higher potential, as a result of the repulsion between the two positive charges.[29,30] Communication between terminal ferrocenyl units can be spatially removed by long chains (alkyl, aryl, amide, amino acid, silyl) and the through space Coulombic interactions appear to be negligible.[29] These dendritic units have been extended to passivate the surfaces of nanoparticles and introduce their anion recognition functionalities. Furthermore, ferrocene containing polymers have also been prepared and been shown to have similar ion sensing capabilities.[30] Depending on the structural framework (polymer, dendrimer, nanoparticle) and the functional groups in the bonding network (amide, silyl, alkyl, aryl etc.) these materials can be tailored to selectively recognize a target molecule.

To further illustrate the progress the ferrocenyl chemistry, examples of ferrocenyl derivatives have also made their way into the field of medicine and there are many reports that have shown that these compounds have promising activity in vitro and in vivo against several diseases.[31,32] Some ferrocene and ruthenocene derivatives, figure 1.4, show promising results as antitumor agents, and are now in clinical trials.[31]

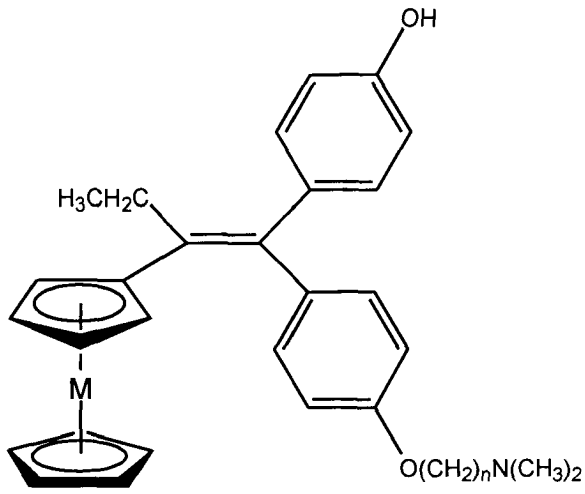

Figure 1.4 Ferrocifin (M = Fe) and Ruthenocifin (M = Ru) show antitumor activity with different strains of breast cancer

Other fields of have also incorporated the ferrocene moiety because of its electron-rich nature, and the focus is on the applications of these compounds in areas such as homogeneous catalysis, polymer chemistry, and nonlinear optical materials.

The chemistry of ferrocene, and to some extent that of other metallocenes, is well understood. However, the potential applications of metallocene complexes have yet to be fully determined. New functionalities and frameworks remain to be explored that require different synthetic strategies that could ultimately lead to novel materials and properties.

1.5. Project Objectives

Nanotechnology is one the fastest growing fields in the science community because of the wide range of applications and potential these materials possess. Several new journals such as Nano Today (2006), Small

(2005), Nano Letters (2001), to name a few, are dedicated to research in this field. The interest stems from the unique properties of these materials and their applications. As mentioned earlier, nanomaterials exhibit properties that can be considered an intermediate of that of the bulk material and molecular unit. In the nano-size regime, the intrinsic physical properties of the material are solely dependent on the size and composition. However, these properties can be modified by altering the surface and interior functionalities, as well as their framework to exhibit specific features. Because of the wide range of applicability these materials have made there way into almost all disciplines of science.

One of the less developed areas of nanoscience is that of nanoclusters. Nanoclusters are commonly grouped with nanoparticles or nanocrystals, however the term here will be reserved for compounds with well defined structures solved by single X-ray crystallography. These compounds can serve as ideal models for optical and electrochemical studies because their structural framework and surface is well defined with little to no ambiguity. The problem remains that there are few general synthetic strategies to target these single crystals. One of the more successful techniques is the use of silylated reagents, in particular chalcogen reagents that have been used to prepare a variety of group 11/12–16 semiconductor cluster molecules in a controlled manner. These reagents have not only been used to prepare metal-chalcogen clusters but also been used to prepare many precursors. It has been demonstrated that redox active ferrocenyl units can be introduced onto the surface of 11/12–16 clusters using silylated reagents. Ferrocenes are suitable donor compounds for the

synthesis of charge transfer complexes where their electron donor ability can be altered based on the choice of functional group on the cyclopentadienyl ring. Recently, the precursors $[(\eta^5\text{-}C_5H_5)Fe(\eta^5\text{-}C_5H_4ESiMe_3)]$ (E = S, Se) were synthesized and used in the synthesis of the M_4 clusters, $[Cd_4Cl_4\{\mu\text{-}(EC_5H_4)Fe(C_5H_5\}_6]^{2-}$ (E=S, Se).[33] Both clusters adopt an adamantane cage framework, with a central core of Cd_4E_6. Electrochemical studies revealed degradation in the cluster framework as a result of oxidative cleavage of the ferrocenyl chalcogenolate unit, leading to the formation of diferrocenyldiselenide (FcSeSeFc), and diferrocenyldisulfide (FcSSFc), respectively.

The introduction of an insulating bridge between the metal chalcogen core and ferrocene unit has been shown to be successful in preventing oxidative degradation.[34] The aim of this research project has been to prepare silylated ferrocenyl chalcogenolate reagents with an alkyl spacer. The spacer is introduced to act as an insulating bridge to eliminate any communication between ferrocenyl units. These reagents will be used as shuttles to introduce the ferrocenyl chalcogen moiety onto metal centers in the synthesis of 12–16 semiconductor nanoclusters.

1.6. References for Chapter 1

1) Brus, L. E. *J. Chem. Phys.* **1984**, 80, 4403.

2) Chestnoy, N.; Harris, T. D.; Hull, R., Brus; L. E. *J. Phys. Chem.* **1986**, 90, 3393.

3) Brus, L. *Appl. Phys. A.* **1991**, 53, 465.

4) a) Brennan, J. G.; Siegrist, T.; Carroll, P. J.; Stuczynski, S. M.; Reynders, P.; Brus, L. E.; Steigerwald, M. L. *Chem. Mater.* **1990**, 2, 403.; b) Bawendi, M. G.; Wilson, W. L.; Rothberg, L.; Carroll, P. J.; Jedju, T. M.; Steigerwald, M. L.; Brus, L. E. *Phys. Rev. Lett.* **1990**, 65, 1623.

5) Murray, C. B.; Norris, D. J.; Bawendi, M. G. *J. Am. Chem. Soc.* **1993**, 115, 8706.

6) Wageh, S.; Shu-Man, L.; Xu-Rong, X. *Physica E* **2003**, 16, 269.

7) Soloviev, V. N., Eichhöfer, A., Fenske, D., Banin, U. *J. Am. Chem. Soc.* **2001**, 123, 2354.

8) Rao, C. N. R.; Kulkarni, G. U.; Thomas, P. J.; Edwards, P. P. *Chem. Eur. J.* **2002**, 8, 29.

9) Housecroft, C. E.; Sharpe, A. G. *Inorganic Chemistry* Pearson Education Limited: Essex, England, 2001, 125-129.

10) Rao, C. N. R.; Müller, A.; Cheetham, A. K. *The Chemistry of Nanomaterials: Synthesis, Properties and Applications* Weinheim: Wiley-VCH, Chichester, 2004, 3-4.

11) Degroot, M. W., Corrigan, J. F. *Z. Anorg. Allg. Chem.* **2006**, 632, 19.

12) Dehnen, S., Fenske, D. *Chem. Eur. J.* **1996**, 2, 1407.

13) Aharoni, A.; Eichhöfer, A.; Fenske, D. *Opt. Mater.* **2003**, 24, 43.

14) S.W. Benson, *J. Chem. Educ.* **1965**, 42, 502.

15) Müller, A.; Diemann, E.; Jostes, R.; Bögge, H. *Angew. Chem. Int. Ed. Engl.* **1981**, 20, 934.

16) So, J.; Boudjouk, P. *Synthesis* **1989**, 306.; Thompson, D. P.; Boudjouk, P. *J. Org. Chem.* **1988**, 53, 2109.

17) a) Schmidt, M.; Kiewert, E.; Lux, H.; Sametschek, C. *Phosphorus, Sulfur Silicon Relat. Elem.* **1986**, 26, 163.; b) Haller, W. S.; Irgolic, K. J. *J. Organomet. Chem.* **1972**, 38, 97.

18) DeGroot, M. W.; Taylor, N. J.; Corrigan, J. F. *Inorg. Chem.* **2005**, 44, 5447.

19) Kealy, T. J., Pauson, P. L. *Nature* **1951**, 168, 1039.

20) Wilkinson, G., Rosenblum, M., Whiting, M. C., Woodward, R. B. *J. Am. Chem. Soc.* **1952**, 74, 2125.

21) Dunitz, J., Orgel, L., Rich, A. *Acta Crystallogr.* **1956**, 9, 373.

22) Yamaguchi, Y., Ding, W., Sanderson, C. T., Borden, M. L., Morgan, M. J., Kutal, C. *Coord. Chem. Rev.* **2007**, 515.

23) Housecroft, C. E.; Sharpe, A. G. *Inorganic Chemistry* Pearson Education Limited: Essex, England, 612-619.

24) Beswick, M. A.; Palmer, J. S.; Wright, D. S. *Chem. Soc. Rev.* **1998**, 27, 225.

25) Beer, P. D.; Hesek, D.; Kingston, J. E.; Smith, D. K.; Stokes, S. E. *Organometallics* **1995**, 14, 3288.

26) Beer, P. D. *Chem. Commun.* **1996**, 689.

27) Beer, P. D.; Cadman, J. *Coord. Chem. Rev.* **2000**, 205, 131.

28) Supritz, C.; Engelmann, A.; Reineker, P. *J. Lumin.* **2005**, 111, 367.

29) Astruc, D., Daniel, M.C., Ruiz, J. *Chem. Commun.,* **2004**, 2637.

30) Casado, C. M.; Cuadrado, I.; Moran, M.; Alonso, B.; Garcia, B.; Gonzalez, B.; Losada, J. *Coordination Chemistry Reviews* **1999**, 53.

31) Top, S.; Vessieres, A.; Cabestaing, C.; Laios, I.; Leclercq, G.; Provot, C.; Jaouen, G. *J. Organomet. Chem.* **2001**, 637, 500.

32) Rajput, J.; Moss, J. R.; Hutton, A. T.; Hendricks, D. T.; Arendse, C. E.; Imrie, C. *J. Organomet. Chem.* **2004**, 689, 1553.

33) a) Lebold, T. P.; Stringle, D. L.; Workentin, M. S.; Corrigan, J. F. *Chem. Commun.* **2003**, 1398.; b) Borecki, A. Undergraduate Chemistry 490 Thesis, *The* University *of* Western Ontario, **2004**.

34) a) Labande, A.; Ruiz, J.; Astruc, D. *J. Am. Chem. Comm.* **2002**, 124, 1782.; b) Astruc, D.; Daniel, M. C.;Ruiz, J. *Chem. Commun.* **2004,** 23, 2637.

CHAPTER 2

Preparation and Characterization of Novel Silylated Ferrocenylmethyl Chalcogenolate Ligands

2.1. Introduction

Although ferrocene was discovered over fifty years ago, new ferrocenyl derivatives and ferrocene containing compounds are still being reported and actively studied.[1] The stability and ease of derivatization of the cyclopentadienyl groups make ferrocene an attractive source for an active redox centre. Continued interest stems from the potential applications in electronic devices and biosensors.[2] One of the challenges faced by synthetic chemists is designing synthetic methodologies that will allow for the incorporation of the desired redox centre into different frameworks.

It has been demonstrated that the optical properties of semiconductor metal-chalcogen nanoclusters can be altered by the incorporation of ferrocenyl units.[3] Also, ferrocenyl units allow for ion sensing similar to that reported for dendrimers.[4] However, there are few examples of well defined nanosized structural frameworks with multiple ferrocenyl units. One of the reasons is the lack of ferrocenylchalcogenolate ligands available for the preparation of well defined structures. Some examples of ferrocenylchalcogenolate ligands reported include: $Fe(\eta^5\text{-}C_5H_4EPh)_2$ (E = S, Se) used in the synthesis of monomeric and polymeric Au and Ag complexes[5]; $Fe(\eta^5\text{-}C_5H_4ESiMe_3)_2$ (E = S, Se) used in the preparation of polynuclear Cu and Ag cluster with multiple ferrocenyl units and monomeric Pt and Pd complexes[6,7]; $CpFe(\eta^5\text{-}C_5H_4ESiMe_3)$ (E = S, Se) in the

synthesis of polynuclear Cd clusters.[8] These reagents are typically prepared by the lithiation of ferrocene with *n*-butyllithium in the presence of tetramethylethylenediamine (TMEDA) to give either $FcLi_2$ or FcLi depending on the molar ratios used. $FcLi_2$ can be reacted with E_2Ph_2 to give $Fe(\eta^5\text{-}C_5H_4EPh)_2$ (E = S, Se),[5] or with elemental sulfur/selenium followed by the addition of chlorotrimethylsilane to give $Fe(\eta^5\text{-}C_5H_4ESiMe_3)_2$ (E = S, Se).[6] FcLi can be reacted with elemental sulfur/selenium to give FcEEFc. Sonochemical reduction of the diferrocenyldiselenide with sodium metal and Ph_2CO followed by silylation with chlorotrimethylsilane results in $CpFe(\eta^5\text{-}C_5H_4ESiMe_3)$ (E = S, Se).[8] In the following sections the preparation and characterization of two new ferrocenylmethylchalcogenolates reagents , $CpFe(\eta^5\text{-}C_5H_4CH_2ESiMe_3)$ [E = S **(1)**, Se **(2)**], will be presented.

2.2. Materials and Methods

2.2.1. General Synthetic Techniques and Starting Materials

Due to the air and moisture sensitivity of the reagents and products, all synthetic and handling procedures were carried out under an inert atmosphere of high purity, dried nitrogen using standard double manifold Schlenk-line techniques or a MBraun inert atmosphere (N_2) glovebox. Tetrahydrofuran and diethyl ether purchased from Caledon were dried and collected using an MBraun MB-SPS solvent purification system with tandem activated alumina/activated copper redox catalyst.[9] Chloroform-d (Cambridge Isotope Laboratories) was dried and distilled over phosphorus pentoxide. Pyridine (Aldrich) and phosphorus

trichloride (Aldrich) were dried and distilled over calcium hydride. Celite was dried by heating at 100°C under vacuum for 48hr. The reagents $E(SiMe_3)_2$ (E = S, Se),[10] and ferrocene carboxylic acid were synthesized according to literature procedures. All other chemicals were used as received from Strem Chemicals and/or Aldrich.

2.2.2. Characterization (NMR Spectroscopy and Mass Spectrometry)

Solution ^1H NMR and ^{13}C NMR spectra were recorded on a Varian Inova 400 NMR spectrometer with an operating frequency of 399.76 MHz and 100.52 MHz respectively, and referenced internally to the residual proton signals of the deuterated solvent, relative to tetramethylsilane (δ = 0.00 ppm). Mass spectrometry was recorded on a Finnigan MAT 8200 mass spectrometer.

2.3. Experimental

2.3.1. Synthesis of $CpFe(\eta^5\text{-}C_5H_4CH_2OH)$[11]

A modified literature procedure was followed, where a solution of ferrocenecarboxylic acid (3.40 g, 14.8 mmol) in 75 mL of diethyl ether was added slowly to a slightly heated solution of $LiAlH_4$ (3.98 g, 105 mmol) in 130 mL of diethyl ether. The mixture was subsequently refluxed for 13h at 60°C. After cooling, a 1:1 ethanol/ether (50 mL) mixture was carefully added to destroy any excess $LiAlH_4$. The reaction mixture was poured into an excess of cold 2 M NaOH solution and the ether and aqueous phases were separated. $MgSO_4$ was added to the ether layer to remove any water and the solvent was removed *in*

vacuo to give a dark orange solid. Using ^{1}H-NMR spectroscopy the orange solid was identified as ferrocenylmethanol. Yield: 2.71 g (85%).

^{1}H NMR ($CDCl_3$): δ = 4.32 (s, 2H), 4.24 (t, 2H, $^3J_{HH}$ = 2 Hz), 4.17(s, 5H), 4.16 (t, 2H, $^3J_{HH}$ = 2 Hz), 2.04 (s, 1H) ppm.

2.3.2. Synthesis of $CpFe(\eta^5\text{-}C_5H_4CH_2Cl)$[12]

Ferrocenylmethanol (2.71 g, 12.5 mmol) dissolved in anhydrous tetrahydrofuran (65 mL) was deprotonated with pyridine (0.95 mL, 12.5 mmol). The solution mixture was cooled to 0°C and freshly distilled phosphorus trichloride (1.1 mL, 12.5 mmol) was slowly added resulting in a colour change from a clear orange solution to a yellow solution with a pale yellow precipitate. The reaction was stirred for 3 h at room temperature after which the yellow precipitate was filtered off. The solvent was then removed *in vacuo* yielding an orange-yellow solid. Using ^{1}H-NMR spectroscopy the pale orange solid was identified as ferrocenylmethylchloride. Yield: 2.28 g (76%).

^{1}H NMR ($CDCl_3$): δ = 4.47(s, 2H), 4.26(t, 2H, $^3J_{HH}$ = 2 Hz), 4.20(t, 2H, $^3J_{HH}$ = 2 Hz), 4.16 (s, 5H) ppm.

2.3.3. Synthesis of $Li^+[SSiMe_3]^-$[13]

A literature procedure was followed where bis(trimethylsilyl)sulfide (0.38 mL, 1.83 mmol) was diluted with anhydrous tetrahydrofuran (10 mL) and cooled to 0°C. *n*-Butyl lithium (1.6 M in hexanes,1.14 mL, 1.83 mmol) was slowly added to the cooled solution and stirred for 30 min at 0°C followed by 30 min at room

temperature. The solvent was removed *in vacuo* to yield a white solid. Using ^{1}H-NMR spectroscopy, the white solid was identified as lithium trimethylsilylthiolate. Yield: 0.21 g (99%).

^{1}H-NMR ($CDCl_3$): δ = 0.32 (s, 3H) ppm.

2.3.4. Synthesis of $Li^+[SeSiMe_3]^-$ [13]

A literature procedure was followed where bis(trimethylsilyl)selenide (0.40 mL, 1.83 mmol) in anhydrous tetrahydrofuran (10 mL) was cooled to 0°C and a solution of *n*-Butyl lithium (1.6 M in hexanes, 1.14 mL, 1.83 mmol) was slowly added. The mixture was stirred at 0°C for 30 min followed by 30 min at room temperature. The solvent was removed in vacuo to yield a white solid. Using ^{1}H-NMR spectroscopy, the white solid was identified as lithium trimethylsilylselenolate. Yield: 0.29g (99%).

^{1}H-NMR ($CDCl_3$): δ = 0.45 (s, 3H) ppm.

2.3.5. Synthesis of $CpFe(\eta^5\text{-}C_5H_4CH_2SSiMe_3)$ (1)

Ferrocenylmethylchloride (0.43g, 1.83mmol) and lithium trimethylsilythiolate (0.21 g, 1.83 mmol) were each dissolved in anhydrous tetrahyrdofuran (50 mL and 10 mL, respectively) and cooled to 0°C. The solutions were mixed and stirred for 1h at room temperature. The solvent was removed *in vacuo* and 25 mL of ether was added to solubilize (ferrocenylmethyltrimethylsilyl)sulfide giving a yellow/orange solution with a pale yellow solid. The solid was removed by passing the mixture through a sintered

glass frit packed with Celite. The solvent was again removed *in vacuo* yielding a yellow solid and identified as (ferrocenylmethyltrimethylsilyl)sulfide (**1**). Yield : 0.47 g (85 %).

^{1}H NMR ($CDCl_3$): δ 4.18 (t, 2H, $^3J_{HH}$ = 2 Hz), 4.13(s, 5H), 4.09 (t, 2H, $^3J_{HH}$ = 2 Hz), 3.50(s, 2H), 0.29(s, 9H) ppm. ^{13}C NMR ($CDCl_3$): δ 87.72 (C_5H_5), δ 68.70 (Cp substituted), δ 68.43 (Cp substituted), δ 67.79 (Cp substituted), δ 26.04 (CH_2), δ 0.92 ($SiMe_3$) ppm.

[M^+]: found (calculated) at m/z = 304.0 (304.3)

2.3.6. Synthesis of $CpFe(\eta^5\text{-}C_5H_4CH_2SeSiMe_3)$ (2)

Ferrocenylmethylchloride (0.43 g, 1.83 mmol) and lithium trimethylsilylselenolate (0.29 g, 1.83 mmol) were each dissolved in anhydrous tetrahydrofuran (50 mL and 10 mL respectively) and cooled to 0°C. The solutions were mixed and stirred for 1h at room temperature. The solvent was removed *in vacuo* and 25 mL of ether was added to solubilize the (ferrocenylmethyltrimethylsilyl)selenide resulting in a yellow/orange solution with a pale yellow solid. The solid was removed by passing the mixture through a sintered glass frit packed with Celite. The solvent was again removed *in vacuo* yielding a yellow solid identified as (ferrocenylmethyltrimethylsilyl)selenide (**2**). Yield: 0.53 g (83 %).

^{1}H NMR ($CDCl_3$): δ 4.17 (t, 2H, $^3J_{HH}$ = 2 Hz), 4.12(s, 5H), 4.10 (t, 2H, $^3J_{HH}$ = 2 Hz), 3.52(s, 2H), 0.38 (s, 9H) ppm. ^{13}C NMR ($CDCl_3$): δ 87.95 (C_5H_5), δ 68.74

(Cp substituted) δ 68.62 (Cp substituted), δ 67.90 (Cp substituted), δ 17.28 (CH_2), δ 1.76 ($SiMe_3$) ppm.

[M^+]: found (calculated) at m/z = 351.9 (351.2)

2.3.7. Synthesis of [CpFe(η^5-$C_5H_4CH_2S$)]$_2$ [14]

A few drops of water were added to a solution of **(1)** (0.050 g, 0.16 mmol) that had been dissolved in tetrahydrofuran (5 mL), and the solution was stirred overnight. Removal of the solvent *in vacuo* afforded a yellow solid identified as di(ferrocenylmethyl)disulfide. Yield: 0.038g (100%).

^{1}H NMR ($CDCl_3$): δ 4.20 (t, 2H, $^3J_{HH}$ = 2 Hz), δ 4.14 (t, 2H, $^3J_{HH}$ = 2 Hz), δ 4.12 (s, 5H), δ 3.54 (s, 2H)

2.3.8. Synthesis of [CpFe(η^5-$C_5H_4CH_2Se$)]$_2$ [15]

A few drops of water were added to a solution of **(2)** (0.050 g, 0.14 mmol) dissolved in tetrahydrofuran (5 mL) and the solution was stirred overnight. Removal of the solvent *in vacuo* afforded a yellow solid. The solid was redissolved in chloroform, where slow evaporation of the solvent afforded yellow needles that were suitable for X-ray crystallography, identified as di(ferrocenylmethyl)diselenide. Yield: 0.040g (98%).

^{1}H NMR ($CDCl_3$): δ 4.21 (t, 2H, $^3J_{HH}$ = 2 Hz), δ 4.14 (t, 2H, $^3J_{HH}$ = 2 Hz), δ 4.12 (s, 5H), δ 3.79 (s, 2H) ppm.

^{13}C NMR ($CDCl_3$): δ 109.76 (Substituted Cp), δ 68.71 (Cp), δ 68.24 (Cp), δ 29.33 (CH_2) ppm.

$[M^+]$: found (calculated) at m/z = 556.9 (556.0)

2.4. Results and Discussion

2.4.1. Synthesis of $CpFe(\eta^5\text{-}C_5H_4CH_2SSiMe_3)$ (1) and $CpFe(\eta^5\text{-}C_5H_4CH_2SeSiMe_3)$ (2)

Ferrocene containing molecules continue to be of great interest due to their inherent redox active metal centre and the relative ease of functionalization of the cyclopentadienyl rings that ultimately allows for various modes of ligation to metal centres. The surface of nanoparticles can be functionalized with ferrocenyl units and has been shown to alter the optical properties of the particle.[3] With the success of silylated chalcogen reagents as route to the formation of metal-chalcogen bonds, we sought out to synthesize a new ferrocenyl chalcogenide that would allow for the introduction of redox active iron centres onto metal-chalcogen cluster surfaces.

Recently, the synthesis of silylated and bis-silylated reagents, $CpFe(\eta^5\text{-}C_5H_4ESiMe_3)$ and $Fe(\eta^5\text{-}C_5H_4ESiMe_3)_2$ (where E = S, Se), have been reported.[6,8] Both reagents have been shown to react readily with metal salts to form polynuclear complexes of metal-chalcogenide cores with ferrocenyl units on their surface. With respect to the "mono"-silylated reagent: $CpFe(\eta^5\text{-}C_5H_4ESiMe_3)$, electrochemical studies revealed degradation of the cluster framework as a result of oxidative cleavage of the ferrocenyl chalcogenolate unit, leading to the formation of the diferrocenyldiselenide (FcSeSeFc), and diferrocenyldisulfide (FcSSFc), respectively.[8] Previous reports have shown that the introduction of an insulating bridge between the metal chalcogen core and ferrocene unit has been

successful in preventing oxidative degradation.[16] Therefore the focus of this research has been to generate silylated ferrocenyl chalcogenolate ligands containing an insulating bridge and incorporate them into metal centers in the synthesis of semiconductor nanoclusters.

As a starting point, ferrocenecarboxylic acid was synthesized by following the preparation techniques outlined by Breit and Breuninger.[17] Ferrocenecarboxylic acid was directly reduced to ferrocenylmethanol by the addition of excess $LiAlH_4$ and refluxing this mixture for approximately 13 hours.[11] Excess $LiAlH_4$ is required to ensure the complete reduction to the primary alcohol. After separation of the organic layer from the aqueous layer, no further purification was required and the product was obtained in high yield.

In order to attach our desired silylated chalcogenide, a better leaving group was placed on the methyl group. Ferrocenylmethanol was deprotonated with the addition of a weak base, pyridine, and then chlorinated with phosphorus trichloride to produce the desired product, ferroceneylmethylchloride.[12] The phosphorus-oxide byproduct is not soluble in solution and therefore easily removed by passing the reaction solution through a sintered glass frit. The removal of any excess pyridine and/or phosphorus trichloride is achieved *in vacuo* and no further purification is required.

It has been shown previously by Segi and co-workers and our group that lithium (trimethylsilyl)chalcogenolates can be used as a facile route for the synthesis of trimethylsilyl chalcogenoethers and asymmetric chalcogenoethers respectively, scheme 2.1.[18] Utilizing this methodology, ferroceneylmethylchloride

is readily converted to (ferrocenylmethyltrimethylsilyl)sulfide, $CpFe(\eta^5\text{-}C_5H_4CH_2SSiMe_3)$ **(1)**, and (ferrocenylmethyltrimethylsilyl)selenide, $CpFe(\eta^5\text{-}C_5H_4CH_2SeSiMe_3)$ **(2)**, by nucleophilic displacement with $Li^+[SSiMe_3]^-$ and $Li^+[SeSiMe_3]^-$ respectively. The byproduct of the reaction, lithium chloride, is slightly soluble in tetrahydrofuran and therefore an alternate solvent, diethyl ether, is used to solublize **(1)** and **(2)** leaving the lithium chloride as a separable solid. The overall reaction for the synthesis of **(1)** and **(2)** is shown in figure 2.2.

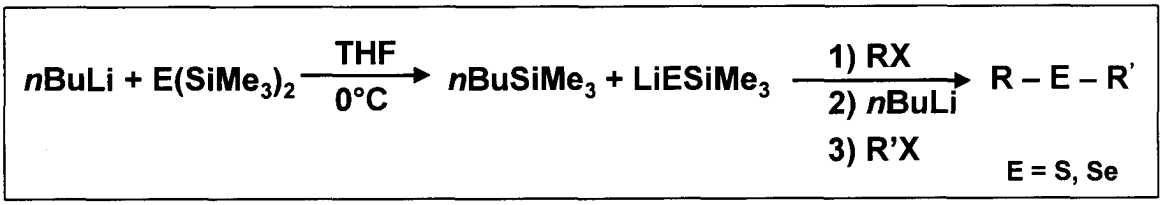

Scheme 2.1 Reaction scheme to asymmetric chalcogenoethers as reported by Segi *et al.*

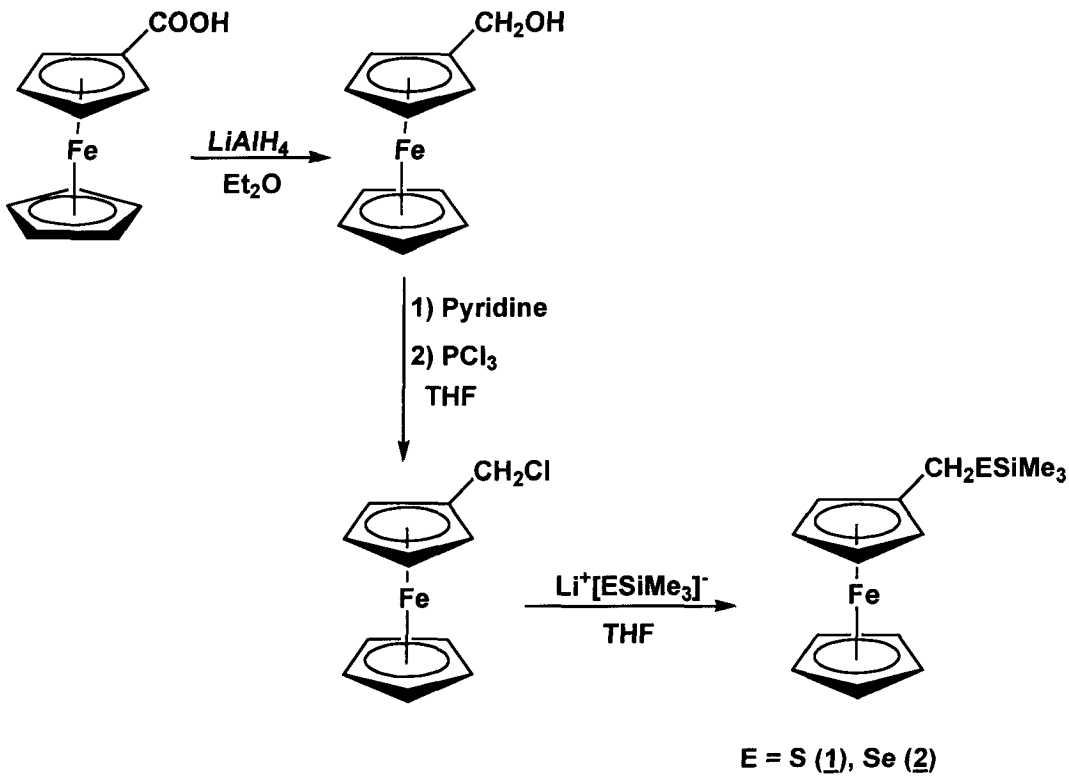

Figure 2.1 Overall synthetic route to $CpFe(\eta^5\text{-}C_5H_4CH_2SSiMe_3)$ **(1)**, and $CpFe(\eta^5\text{-}C_5H_4CH_2SeSiMe_3)$ **(2)**.

Attempts to crystallize (**1**) and (**2**) by a variety of crystallization techniques were unsuccessful, all yielding yellow to pale orange oils. In the proton NMR spectra of (**1**) and (**2**) (figures 2.2 and 2.3 respectively), the relative peak positions are similar except for the methyl group protons [-ESi(CH_3)$_3$] on the silyl groups where there is a 0.10 ppm upfield shift observed for (**2**). The peak position for the trimethyl silyl group allows one to quickly monitor the reactivity of (**1**) and (**2**) by the chemical shift of these peaks upon reacting with metal salts, typically upfield.

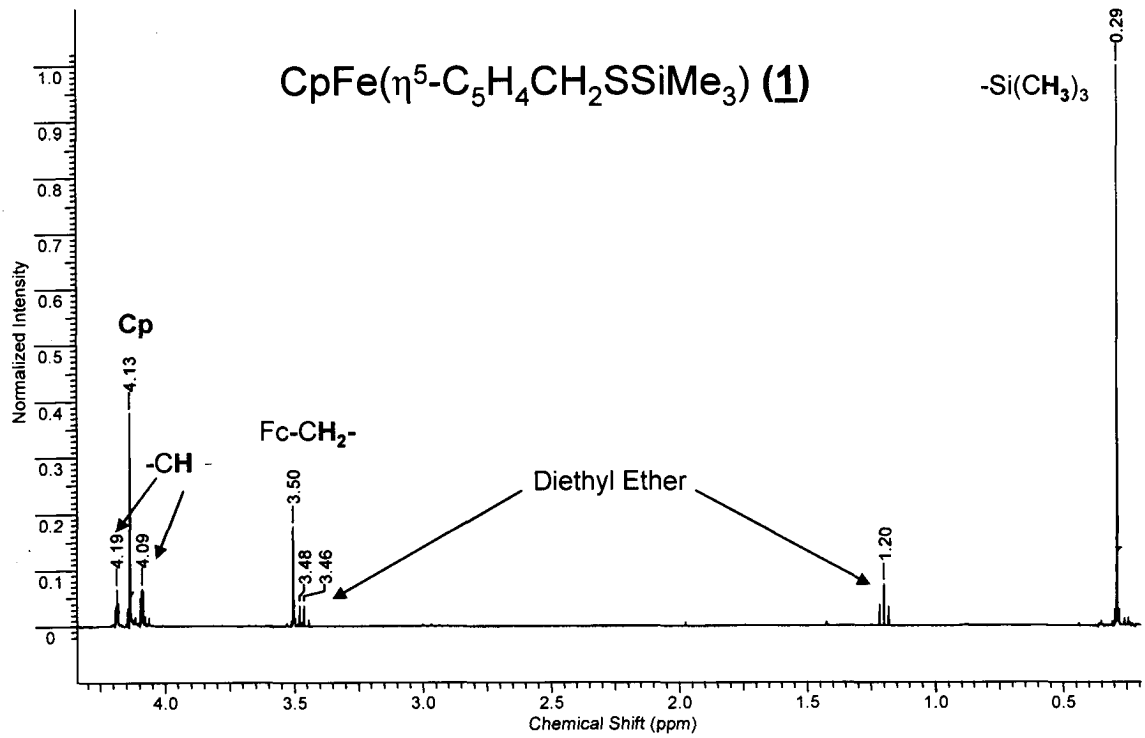

Figure 2.2 ^{1}H-NMR spectrum of (**1**) in $CDCl_3$.

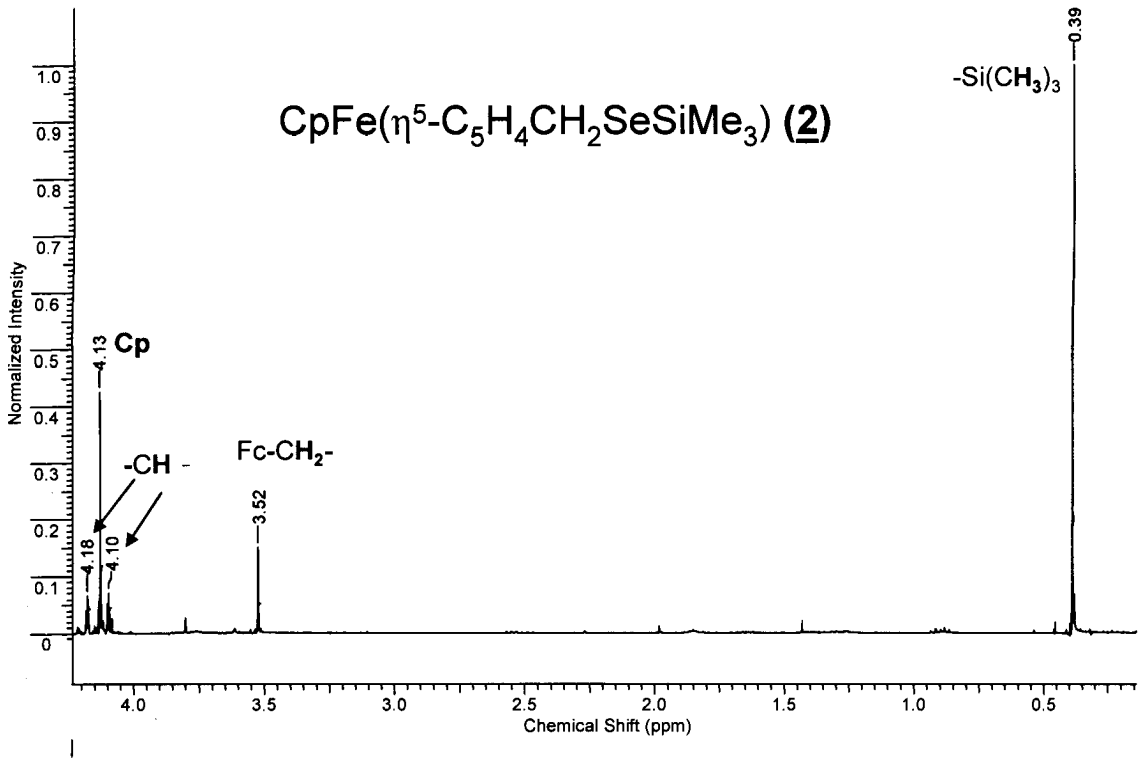

Figure 2.3 ^{1}H-NMR spectrum of (**2**) in $CDCl_3$.

2.4.2 Attempted Functionalization of Various Metal Centres (M = Cd, Zn, and Cu) with $CpFe(\eta^5\text{-}C_5H_4CH_2ESiMe_3)$ (E = S, Se)

As was our initial goal was to functionalize the surface of metal clusters with a redox active unit, the chemistry of group 11–12 metals was explored. Recently, new synthetic strategies have led to structurally characterizable cluster and nanocluster frameworks. The use of silylated reagents, $RESiMe_3$ and $E(SiMe_3)_2$ (E = S, Se, R = alkyl, aryl), are advantageous because they have been shown to react with a wide range metals salts in common organic solvents to form metal-chalcogen clusters. Furthermore, the ability to modify the "R" substitutent allows for a convenient method for the introduction of a desired chemical functionality to polynuclear metal-chalcogen frameworks.

Scheme 2.2 outlines the various metals that were tried, but for all cases and reaction conditions no structurally characterizable products were obtained. From what was expected to be a simple coordination complex reaction (i), three products were obtained: $(FcCH_2)_2E$, $(FcCH_2E)_2$ (E = S, Se) and an unidentified product. To gain a better understanding of the reactivity, reactions were repeated in $CDCl_3$ and monitored, using ^{1}H-NMR spectrometry, by taking aliquots of the reaction mixture. The presence of $(FcCH_2E)_2$ and $AcOSiMe_3$, and the disappearance of any starting reagents suggests that the targeted (*N,N'*-tmeda)$Zn(ECH_2Fc)_2$ (E = S, Se) complex may be unstable and therefore chalcogenolate units are readily oxidized which would explain the presence of

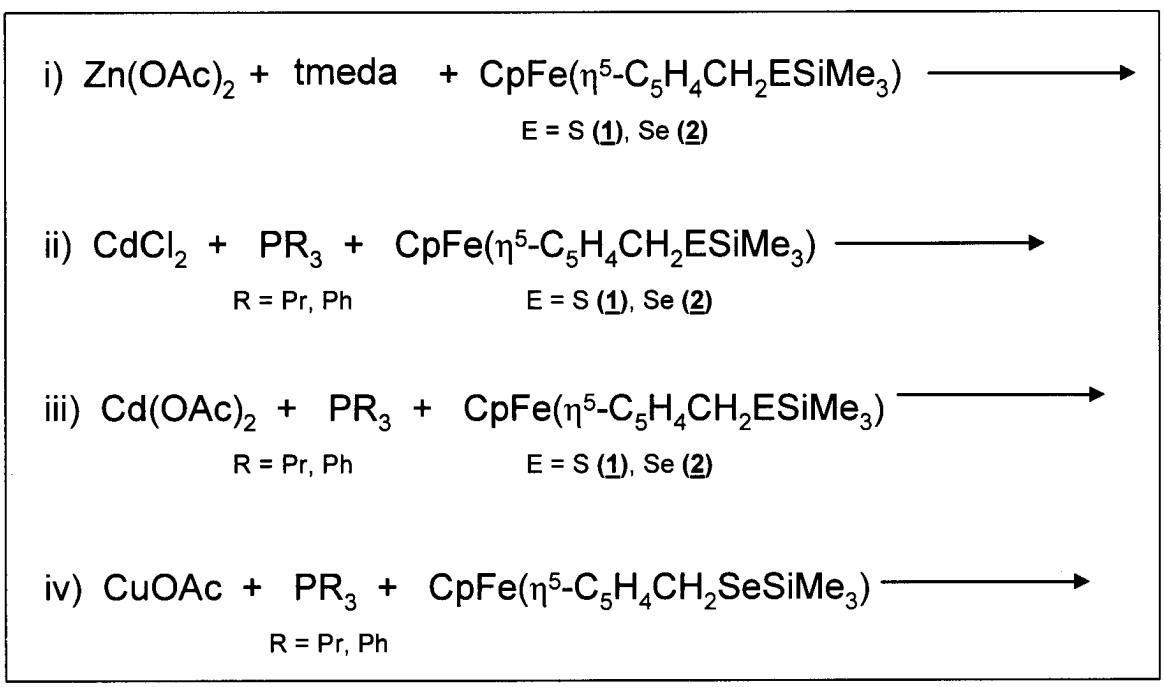

Figure 2.4 Reaction schemes outlining various metals that were targeted with **(1)** and **(2)**.

$(FcCH_2E)_2$. In addition, the presence of $(FcCH_2)_2E$ may also explain the instability of coordination complex, where the lone-pair of electrons on the chalcogenolate can act as a nucleophile and, in a S_N2 reaction, displace a $^-ECH_2Fc$ group on an adjacent molecule, which can in turn react with the ferrocenyl unit on the original nucleophile as illustrated in figure 2.4.

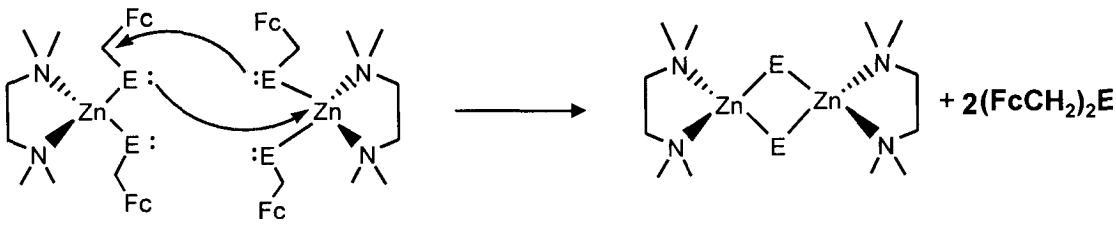

Figure 2.5 Possible mechanism of the nucleophilic displacement of the ferrocenylchalcogenolate unit.

As mentioned, chalcogens can adopt several bridging modes where in this scenario the (*N,N'*-tmeda)Zn$(ECH_2Fc)_n$ complex dimerizes via M–E–M bond formation and could potentially be the unidentified product. Attempts to crystallize and characterize this product proved to be difficult resulting in yellow amorphous solids and/or oils.

It was expected that the reagents CpFe(η^5-$C_5H_4CH_2ESiMe_3$) (E = S (**1**), Se (**2**)) would have similar reactivity to that previously reported with CpFe(η^5-$C_5H_4ESiMe_3$) (E = S, Se) where a Cd_4E_6 adamantoid cluster with six surface ferrocenyl groups was obtained.[8] In addition, by changing the steric properties of the solubilizing ligand, in this case the bulkiness of the R group on the phosphine, and the stoichiometry of starting reagents, a range of M-E frameworks can be achieved.[19] As shown in scheme 3 reactions (ii) – (iii) for all

reaction conditions no single characterizable product was obtained. From the ^{1}H-NMR spectrum of the reaction mixture, no starting reagent was present and the only identifiable product was the $(FcCH_2E)_2$ (E = S, Se). Crystallization attempts gave either amorphous yellow solids or orange oils.

Due to the difficulties experienced with Zn and Cd, the chemistry of the more reactive Hg complexes was not explored. Instead, the focus was shifted to the chemistry of group 11 metals (Fig. 2.3 reaction iv). The reactivity of **(1)** and **(2)** with Cu and Ag proved to be more fruitful where polynuclear complexes of CuS, AgS and AgSe were obtained and will be discussed in the following chapter.

2.5. References for Chapter 2

1) a) Siemeling, U.; Rother, D.; Bruhn, C.; Fink, H.; Weidner, T.; Trager, F.; Rothenberger, A.; Fenske, D.; Priebe, A.; Maurer, J.; Winter, R. *J. Am. Chem. Soc.* **2005**, 127, 1102.; b) Mochida, T.; Shimizu, F.; Shimizu, H.; Okazawa, K.; Sato, F.; Kuwahara, D. *J. Organomet. Chem.* **2007**, 692, 1834.

2) Labande, A.; Ruiz, J.; Astruc, D. *J. Am. Chem. Soc.* **2002**, 124, 1782.

3) Chandler, R. R.; Coffer, J. L.; Atherton, S. J.; Snowden, P. T. *J. Phys. Chem. B.* **1992**, 96, 2713.

4) G. R. Newkome, E. He and C. N. Moorefield, *Chem. Rev.*, **1999**, 99,1689.

5) Canales, S.; Crespo, O.; Fortea, A.; Gimeno, C. M.; Jones, P. G.; Laguna, A. *Dalton Trans.* **2002**, 2250.

6) a) Wallbank, A. I.; Borecki, A.; Taylor, N. J.; Corrigan, J. F. *Organometallics* **2005**, 24, 788.; b) Nitschke, C.; Fenske, D.; Corrigan, J. F. *Inorg. Chem.* **2006**, 45, 9394.; c) Nitschke, C.; Wallbank, A. I.; Fenske, D.; Corrigan, J. F. *J. Cluster. Sci.* **2007**, 18, 131.; d) Wallbank, A. I.; Corrigan, J. F. *Chem. Commun.*, **2001**, 377.

7) Brown, M. J.; Corrigan, J. F. *J. Organomet. Chem.* **2004**, 689, 2872.

8) a) Lebold, T.P.; Stringle, D.L.; Workentin, M.S.; Corrigan, J.F.; *Chem. Commun.*, **2003**, 1398.; b) Borecki, A. Undergraduate Chemistry 490 Thesis, *The* University *of* Western Ontario, **2004**.

9) Pangborn, A. B.; Giardello, M. A.; Grubbs, R. H.; Rosen, R. K.; Timmers, F. J. *Oranometallics* **1996**, 15, 1518.

10) So, J.; Boudjouk, P. *Synthesis* **1989**, 306.; Thompson, D. P.; Boudjouk, P. *J. Org. Chem.* **1988**, 53, 2109.

11) Davis, W. L.; Shago, R. F.; Langner, E.; Swarts, J. C. *Polyhedron,* **2005**, 24, 1611.

12) a) Kaluz, S.; Toma, S. *Collection Czechoslovak Chem. Commun.,* **1988**, 53, 638.; b) Sonoda, A.; Moritani, I. *J. Organometal. Chem.,* **1971**, 133.

13) Taher, D.; Wallbank, A. I.; Turner, E. A.; Cuthbert, H. L.; Corrigan, J. F. *Eur. J. Inorg. Chem.,* **2006**, 4616.

14) Aleksander, R.; Bronislaw, C.; Miroslaw, D.; Adam, P. *Polish Journal of Chemistry*, **1980**, 54, 241.

15) Vijayaratnam, N. Undergraduate Chemistry 490 Thesis, *The* University *of* Western Ontario, **2005**.

16) a) Labande, A.; Ruiz, J.; Astruc, D. *J. Am. Chem. Commun.* **2002**, 124, 1782.; b) Astruc, D.; Daniel, M. C.; Ruiz, J.; *Chem. Commun.* **2004,** 23, 2637.

17) Briet, B.; Breuninger, D.; *Synthesis,* **2005**, 16, 2782.

18) a) Segi, M.; Nakajima, T.; Suga, S.; Murai, S.; Ryu, I.; Ogawa, A.; Sonoda, N. *J. Am. Chem. Soc.* **1988**, 110, 1976.; b) Segi, M.; Kato, M.; Nakajima, T.; Suga, S.; Sonoda, N. *Chem. Lett.* **1989**, 1009.

19) Dehnen, S.; Eichhöfer, A.; Fenske, D. *Eur. J. Inorg. Chem.* **2002**, 279.

Chapter 3

Preparation and Characterization of New Ferrocenylmethylchalcogenolate - Group 11 Metal Clusters.

3.1. Introduction

One area of current research on ferrocene is focused on preparing frameworks that support multi-ferrocenyl units. To date, aromatic,[1] dendrimeric,[2] and inorganic[3] frameworks have been used as cores on which multiple ferrocenyl groups can be attached. Semiconductor nanoparticles offer a unique framework that remains to be explored. The main challenges faced by researchers is developing general synthetic strategies to access well defined structural frameworks, ideally with no size dispersion, and methods for the introduction of ferrocenyl groups to their surfaces.

The use of silylated reagents has been shown to be very fruitful in metal-chalcogen chemistry. The size of the final product obtained in the reactions of silylated chalcogen reagents with metal salts depends on the ratio of starting reagents, the steric demands of the phosphine ligand, and solvent used.[7] A series of group 11-16 nanoclusters have been prepared by Fenske and Corrigan, where the largest clusters of the series, $[Cu_{146}Se_{73}(PPh_3)_{30}]$[4] and $[Ag_{188}S_{94}(PR_3)_{30}]$[5] have been characterized by X-ray crystallography. The series of $Cu_{2n}E_n$ (E = S, Se) clusters obtained using silylated reagents ranges from $Cu_{12}Se_6$ to $Cu_{146}Se_{73}$. These clusters exhibit some interesting structural and physical properties. In particular, various coordination modes are observed depending on the bridging chalcogen (S versus Se) and size of the cluster,

where the larger clusters in the series, $[Cu_{70}Se_{35}(PEt_3)_{22}]$ and $[Cu_{146}Se_{73}(PPh_3)_{30}]$, have been shown to have layer type structural frameworks similar to that found in the bulk material.[6,7] Preliminary studies of these clusters show that their electrical conductivity is also dependent on their size.[7] Computational calculations have shown that the phosphane-stabilized, PR_3, cluster complexes are metastable.[8] Therefore these clusters can be described as a section of the structure of the bulk binary Cu_2E phase material (E = S, Se) surrounded by PR_3 ligands[8] and can serve as potential models for the study of the change in physical and chemical properties observed when going from small molecules to bulk materials. These molecular clusters have the advantage over other nanomaterials because there is no particle size distribution due to their well defined structure.

The isolation, characterization and investigation of metal-chalcogen clusters could provide insight into new nanomaterials with interesting properties. It has been demonstrated that the incorporation of a redox centre, such as ferrocene based ligands, onto metal-chalcogen nanoparticles can alter the optical properties of these materials.[9] These complexes have gained much attention in material sciences, where the focus has been on preparing functional materials such as biosensors.[10] While these compounds exhibit interesting properties there are few examples of ferrocenyl-chalcogen ligands reported for accessing such materials.

Silylated chalcogen reagents of the type $RESiMe_3$ (R = organic group; E = S, Se, Te) are soluble in most common organic solvents and have the benefit of

introducing various functionalities, "R", into metal-chalcogen architectures. Furthermore, they allow for homogeneous reaction conditions which are essential for the formation and crystallization of larger complexes. The reagents $Fe(\eta^5\text{-}C_5H_4ESiMe_3)_2$[11,12] and $CpFe(\eta^5\text{-}C_5H_4ESiMe_3)$[13] (E = S, Se) have been used to passivate cluster surfaces. However, electrochemical analysis using cyclic voltammetry of $Cd_6(EFc)_6$ clusters showed a single irreversible anodic oxidation wave followed by two reversible oxidation waves seen after repetitive cycles. The irreversible wave was attributed to the oxidation of ferrocenyl units, which then initiates the oxidative cleavage of the ferrocenylchalcogenolate units leading to the formation of di(ferrocenylsulfide) and selenide (FcE-EFc) (E = S, Se).[13] Similar cluster degradation was observed for clusters prepared with $Fe(\eta^5\text{-}C_5H_4ESiMe_3)_2$.[11,12] Therefore, it is essential to prepare ferrocenyl ligands that will remain attached to cluster frameworks to allow electrochemical studies of these clusters. The successful synthesis of $FcCH_2ESiMe_3$ [E = S (**1**), Se (**2**)] reagents was described in the previous section and its reactivity for the preparation and characterization of $[Cu_3(SCH_2Fc)_3(PPh_3)_3]$ (**3**), $[Ag_{48}S_6(SCH_2Fc)_{36}]$ (**4**) and $[Ag_{10}(SCH_2Fc)_{10}(PPh_3)_4]$ (**5**) and $[Ag_8(SeCH_2Fc)_8(PPh_3)_4]$ (**6**) clusters will be discussed in the following sections.

3.2. Materials and Methods

3.2.1. Starting Materials

All synthetic and handling procedures were carried out under an inert atmosphere of high purity dried nitrogen using standard double manifold

Schlenk-line techniques and a MBraun inert atmosphere (N_2) glovebox. Tetrahydrofuran, toluene, pentane, hexanes and diethyl ether purchased from Caledon were dried and collected using an MBraun MB-SPS solvent purification system with activated alumina catalyst.[14] Chloroform (purchased from) and chloroform-d (Cambridge Isotope Laboratories) were dried and distilled over phosphorus pentoxide. Deuterated THF (d_8-THF) was purchased from Aldrich and used as received. Copper (I) acetate was prepared according to literature procedures. All other chemicals were used as received from Strem and/or Aldrich. The reagents $FcCH_2ESiMe_3$ [E = S (**1**), Se (**2**)] were prepared as outlined in the previous chapter.

3.2.2. Characterization

Single crystal X-ray diffraction measurements were performed on an Enraf-Nonius KappaCCD X-ray diffractometer in a cold nitrogen stream at 150K using graphite-monochromated Mo-Kα radiation (λ=0.71073 Å) with φ and ω scans. Data reduction was performed using Nonius HKL DENZO and SCALEPACK software. Molecular structures were determined via direct methods and Patterson (SHELXS-97) and refined by a full matrix least squares method based on F^2 using *SHELXTL 5.0* software.

Diffraction data for (**3**) and (**4**) were collected by Dr. Mike Jennings and solved and refined by Dr. John Corrigan. Diffraction data for (**5**) and (**6**) were collected, solved and refined by Dan MacDonald.

Elemental analyses were performed by Guelph Chemical Laboratories (Guelph, Canada). Solution ^{1}H NMR and ^{31}P spectra were recorded on a Varian Inova 400 NMR spectrometer with an operating frequency of 399.76 MHz and 161.96 MHz respectively. ^{1}H NMR samples were referenced internally to the residual proton signals of the deuterated solvent, relative to tetramethylsilane (δ = 0.00 ppm).

3.3. Experimental

3.3.1. Synthesis and characterization of $[Cu_3(SCH_2Fc)_3(PPh_3)_3]$ (3)

Copper (I) acetate (0.84 g, 0.69 mmol) was solubilized with 2 equivalents of triphenylphosphine (0.36 g, 1.4 mmol) in chloroform (5 mL). **(1)** (0.21 g, 0.69 mmol) was dissolved in chloroform (5 mL) and the temperature of both solutions was reduced to 0°C. The clear colourless solution of copper (I) acetate/triphenylphosphine was added to the yellow/orange solution of **(1)** and stirred for two hours at room temperature. The resultant solution had a darker orange colour. Layering the reaction mixture with hexanes (30 mL) afforded light orange block-like single crystals within 48 hours. The structure was identified by X-ray crystallography to be $[Cu_3(SCH_2Fc)_3(PPh_3)_3]$ **(3)**. Yield: 0.23 g (60%).

Spectroscopic Data:

^{1}H NMR ($CDCl_3$): δ = 7.36–7.49 (m, br, Cu-P**Ph**$_3$), 3.91 and 4.05. (s, br, $C_5\mathbf{H}_4$), 4.00 (s, br, $C_5\mathbf{H}_5$), 3.79 (s, -C$\mathbf{H}_2$-) ppm.

Elemental Analysis: Calc. (found)

(3) C, 62.54 (62.53); H, 4.71 (5.32)

3.3.2. Synthesis and characterization of $[Ag_{48}S_6(SCH_2Fc)_{36}]$ (4) and $[Ag_{10}(SCH_2Fc)_{10}(PPh_3)_4]$ (5)

Silver (I) acetate (0.12 g, 0.70 mmol) was solubilized with 2 equivalents of triphenylphosphine (0.37 g, 1.4 mmol) in chloroform (5 mL). **(1)** (0.21 g, 0.70 mmol) was dissolved in chloroform (5 mL) and the temperature of both solutions was reduced to –60°C. The solutions were mixed at –60°C and the reaction mixture was slowly warmed to room temperature and was stirred for 2 hours, after which an intense orange-red coloured solution is observed. Pentane (35 mL) was diffused over the reaction solution and after 48 hours two different types of crystals were obtained. The major product was isolated as orange square pyramidal crystals, and secondary product was isolated as small yellow cubes. The structures of both were determined by X-ray crystallography to be $[Ag_{48}S_6(SCH_2Fc)_{36}]$ **(4)** (orange crystals) and $[Ag_{10}(SCH_2Fc)_{10}(PPh_3)_4]$ **(5)** (yellow crystals). Yield: **(4)** 0.098 g (43%), **(5)** 0.095 g (30%).

Elemental Analysis: Calc. (found)

(4) C, 37.74 (35.29); H, 2.92, (2.01), **(5)** C, 49.29 (49.19);H, 3.86 (4.00)

3.3.3. Synthesis and Characterization of $[Ag_8(SeCH_2Fc)_8(PPh_3)_4]$ (6)

Silver (I) acetate (0.13 g, 0.74 mmol) was solubilized with 2 equivalents of triphenylphosphine (0.39 g, 1.5 mmol) in chloroform (5 mL). **(2)** (0.26 g, 0.74 mmol) was dissolved in chloroform (5 mL) and the temperature of both solutions was reduced to –75°C. The two solutions were mixed at –75°C and the reaction mixture was slowly warmed to –20°C and stirred at this temperature for 2 hours resulting in a deep red solution. The reaction solution was cooled to –40°C and

layered with hexanes (35 mL). Several weeks later orange block-like single crystals were obtained and identified by X-ray crystallography to be $[Ag_8(SeCH_2Fc)_8(PPh_3)_4]$ (**6**). Yield: (**6**) 0.16 g (44%)

Elemental Analysis: Calc. (found)

(**6**) C, 46.46 (46.66); H, 3.61, (4.23).

3.4. Results and Discussion

3.4.1. Synthesis of $[Cu_3(SCH_2Fc)_3(PPh_3)_3]$ (3), $[Ag_{48}S_6(SCH_2Fc)_{36}]$ (4) and $[Ag_{10}(SCH_2Fc)_{10}(PPh_3)_4]$ (5) and $[Ag_8(SeCH_2Fc)_8(PPh_3)_4]$ (6)

One of the most versatile synthetic strategies for the synthesis of metal chalcogen nanocluster complexes involves the use of silylated chalcogen reagents such as $E(SiMe_3)_2$ and $RESiMe_3$ (E = S, Se, Te; R = organic moiety). The synthesis of silylated ferrocenyl chalcogenlate reagents, $Fe(\eta^5\text{-}C_5H_4ESiMe_3)_2$ and $CpFe(\eta^5\text{-}C_5H_4ESiMe_3)$, used in the preparation of polynuclear clusters prompted us to investigate the effects of an alkyl spacer between the cyclopentadienyl group and the chalcogen atom. The aim is to eliminate any communication between the redox centre and the chalcogen that was observed with $Fe(\eta^5\text{-}C_5H_4ESiMe_3)_2$ and $CpFe(\eta^5\text{-}C_5H_4ESiMe_3)$ resulting in oxidative cleavage of the ferrocenyl chalcogen groups.[11,13]

A freshly prepared solution of $FcCH_2SSiMe_3$ (**1**) was reacted with copper(I) acetate in the presence of a triphenylphosphine at 0°C in chloroform, resulting a clear orange solution. The reaction mixture was stirred and the temperature was gradually warmed to room temperature resulting in a darker orange coloured solution. ^{1}H-NMR spectroscopy can be used to monitor the

overall reaction, figure 3.1. There is an upfield shift and broadening of the peaks associated with the ferrocenyl protons and a downfield shift of methylene protons (Fc-C**H**$_2$-S). Although not shown in figure 3.1, there is also an upfield shift observed for the acetate peak of copper-acetate and down field shift for the trimethylsilane group of (**1**), as a result of the formation of acetoxytrimethylsilane (C**H**$_3$COO-Si**Me**$_3$) indicating the absence of any starting reagents. Layering the reaction mixture with hexanes affords pale orange block-like crystals of [$Cu_3(SCH_2Fc)_3(PPh_3)_3$] (**3**), suitable for analysis by single crystal X-ray crystallography, in good yield.

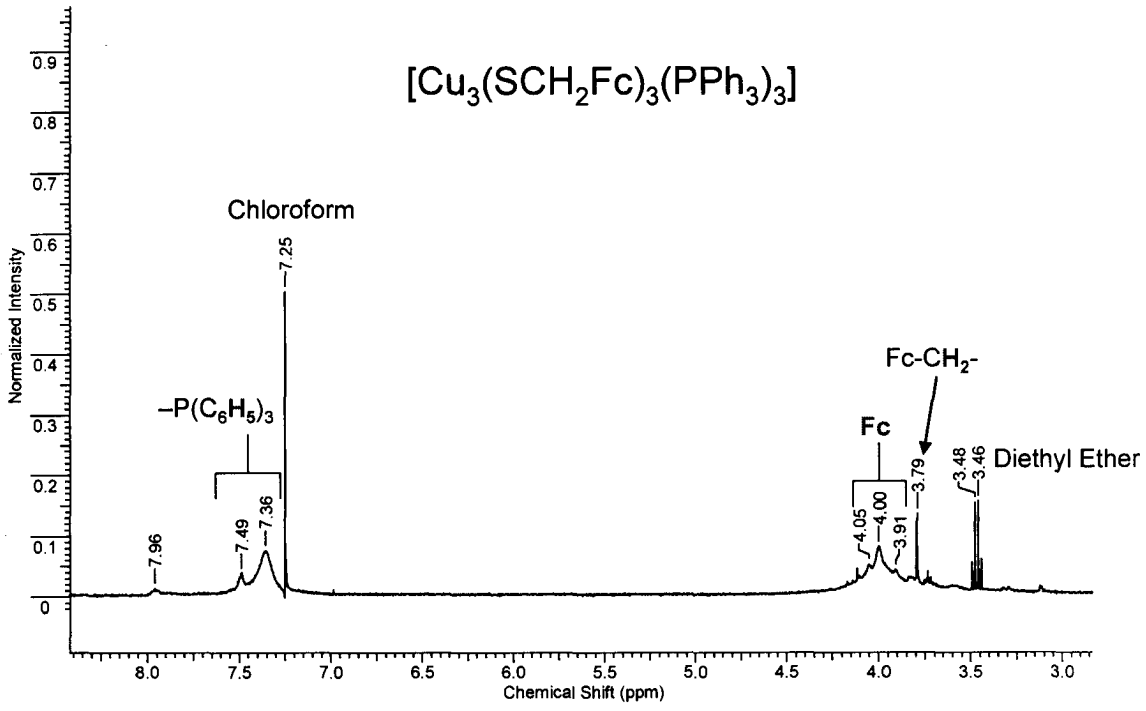

Figure 3.1 ^{1}H NMR spectrum of (**3**) in $CDCl_3$.

Unlike copper acetate, silver acetate requires more time to be fully solubilized with triphenylphosphine in chloroform to give a clear colourless

solution. To this solution a freshly prepared solution of **(1)** in chloroform is added at –60°C resulting in a clear pale orange solution. The reaction mixture is stirred and slowly warmed to room temperature where a gradual colour change was observed to a darker orange-red solution. Filtration was sometimes necessary to remove any turbidity to give a clear homogeneous solution required for crystallization. Slow diffusion of pentane over the reaction mixture affords two crystalline products suitable for analysis by single crystal X-ray crystallography: the major product was single orange square pyramidal crystals of $[Ag_{48}S_6(SCH_2Fc)_{36}]$ **(4)**, and the secondary product was single yellow block-like crystals of $[Ag_{10}(SCH_2Fc)_{10}(PPh_3)_4]$ **(5)**.

In a similar manner, $[Ag_8(SeCH_2Fc)_8(PPh_3)_4]$ **(6)** was prepared by reacting a solution of silver acetate solubilized with triphenylphosphine with $FcCH_2SeSiMe_3$ **(2)** at –70°C in chloroform. The initial solution was a pale orange colour, however upon warming to –25°C a dark red solution was obtained. Reactions that were warmed up above –15°C resulted in the precipitation of an amorphous black solid, and ^{1}H-NMR analysis of the supernatant revealed the presence of (diferrocenyl)diselenide $(FcCH_2Se)_2$, suggesting thermal decomposition of the cluster. No further characterization was done on these decomposition products. To avoid thermal decomposition, reactions were kept below –25°C and layered with hexane, and then stored at –40°C. After several weeks, single orange block-like crystals of **(6)** suitable of X-ray crystallography were obtained.

3.4.2. Structural Characterization of $[Cu_3(SCH_2Fc)_3(PPh_3)_3]$ (3), $[Ag_{48}S_6(SCH_2Fc)_{36}]$ (4) and $[Ag_{10}(SCH_2Fc)_{10}(PPh_3)_4]$ (5) and $[Ag_8(SeCH_2Fc)_8(PPh_3)_4]$ (6)

Clusters (3), (4), (5) and (6) have all been structurally characterized by X-ray crystallography. Scheme 3.1 outlines the reaction conditions used to obtain clusters (3), (4), (5) and (6). In figure 3.2 the molecular structure of (3) is shown, which was satisfactorily solved and refined in the triclinic space group $P\bar{1}$ with two independent molecules in the asymmetric unit cell. Discussions here refer to molecule one. The core of the cluster is a closed ring consisting of alternating Cu-S-Cu bonds, where the thiolate ions adopt a μ_2-bridging mode, and each Cu atom is also bonded to a phosphine ligand giving an almost trigonal planar geometry (Σ(bond angles) = 358.27–359.99°) about the copper centres. The copper-thiolate distances for (3) [2.215(3)–2.306(3) Å] are slightly longer than in the related trinuclear complex $[CpFe\{\eta^5\text{-}C_5H_3(1\text{-}PPh_2)(2\text{-}CH\text{-}(CH_3)S)\}Cu]_3$ (Cu–S = 2.178(6)–2.251(6) Å)[16], but are within range of three coordinate Cu(I)–S complexes reported [2.103–2.673 Å].[17] Table 3.1 summarizes selected bond lengths and angles for (3). The internal core is protected from further condensation by the ferrocenyl and phenyl groups covering the surface of the cluster. In figure 3.3, a space filling diagram of (3) illustrates that the internal core is completely covered by the ferrocenyl and phenyl groups. Two chloroform molecules, represented as blue balls, are also found on the surface of (3). Elemental analysis of (3) was found to be 62.53 and 5.32 % for C and H atoms respectively. These values are within range of the calculated values C:H, 62.54:4.71 %.

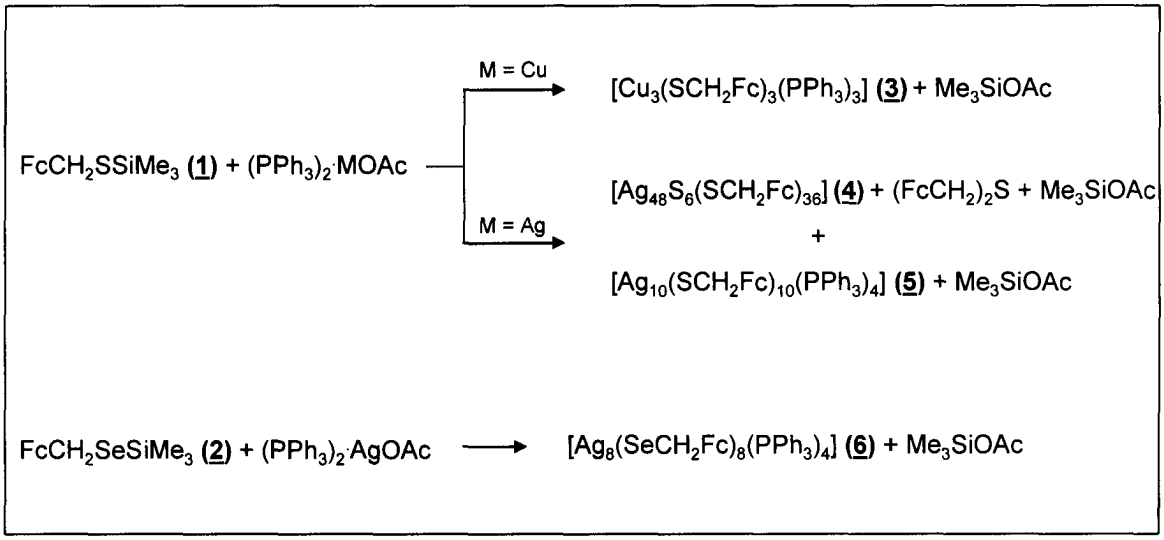

Scheme 3.1 Reaction schemes outlining the preparation of (3), (4), (5) and (6).

Cu(11)-P(11)	2.203(3)	P(11)-Cu(11)-S(11)	135.14(13)
Cu(11)-S(11)	2.215(3)	P(11)-Cu(11)-S(31)	116.35(13)
Cu(11)-S(31)	2.306(3)	S(11)-Cu(11)-S(31)	106.78(12)
Cu(21)-P(21)	2.232(3)	P(21)-Cu(21)-S(11)	122.48(12)
Cu(21)-S(11)	2.240(3)	P(21)-Cu(21)-S(21)	119.97(11)
Cu(21)-S(21)	2.284(3)	S(11)-Cu(21)-S(21)	117.34(12)
Cu(31)-P(31)	2.195(4)	P(31)-Cu(31)-S(21)	116.30(13)
Cu(31)-S(21)	2.227(4)	P(31)-Cu(31)-S(31)	133.32(13)
Cu(31)-S(31)	2.233(3)	S(21)-Cu(31)-S(31)	110.37(13)
		Cu(11)-S(11)-Cu(21)	98.61(12)
		Cu(31)-S(21)-Cu(21)	85.98(10)
		Cu(31)-S(31)-Cu(11)	94.92(13)

Table 3. 1 Selected intramolecular bond lengths [Å] and angles [°] for (3).

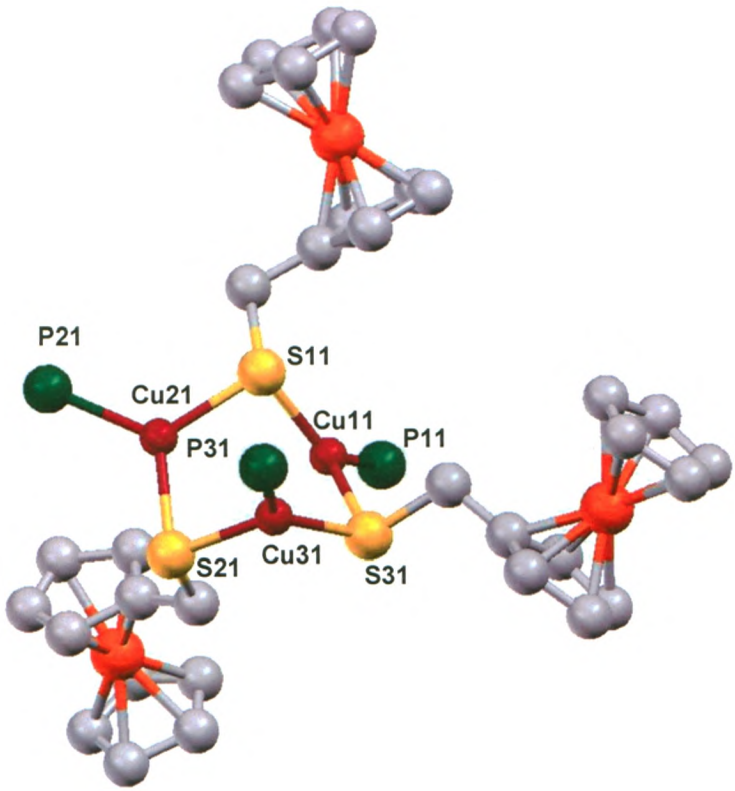

Figure 3.2 Ball and stick diagram of the molecular structure of $[Cu_3(SCH_2Fc)_3(PPh_3)_3]$ **(3)**. Cu, Fe, S, P and C atoms are represented as red, orange, yellow, dark green and grey spheres, respectively. Hydrogen atoms and phenyl groups have been omitted for clarity.

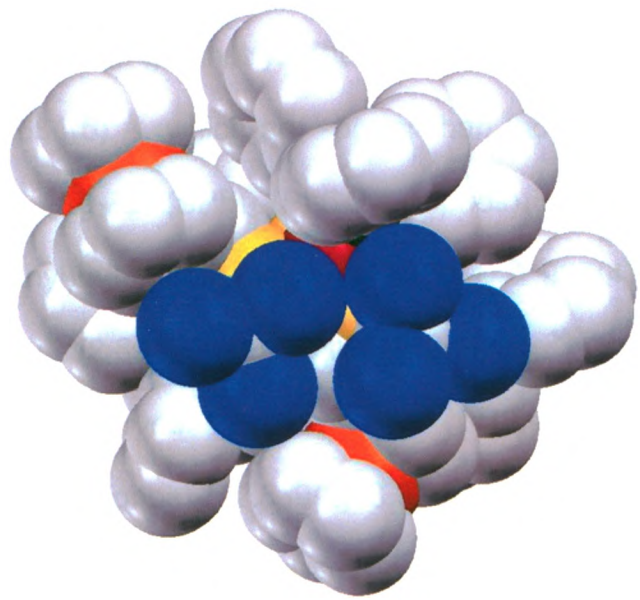

Figure 3.3 Spacefilling diagram of the molecular structure of $[Cu_3(SCH_2Fc)_3(PPh_3)_3]\cdot(CHCl_3)_2$ **(3)**. Cu, Fe, S, P, C and Cl atoms are represented as red, orange, yellow, dark green, grey and blue spheres, respectively. Hydrogen atoms have been omitted for clarity.

Figures 3.4, 3.5 and 3.6 all display the molecular structure of $[Ag_{48}S_6(SCH_2Fc)_{32}]$ **(4)** which was solved and refined in the monoclinic space group C2/c. The core of the structure can be described as a compressed disk consisting of forty-eight silver atoms bonded to both sulfide (S^{2-}) and thiolate ($FcCH_2S^-$) ions. The six interstitial sulfides (S^{2-}) adopt a μ_4-bridging mode, where each atom is bonded to four silver atoms. The thiolates ($FcCH_2S^-$) ions form either μ_2 or μ_3 bridges to silver atoms. Silver atoms have either a distorted linear geometry or trigonal planar geometry. The Ag–S bond lengths for **(4)** range between 2.144(8)–2.684(5) Å, which are shorter than those reported for similar sized clusters, $[Ag_{70}S_{16}(SPh)_{34}(PhCO_2)_4(triphos)_4]$, triphos [1,1,1-tris{(diphenylphosphanyl)methyl}ethane], [2.370(4)–2.927(4) Å][5] and $[Ag_{50}S_7(SC_6H_4Bu^t\text{-}4)_{40}]^{4-}$ [2.394–2.668 Å] for μ_3 bridging.[18] Comparable Ag–Ag distances are observed for **(4)** [2.952(2)–3.324(2) Å], $[Ag_{70}S_{16}(SPh)_{34}(PhCO_2)_4(triphos)_4]$ [2.889(2)–3.380(2) Å], and $[Ag_{50}S_7(SC_6H_4Bu^t\text{-}4)_{40}]^{4-}$ [2.950–3.458 Å]. Since all Ag atoms in these clusters have the formal charge of +1 and therefore a d^{10} configuration, it was concluded that there are no significant Ag-Ag interactions.[18] The most interesting structural feature found in **(4)** are the thirty-six ferrocenyl units found on the surface, which inhibit the further growth of the cluster core towards crystalline Ag_2S. This is the largest number of ferrocenyl units to cover the surface of a cluster that has been structurally characterized by single X-ray crystallography. It is also worth mentioning the absence of any phosphine ligands on the surface of **(4)** that was used to solubilize the silver carboxylate. ^{1}H-NMR spectroscopy on isolated crystals of **(4)**

was attempted in various deuterated solvents due to solubility issues, where d_8-THF had the best solubility after sonication (Appendix A). Peak assignments remain ambiguous as a result of overlapping peaks, suggesting that some the ferrocene groups are magnetically nonequivalent. Elemental analysis of **(4)** was found to be 35.29 and 2.01% for C and H atoms respectively. These values are within the calculated values for C:H, 37.74:2.92 %.

As a second product, single crystals of **(5)** were obtained from the same reaction that crystals of **(4)** were obtained (scheme 3.1), and satisfactorily solved and refined in the triclinic space group $P\bar{1}$. The molecular structure of **(5)** is illustrated in figures 3.7, 3.8 and 3.9, where the core is exclusively made up ten silver atoms bonded ten ferrocenylmethylthiolate ligands ($^{-}SCH_2Fc$) which adopt either a μ_2 or μ_3 bridging mode. Three different coordination environments are observed for the Ag atoms, where shorter bond Ag-S lengths are observed for distorted linear coordination, [2.373(2)–2.406(2) Å], compared to trigonal planar and tetrahedral coordination [2.442(2)–2.726(2) Å]. Similar Ag-Ag distances are also observed for **(5)** [2.9714(9)–3.3436(9) Å] as was observed for **(4)**. A summary of selected bond lengths and angles for **(5)** is given in table 3.2. The core of **(5)** is protected by a shell of ferrocenylmethyl units and triphenylphosphine ligands.

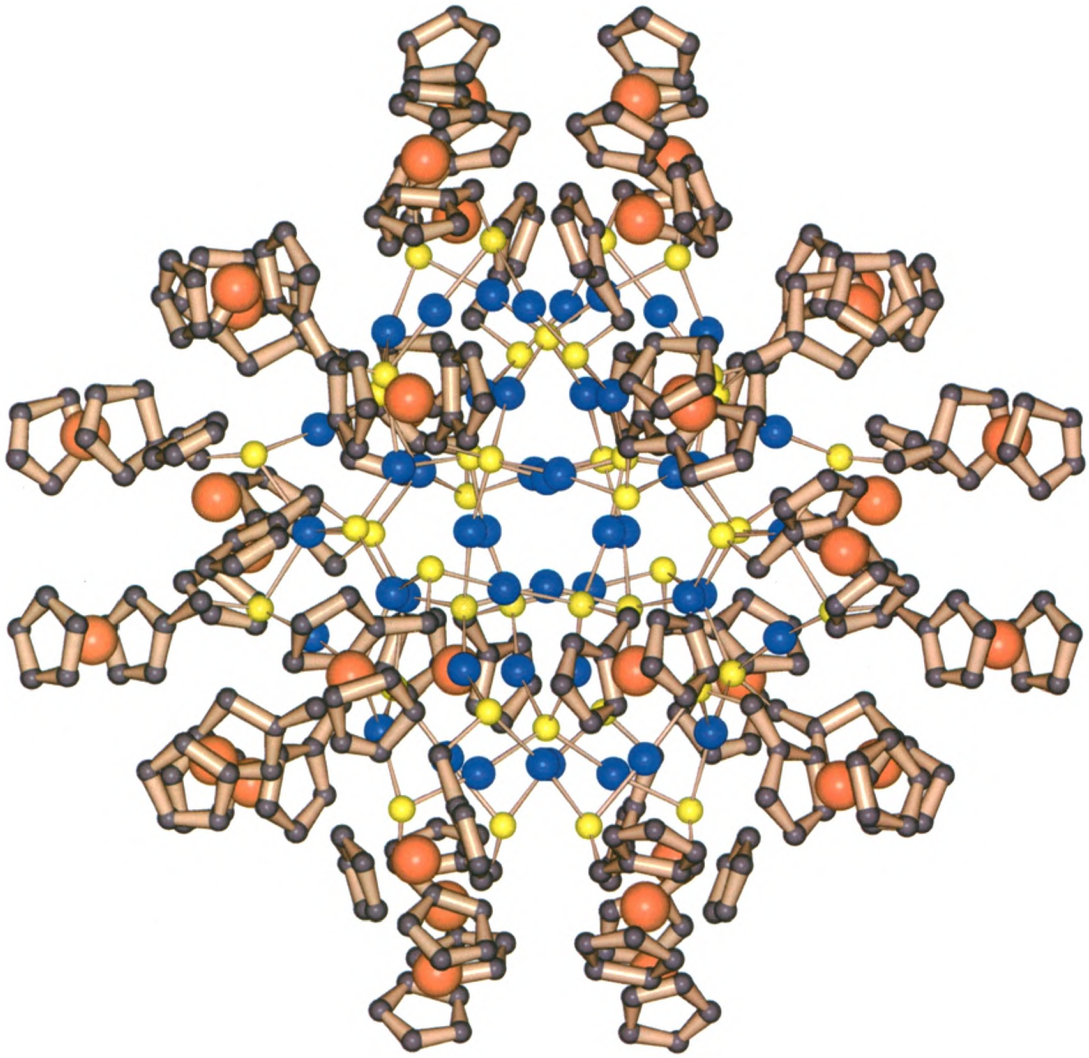

Figure 3.4 Ball and stick diagram of the molecular structure of $[Ag_{48}S_6(SCH_2Fc)_{36}]$ **(4)**. Ag, Fe, S and C atoms are represented as blue, orange, yellow and grey spheres, respectively. Hydrogen atoms have been omitted for clarity.

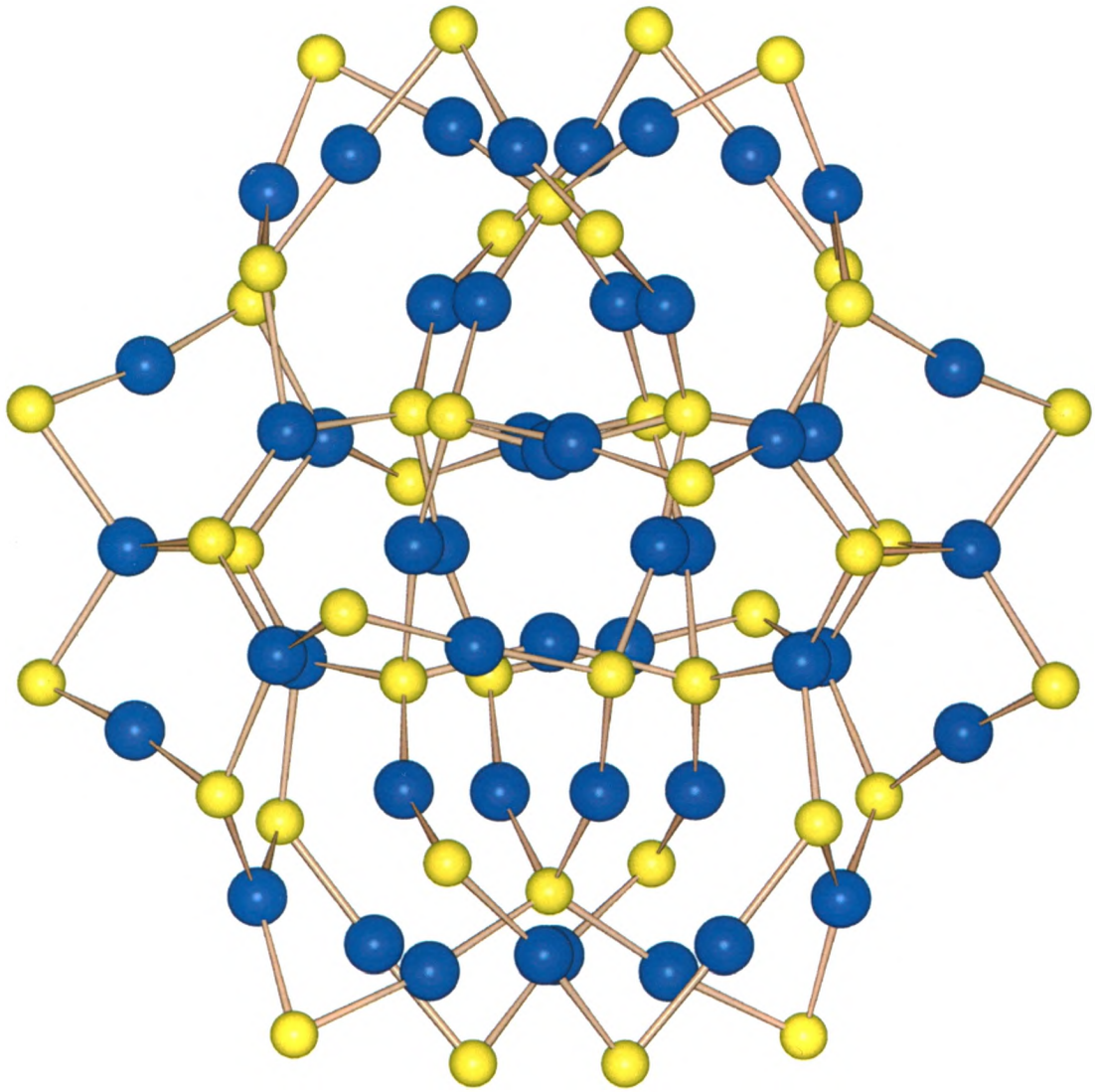

Figure 3.5 Ball and stick diagram of the molecular structure of $Ag_{48}S_{42}$ core of $[Ag_{48}S_6(SCH_2Fc)_{36}]$ **(4)**. Ag and S atoms are represented as blue and yellow spheres, respectively.

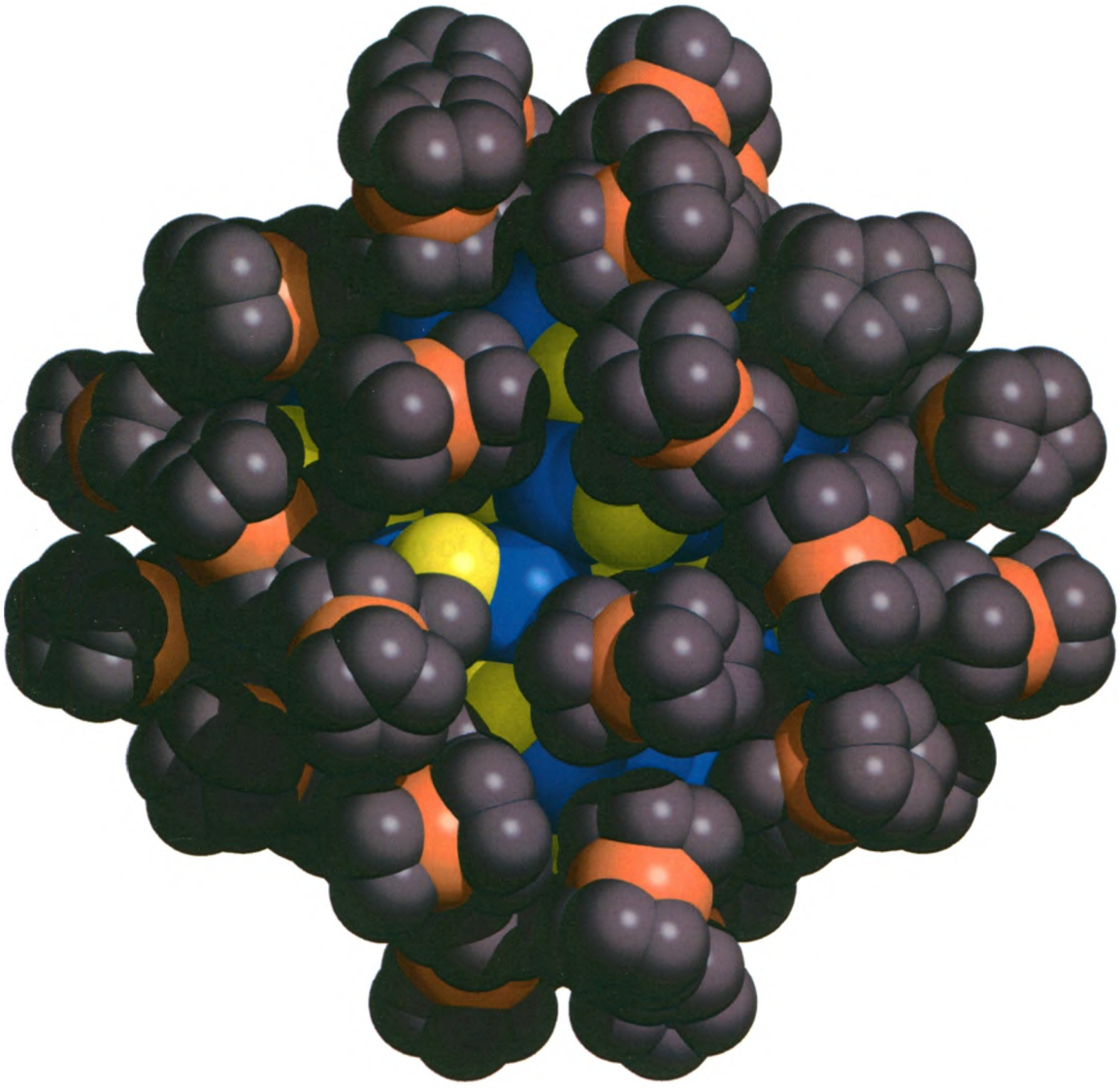

Figure 3.6 Space filling diagram of the molecular structure of $[Ag_{48}S_6(SCH_2Fc)_{36}]$ **(4)**. Ag, Fe, S and C atoms are represented as blue, orange, yellow and grey spheres, respectively. Hydrogen atoms have been omitted for clarity.

Although one cannot predict the final product in cluster formation, the synthesis of **(4)** as the major product over **(5)** was somewhat unexpected. Group 11-16 metal chalcogen clusters obtained using $Fe(\eta^5\text{-}C_5H_4ESiMe_3)_2$ (E = S, Se) revealed that only metal-chalcogenolate complexes $(M–ER–M)_x$ are formed. It was assumed that using analogous reaction conditions with reagent **(1)** would result in similar sized clusters, as indeed this is the case in the formation **(5)**. In cluster **(4)** however, there are six S^{2-} ions in the core which allow for interstitial bonding and results in cluster growth due to higher coordination modes. Since there is no direct source of S^{2-}, the potential source was investigated. A closer examination of the preparation of **(1)** using ^{1}H-NMR spectroscopy revealed the presence of unreacted $[Me_3SiS]^-$ which could explain the source of S^{2-}. However, subsequent reactions with and without any $[Me_3SiS]^-$ present in the reaction solution still resulted in crystals of **(4)** and **(5)**. It is also possible that **(4)** is the thermodynamically stable product, where it is formed by the cleavage of $MS–CH_2Fc$ to allow for the formation of interstitial sulfides and $(FcCH_2)_2S$ as the byproduct. Such bond cleavage is not uncommon, clusters such as $[Ag_{70}S_{20}(SPh)_{28}(dppm)_{20}]$ (dppm = bis(diphenylphosphanyl)methane) , $[Ag_{123}S_{35}(S\textit{t}Bu)_{50}]$,[19] $[Ag_{30}Se_8(Se\textit{t}Bu)_{14}(P\textit{n}Pr_3)_8]$ and $[Ag_{90}Se_{38}(Se\textit{t}Bu)_{14}(PEt_3)_{22}]$ have all been prepared by the reaction of silver carboxylates with $RESiMe_3$ (E = S, Se; R = organic group) in the presence of tertiary phosphines. The byproduct $(FcCH_2)_2S$ can be screened for by gas chromatography and/or ^{1}H-NMR spectroscopy, and if the presence is confirmed then it would help confirm the bond cleavage mechanism for the formation of the interstitial sulfides.

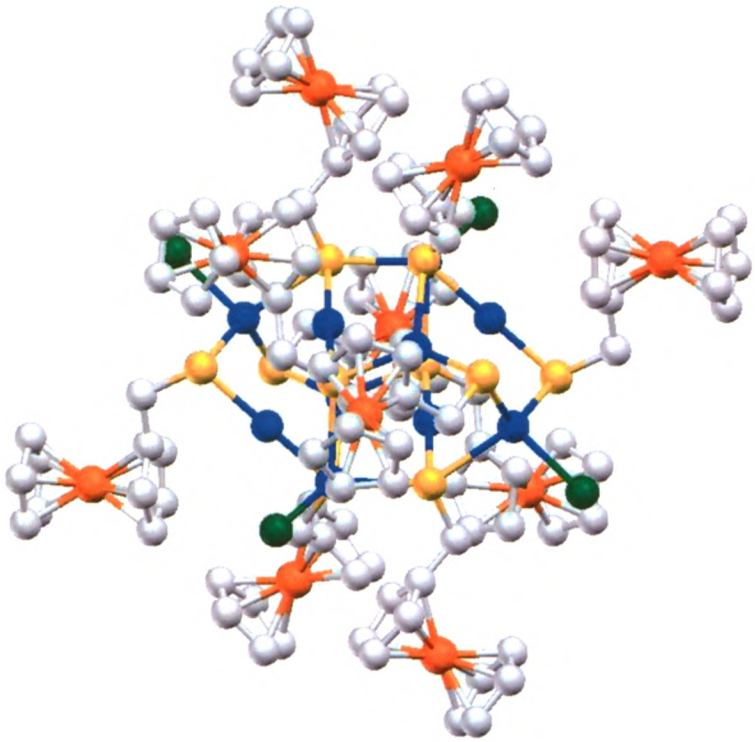

Figure 3.7 A ball and stick representation of $[Ag_{10}(SCH_2Fc)_{10}(PPh_3)_4]$ (**5**). Ag, Fe, S, P, C are represented by blue, orange, yellow, green and grey spheres, respectively. Phenyl groups and hydrogen atoms have been omitted for clarity.

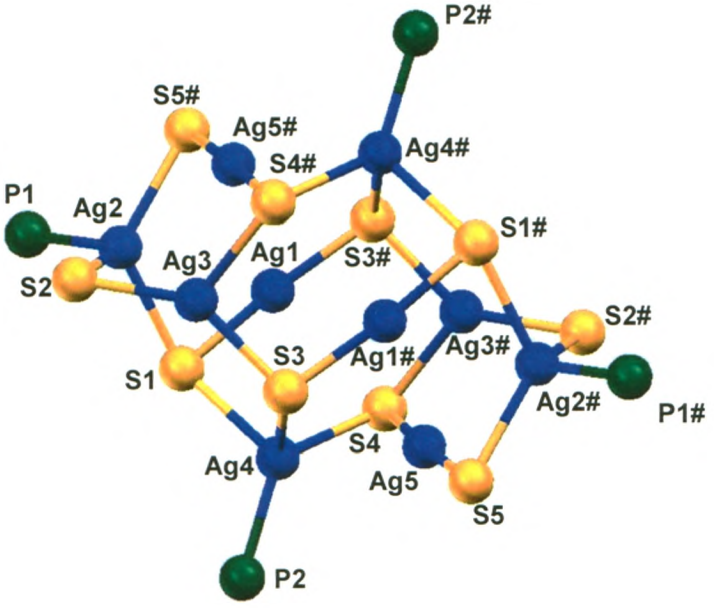

Figure. 3.8 A ball and stick representation of the $Ag_{10}S_{10}$ core of $[Ag_{10}(SCH_2Fc)_{10}(PPh_3)_4]$ **(5)**. Ag, S, P, are represented by blue, yellow, and green spheres, respectively. Phenyl groups and hydrogen atoms have been omitted for clarity.

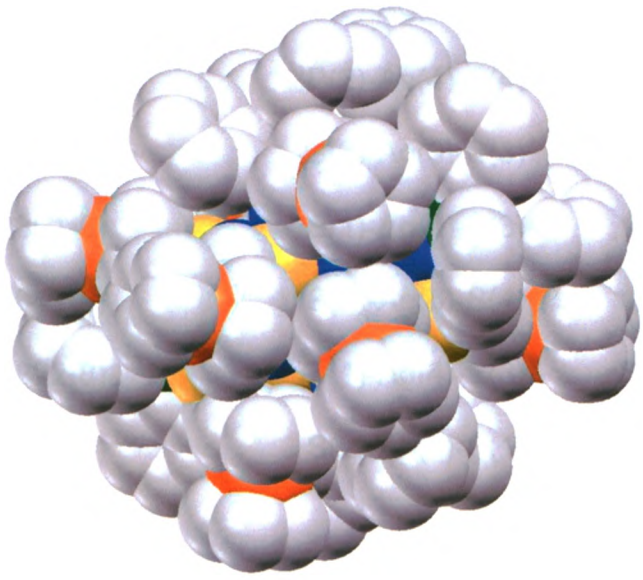

Figure 3.9 Space filling diagram of the molecular structure of $[Ag_{10}(SCH_2Fc)_{10}(PPh_3)_4]$ **(5)**. Ag, Fe, S, P, C are represented by blue, orange, yellow, green and grey spheres, respectively. Hydrogen atoms have been omitted for clarity.

Ag(5)-S(5)	2.373(2)	S(3)-Ag(3)-S(4)#1	100.15(6)
Ag(1)-S(1)	2.395(2)	P(1)-Ag(2)-S(5)#1	100.39(7)
Ag(1)-S(3)#1	2.401(2)	S(4)-Ag(4)-S(1)	100.65(6)
Ag(4)-P(2)	2.443(2)	S(4)-Ag(4)-S(3)	102.94(6)
Ag(4)-P(2)	2.443(2)	P(1)-Ag(2)-S(1)	103.33(7)
Ag(3)-S(3)	2.5170(18)	P(2)-Ag(4)-S(3)	113.57(7)
Ag(2)-P(1)	2.558(2)	P(1)-Ag(2)-S(2)	114.67(7)
Ag(2)-P(1)	2.558(2)	P(2)-Ag(4)-S(1)	116.56(7)
Ag(2)-S(2)	2.571(2)	S(2)-Ag(2)-S(5)#1	118.79(7)
Ag(2)-S(5)#1	2.635(2)	S(5)#1-Ag(2)-S(1)	120.76(6)
Ag(4)-S(4)	2.6470(19)	S(2)-Ag(3)-S(4)#1	120.77(7)
Ag(4)-S(3)	2.726(2)	P(2)-Ag(4)-S(4)	127.54(6)
Ag(5)-Ag(3)#1	2.9174(9)	S(2)-Ag(3)-S(3)	138.97(7)
Ag(4)-Ag(5)	2.9851(9)	S(1)-Ag(1)-S(3)#1	172.83(6)
Ag(1)-Ag(2)	3.0811(8)	S(5)-Ag(5)-S(4)	176.16(7)
Ag(5)-Ag(1)#1	3.1822(8)	S(1)-Ag(4)-S(3)	87.75(6)
Ag(2)-Ag(5)#1	3.2547(9)	S(2)-Ag(2)-S(1)	98.62(6)
Ag(1)-Ag(3)	3.2820(8)		

Table 3.2 Selected intramolecular bond lengths [Å] and angles [°] for (**5**).

Figure 3.10, 3.11 and 3.12 illustrate the molecular structure of $[Ag_{10}(SeCH_2Fc)(PPh_3)_3]$ **(6)** that was satisfactorily solved and refined in the monoclinic space group C2/c. The Ag-Se framework can be described as consisting of four and eight membered rings (Fig. 3.11). There are four μ_2 and four μ_3 bridging selenolate ligands ($^-SeCH_2Fc$) with Ag–Se distances ranging from 2.594(1)–2.621(1) Å and 2.632(1)–2.665(1) Å respectively. The Ag–Se bond distances are within range of similarly sized AgSe clusters: $[Ag_8(2,4,6\text{-}Pr^i_3C_6H_2Se)_8]$ [only μ_2: 2.465(1)–2.526(1) Å][21] and $[Ag_8(Se_2Fc)_4(PnPr_3)_4]$ [μ_2: 2.478(2)–2.633(2) Å; μ_3: 2.504(3)–2.933(3) Å].[22] Comparing the coordination geometry about the Ag centres of both $[Ag_8(2,4,6\text{-}Pr^i_3C_6H_2Se)_8]$ and $[Ag_8(Se_2Fc)_4(PnPr_3)_4]$ with **(6)**, where distorted linear to tetrahedral geometries are observed for the first two clusters, in **(6)** all Ag atoms are exclusively in a distorted trigonal planar geometry (Fig. 3.11). Four Ag centres are bonded to one μ_2-Se and two μ_3-Se atoms, and the other four are bonded to two $\mu_{2/3}$-Se atoms and one triphenylphosphine ligand. Ag–Ag contact distances in **(6)** are all greater than 2.87 Å where no significant bonding interactions are present. Selected bond lengths and angles for **(6)** are summarized in Table 3.3.

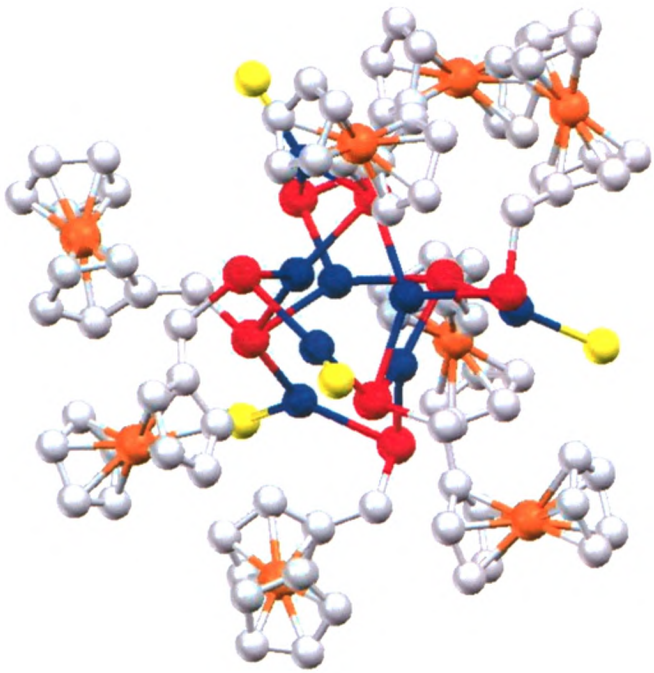

Figure 3.10 A ball and stick representation of the molecular structure of $[Ag_8(SeCH_2Fc)_8(PPh_3)_4]$ **(6)**. Ag, Fe, Se, P, C are represented by blue, orange, red, yellow and grey spheres, respectively. Phenyl groups and hydrogen atoms have been omitted for clarity.

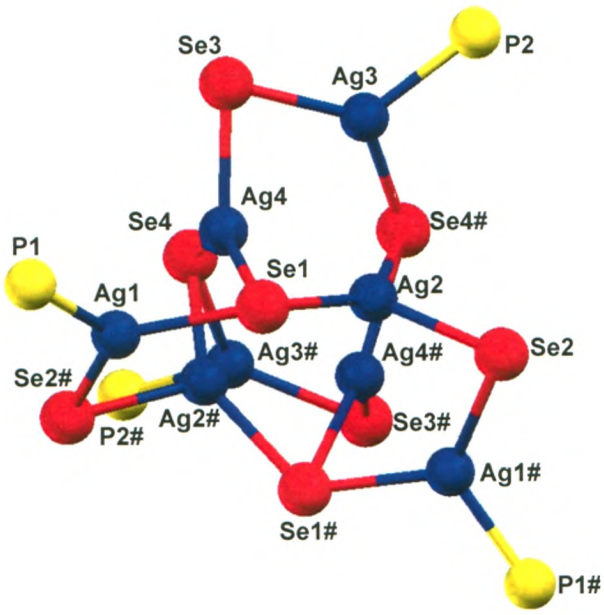

Figure. 3.11 A ball and stick representation of the Ag_8Se_8 core of $[Ag_8(SeCH_2Fc)_8(PPh_3)_4]$ **(6)**. Ag, P, and Se, are represented by blue, yellow and red spheres, respectively. Phenyl groups and hydrogen atoms have been omitted for clarity.

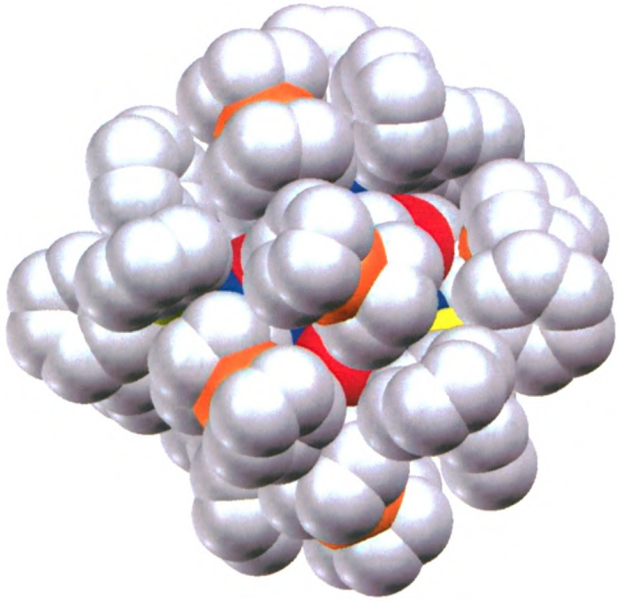

Figure 3.12 Space filling diagram of the molecular structure of $[Ag_8(SeCH_2Fc)_8(PPh_3)_4]$ **(6)**. Ag, Fe, Se, P, C are represented by blue, orange, red, yellow and grey spheres, respectively. Hydrogen atoms have been omitted for clarity.

Ag(1)-P(1)	2.466(3)	Ag(1)#1-Se(2)-Ag(2)	80.02(4)
Ag(3)-P(2)	2.488(3)	Ag(3)#1-Se(4)-Ag(2)#1	75.19(4)
Ag(3)-Se(3)	2.5938(14)	Ag(3)-Se(3)-Ag(4)	75.09(4)
Ag(1)-Se(2)#1	2.5958(15)	Ag(1)-Se(1)-Ag(4)	72.79(4)
Ag(4)-Se(3)	2.6085(13)	Ag(2)-Se(1)-Ag(4)	66.35(3)
Ag(2)-Se(2)	2.6211(13)	Se(4)-Ag(4)-Se(1)	140.40(4)
Ag(2)-Se(1)	2.6323(13)	Se(1)-Ag(2)-Se(4)#1	139.70(4)
Ag(3)-Se(4)#1	2.6339(13)	Ag(2)-Se(1)-Ag(1)	127.59(5)
Ag(2)-Se(4)#1	2.6397(12)	Se(3)-Ag(3)-Se(4)#1	125.72(5)
Se(4)-Ag(2)#1	2.6398(12)	P(1)-Ag(1)-Se(2)#1	123.17(9)
Ag(1)-Se(1)	2.6442(15)	Se(2)#1-Ag(1)-Se(1)	123.15(5)
Ag(4)-Se(4)	2.6635(13)	P(2)-Ag(3)-Se(3)	122.25(8)
Ag(4)-Se(1)	2.6653(12)	P(1)-Ag(1)-Se(1)	113.42(9)
Ag(2)-Ag(4)#1	2.8729(11)	Se(2)-Ag(2)-Se(1)	111.57(4)
Ag(2)-Ag(4)	2.8989(11)	P(2)-Ag(3)-Se(4)#1	111.51(8)
Ag(1)-Ag(4)	3.1503(11)	Se(3)-Ag(4)-Se(4)	110.34(4)
Ag(3)-Ag(4)	3.1700(12)	Se(3)-Ag(4)-Se(1)	109.16(4)
Ag(2)-Ag(3)	3.2173(11)	Se(2)-Ag(2)-Se(4)#1	107.83(4)
Ag(1)-Ag(2)#1	3.3539(11)		

Table 3.3 Selected intramolecular bond lengths [Å] and angles [°] for (**6**).

3.4.3. Electrochemistry of $[Cu_3(FcCH_2S)_3(PPh_3)_3]$ (3), $[Ag_{48}S_6(FcCH_2S)_{36}]$ (4)

Electrochemical measurements were obtained using a BAS 100W version 2.0 Electrochemical Analyzer potentiostat interfaced to a personal computer using BAS 100W version 2.0 software. A standard 3-electrode arrangement was used with a Pt working electrode, platinum flag counter electrode, and silver wire reference electrode in tetrahydrofuran with Bu_4NPF_6 (0.1M) as the supporting electrolyte for both (3) and (4). Scan rates were run between 50 and 200 mV/s at room temperature in an inert atmosphere glovebox. All potentials are reported versus S.C.E. and were referenced internally to ferrocene (E^o = 0.528 V),[12] added at the end of the experiment.

Cyclic voltammetry was used to investigate the redox activity of the iron centres and any iron-chalcogen communication in (3) and (4). The cyclic voltammograms are shown in figures 3.13 and 3.14 for (3) and (4), respectively. For (3), a single quasi-reversible oxidation wave was observed at all scan rates with ΔE_p ($E_{pa} - E_{pc}$) ranging from 227 mV for slower scan rates up to 347 mV at higher scan rates. The determined peak cathodic/peak anodic current ratios for (3) were in the range of $0.91 < i_{pc}/i_{pa} < 1$, and the formal reduction potentials, $E^{o'} = (E_{pa} + E_{pc})/2 = E_{1/2}$ = 490 mV, were scan rate independent between 50 and 200 mV/s.

For (4), a single quasi-reversible oxidation wave was observed at all scan rates with ΔE_p = 339 – 655 mV. Figure 3.14 shows the votammograms for (4) where $E_{1/2}$ values remained relatively constant ranging between 466 to 495 mV at all scan rates. The i_{pc}/i_{pa} ratios range between 0.78 and 0.90.

The ΔE values for (**3**) and (**4**) suggest that the oxidation of the ferrocenyl units are electrochemically irreversible, but the shape of the voltammograms shows that they are chemically reversible at all scan rates and suggests that the cluster framework remains intact. The values for i_{pa}:i_{pc} should be 1 for a simple reversible couple,[23] and values found were close to or in the range thereof for (**3**). Greater deviations from the ideal values for a reversible electronic process are observed for (**4**). Large ΔE values are typically indicative of simple irreversible electronic species, however, as the number of identical redox sites increases, a significant amount of overlapping concentrations of partially reduced species results in the broadening of the voltammogram and greater separation between reduction potentials.[24] Furthermore, slower diffusion, because of the large size of the compound, to the electrode surface, solvent and electrolyte used all have an effect on the reduction potentials. The presence of a single reversible oxidation wave implies that the ferrocenyl units are oxidized independently at similar potentials and that the alkyl spacer helps prevent any communication between redox centres and chalcogen atoms

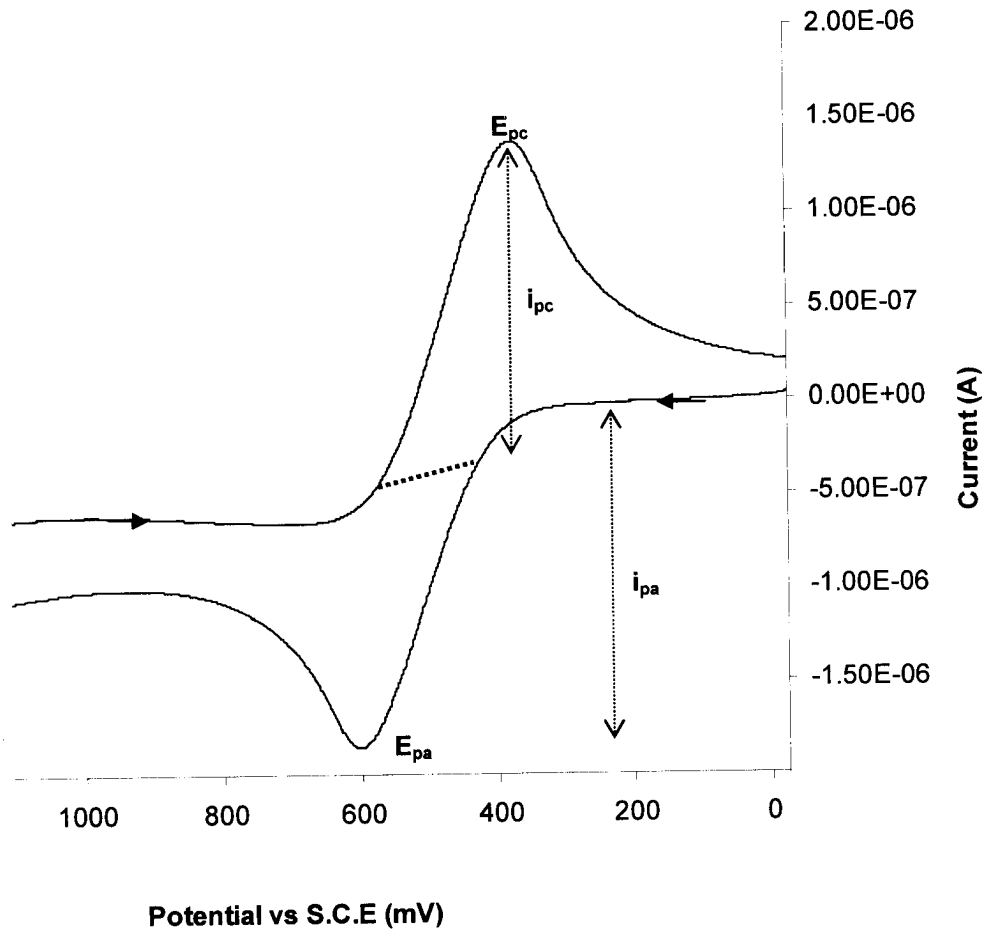

Figure 3.13 Cyclic voltammogram of **(3)** (0.5 mM) in dry THF and Bu_4NPF_6 (0.1M) as the supporting electrolyte at a scan rate of 50 mV/s.

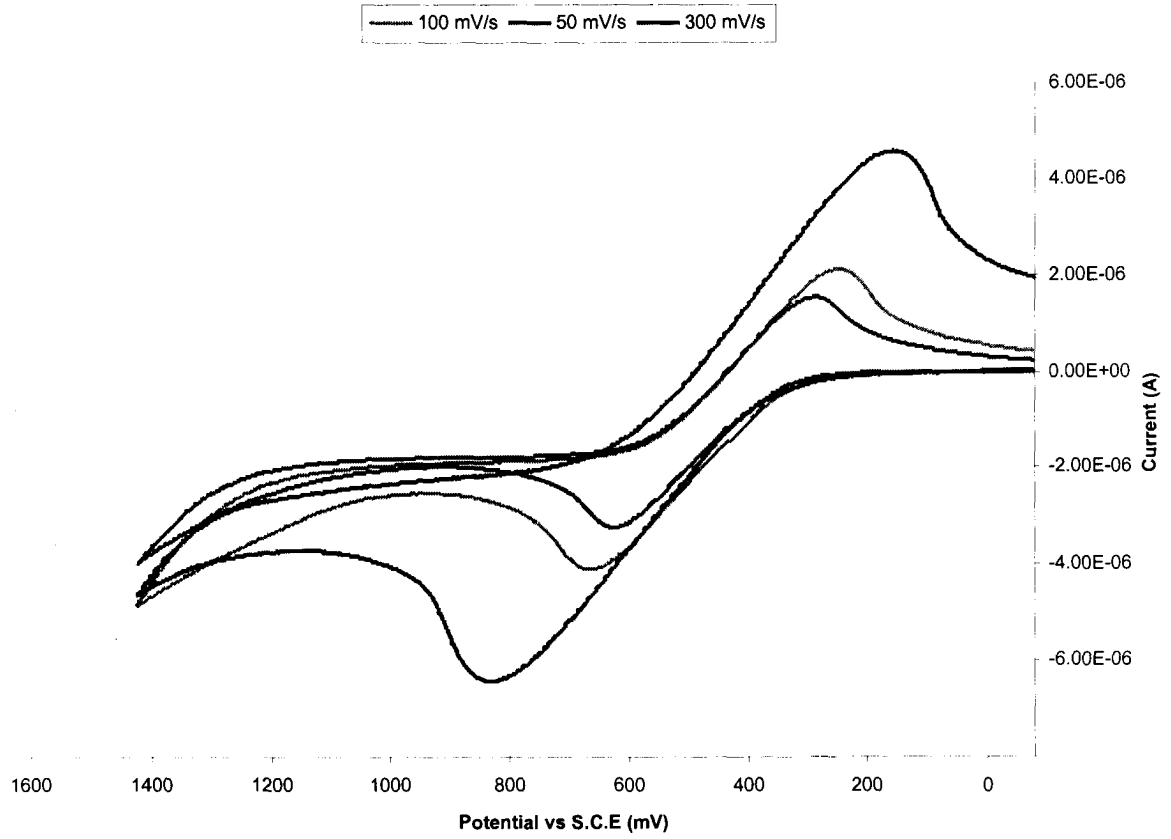

Figure 3.14 Cyclic voltammogram for **(4)** (0.2 mM) in dry THF and Bu_4NPF_6 (0.1M) as the supporting electrolyte. Potential in mV is shown on the horizontal axis and current in A is shown on the vertical axis.

3.5. References for Chapter 3

1) Nakashima, S.; Nakazaki, S.; Sakai, H.; Watanabe, M.; Motoyama, I.; Sato, M. *Inorg. Chem.,* **1998**, 37, 1959.

2) G. R. Newkome, E. He and C. N. Moorefield, *Chem. Rev.*, **1999**, 99,1689.

3) Canales, S.; Crespo, O.; Fortea, A.; Gimeno, C. M.; Jones, P. G.; Laguna, A. *Dalton Trans.* **2002**, 2250.

4) H. Krautscheid, H.; Fenske, D.; Baum, G.; Semmelmann, M. *Angew. Chem., Int. Ed. Engl.*, **1993**, 32, 1303.

5) Wang, X. J.; Langetepe, T.; Persau, C.; Kang, B. S.; Sheldrick, G. M.; Fenske, D. *Angew. Chem. Int. Ed. Engl.* **2002**, 41, 3818.

6) Dehnen, S.; Fenske, D. *Chem. Eur. J.* **1996**, 2, 1407.

7) Devenson, A.; Dehnen, S.; Fenske, D. *Dalton Trans.* **1997**, 4491.

8) Schafer, A.; Fenske, D.; Ahlrichs, R. *Angew. Chem. Int. Ed. Engl.* **1994**, 33, 746.

9) Chandler R. R.; Coffer, J. L.; Atherton, S. J.; Snowden, P. T. *J. Phys. Chem. B* **1992**, 96, 2713.

10) Labande, A.; Ruiz, J.; Astruc, D. *J. Am. Chem. Soc.* **2002**, 124, 1782.

11) a) Wallbank, A. I.; Corrigan, J. F. *J. Cluster Sci.* **2004**, 225.; b) Nitschke, C.; Fenske, D.; Corrigan, J. F. *Inorg. Chem.* **2006**, 45, 9394.

12) Brown, M. J.; Corrigan, J. F. *J. Organomet. Chem.* **2004**, 689, 2872.

13) a) Lebold, T.P.; Stringle, D.L.; Workentin, M.S.; Corrigan, J.F.; *Chem. Commun.,* **2003**, 1398.; b) Borecki, A. Undergraduate Chemistry 490 Thesis, *The* University *of* Western Ontario, **2004**.

14) Pangborn, A. B.; Giardello, M. A.; Grubbs, R. H.; Rosen, R. K.; Timmers, F. J. *Oranometallics* **1996**, 15, 1518

15) Lopez-Dellamary, T.; Sampedro, J. A.; Fontes, C. M.; Ogura, T. *Transition Met. Chem.* **1978**, 3, 342.

16) Togni, A.; Rihs, G.; Blumer, R. E. *Organometallics* **1992**, 11, 613.

17) Dehnen, S.; Eichhöefer, A.; Fenske, D. *Eur. J. Inorg. Chem.* **2002**, 279.

18) Tang, K.; Xie, X.; Zhang, Y.; Zhao, X.; Jin, X. *Chem. Commun.* **2002**, 1024.

19) Anson, C. E.; Eichhöfer, A.; Issac, I.; Fenske, D.; Fuhr, O.; Sevillano, P.; Persau, C.; Stalke, D.; Zhang, J. *Angew. Chem. Int. Ed.* **2008**, 47, 1326.

20) Fenske, D.; Zhu, N.; Langetepe, T. *Angew. Chem. Int. Ed.* **1998**, 37, 2640.

21) Tang, K.; Jin, X.; Yan, H.; Xie, X.; Liu, C.; Gong, Q. *J. Chem. Soc., Dalton Trans.*, **2001**, 1374.

22) Nitschke, C.; Wallbank, A. I.; Fenske, D.; Corrigan, J. F. *J. Cluster. Sci.* **2007**, 18, 131.

23) Kissinger, P. T.; Heineman, R. W. *J. Chem. Educ.* **1983**, 60, 702.

24) Kaifer, A. E.; Gomez-Kaifer, M. *Supramolecular Electrochemistry* Wiley-VCH: New York; Chichester; Brisbane; Singapore; Toronto, 89-92, 94-102.

Chapter 4

General Conclusions and Future Outlook

4.1 Summary

Nanometer-sized metal chalcogen clusters, "nanoclusters", make up small but quickly growing field of nanotechnology. In this subfield, the isolation and structural characterization of monodisperse products has allowed researchers to study the physical properties of semiconducting materials as a function of decreasing size.[1] Silylated chalcogen reagents, $E(SiMe_3)_2$ and $RESiMe_3$ (E = S, Se, Te; R = organic group), offer a soluble source of E^{2-} and/or RE^- and have been used extensively in the preparation of metal-chalcogen nanoclusters. The mild reaction conditions and wide range of reactivity of silylated reagents with transition metal salts have resulted in a series of novel group 10–12/16 clusters.[2-9] Reaction conditions are critical for the final product obtained and particularly dependent on the stoichiometry of starting reagents, temperature, solvent and steric effects of the solubilizing ligand, $PR'R_2$.[2-9] Further structural diversity can be introduced to the surface of metal chalcogen clusters by varying the R group of chalcogenolate reagents $RESiMe_3$, where R is an organic group. The reagents $Fe(\eta^5\text{-}C_5H_4ESiMe_3)_2$[4,6,8] and $CpFe(\eta^5\text{-}C_5H_4ESiMe_3)$[9] (E = S, Se) have been recently reported and used to passivate the surface of metal chalcogen clusters. The ferrocenyl units help stabilize the cluster core from further random condensation, but more importantly, they functionalize the surface with redox active centres. Electrochemical studies of the clusters obtained from the silylated chalcogenolate reagents, $Fe(\eta^5\text{-}C_5H_4ESiMe_3)_2$ and $CpFe(\eta^5\text{-}C_5H_4ESiMe_3)$ (E = S,

Se), all resulted in cluster degradation as a result of oxidative cleavage of the ferrocenylchalcogenide. The degradation of cluster was attributed to the instability of the oxidized ferrocenyl unit ($Fe^{II} \rightarrow Fe^{III}$) communicating with the chalcogen atom and resulted in the formation of the stable di(ferrocenylchalcogenide) [FcEEFc or $(FcE_2)_2$; E = S, Se].[6,8,9] Communication between iron centres and chalcogen atoms can be eliminated by alkyl or aryl spacers.[10,11] Therefore, in order to study the electronic properties of ferrocenyl passivated metal-chalcogen cluster, silylated ferrocenyl chalcogenolate reagents with an alkyl spacer, $-CH_2-$ were prepared and used in the synthesis of novel metal-chalcogen clusters: $[Cu_3(SCH_2Fc)_3(PPh_3)_3]$ **(3)**, $[Ag_{48}S_6(SCH_2Fc)_{36}]$ **(4)** and $[Ag_{10}(SCH_2Fc)_{10}(PPh_3)_4]$ **(5)** and $[Ag_8(SeCH_2Fc)_8(PPh_3)_4]$ **(6)**.

The successful preparation of ferrocenylmethylchalcogenolates ligands , $CpFe(\eta^5\text{-}C_5H_4CH_2ESiMe_3$ (E = S **(1)**, Se **(2)**), are prepared directly from ferrocene as outlined in chapter 2. Long term storage of **(1)** and **(2)** proved to be difficult even in the solid state, where **(1)** and **(2)** slowly decompose to $(FcCH_2E)_2$ within a week. Therefore, **(1)** and **(2)** were generated in situ and reacted immediately with metal salts as described in chapter 3.

Single crystals of $[Cu_3(SCH_2Fc)_3(PPh_3)_3]$ **(3)**, $[Ag_{48}S_6(SCH_2Fc)_{36}]$ **(4)** and $[Ag_{10}(SCH_2Fc)_{10}(PPh_3)_4]$ **(5)** and $[Ag_8(SeCH_2Fc)_8(PPh_3)_4]$ **(6)** were obtained and allowed for the satisfactory refinement of their molecular structure. With respect to their structural frameworks, these cluster exhibit characteristic coordinations for group 11 metals, ranging from linear to tetrahedral geometries. Also, typical bridging modes were observed for the chalcogen atoms, μ_2 to μ_4. The most

notable structural feature was observed in (**4**), where thirty-six ferrocenylmethyl groups exclusively stabilize a $Ag_{48}S_{42}$ core. To date, (**4**) is the largest cluster with the greatest number of ferrocenyl units to be structurally characterized. Electrochemical studies were conducted on the (**3**) and (**4**) and revealed that the alkyl spacer prevented oxidative cleavage previously observed for $Fe(\eta^5\text{-}C_5H_4ESiMe_3)_2$ and $CpFe(\eta^5\text{-}C_5H_4ESiMe_3)$. Single pseudo-reversible peaks were observed at all scan rates and after repetitive cycles which suggests that metal chalcogen framework remain intact. Future electrochemical studies on (**5**) and (**6**) remain to be examined. In addition, in CV experiments, electrolyte and solvent both have an effect on the shape of the voltammogram, where single broad reversible peaks become resolved into two peaks by changing the electrolyte.[11] Therefore, these variables need to be addressed to have a comprehensive understanding of the insulating effects of the alkyl spacer and reversibility of the ferrocenyl units.

Thus, the synthesis and reactivity of (**1**) and (**2**) towards the formation of metal-chalcogen bonds has been discussed in this thesis. The isolation and characterization of group 11/16 clusters, (**3**), (**4**), (**5**) and (**6**), further illustrates the utility and applicability of silylated chalcogen reagents, $-ESiMe_3$. By changing the reaction conditions, for example the temperature, solvent and tertiary phosphine used, it should be possible to isolate ME clusters (M = group 10-12 transition metal; E = S, Se) of different sizes and number of ferrocenyl units. Also, the

ferrocenyl chalcogen reagents with longer alkyl spacers, amide and ester spacers are currently be pursued, where the latter have been prepared and their reactivity is currently being investigated. Future work of ferrocenyl chalcogen reagents will be directed at use of these reagents in formation of a series metal-chalcogen clusters with surface ferrocenyl groups that can be used in ion sensing studies and optical studies.

4.2. References for Chapter 4

1) Soloviev, V. N., Eichhöfer, A., Fenske, D., Banin, U. *J. Am. Chem. Soc.* **2001**, 123, 2354.

2) Fenske, D.; Ohmer, J.; Hachgenei J. *Angew. Chem. Int. Ed. Engl.* **1985**, 24, 993.

3) Dehnen, S.; Eichhöfer, A.; Fenske, D. *Eur. J. Inorg. Chem.* **2002**, 279.

4) a) Wallbank, A. I.; Borecki, A.; Taylor, N. J.; Corrigan, J. F. *Organometallics,* **2005**, 24, 788.; b) Nitschke, C.; Fenske, D.; Corrigan, J. F. *Inorg. Chem.* **2006**, 45, 9394.

5) Fenske, D.; Langetepe, T.; Kappes, M. M.; Hampe, O.; Weis, P. *Angew. Chem. Int. Ed.* **2000**, 39, 1857.

6) Nitschke, C.; Wallbank, A. I.; Fenske, D.; Corrigan, J. F. *J. Cluster. Sci.* **2007**, 18, 131.;

7) Chitsaz, S.; Fenske, D.; Fuhr, O. *Angew. Chem. Int. Ed.* **2006**, 45, 8055.

8) Brown, M. J.; Corrigan, J. F. *J. Organomet. Chem.* **2004**, 689, 2872.

9) Lebold, T. P.; Stringle, D.L.; Workentin, M.S.; Corrigan, J. F.; *Chem. Commun.,* **2003**, 1398.

10) a) Ruiz, J.; Astruc, D. *J. Am. Chem. Comm.* **2002**, 124, 1782.; b) Astruc, D.; Daniel, M. C.; Ruiz, J.; *Chem. Comm.* **2004,** 23, 2637.; c) Burgess, M. R.; Jing, S.; Morley, C. P. *J. Organomet. Chem.,* **2006**, 691, 3484.

11) Davis, W. L.; Shago, F.; Langner, E.; Swarts, J. C. *Polyhedron,* **2005**, 24, 1611.; Labande, A.

APPENDIX A:

^{1}H-NMR Data for (**4**) and X-ray Crystallographic Data Parameters and Atomic Positions for (**3**), (**4**), (**5**) and (**6**).

APPENDIX A.1.

Crystal data and structure refinement for $[Cu_3(SCH_2Fc)_3(PPh_3)_3]$ **(3)**

Empirical formula	$C_{90}\ H_{81}\ Cl_9\ Cu_3\ Fe_3\ P_3\ S_3$	
Formula weight	2028.86	
Temperature	150(2) K	
Wavelength	0.71073 Å	
Crystal system	Triclinic	
Space group	P-1	
Unit cell dimensions	a = 16.617(2) Å	α= 103.077(6)°
	b = 22.427(2) Å	β = 107.624(4)°.
	c = 25.705(3) Å	γ = 91.818(6)°.
Volume	8841.1(17) $Å^3$	
Z	4	
Density (calculated)	1.524 Mg/m^3	
Absorption coefficient	1.630 mm^{-1}	
F(000)	4128	
Crystal size	0.48 x 0.30 x 0.08 mm^3	
Theta range for data collection	2.15 to 25.00°.	
Index ranges	-19<=h<=18, -22<=k<=26, -30<=l<=22	
Reflections collected	30249	
Independent reflections	22344 [R(int) = 0.0693]	
Completeness to theta = 25.00°	71.8 %*	
Absorption correction	None	
Max. and min. transmission	0.8807 and 0.5084	
Refinement method	Full-matrix-block least-squares on F^2	
Data / restraints / parameters	22344 / 190** / 1857	
Goodness-of-fit on F^2	0.944	
Final R indices [I>2sigma(I)]	R1 = 0.0803, wR2 = 0.1832	
R indices (all data)	R1 = 0.2044, wR2 = 0.2186	
Largest diff. peak and hole	1.099 and -0.899 $e.Å^{-3}$	

*The weakly diffracting nature of the crystal limited the number of data that could be indexed.

**Disordered Cp rings were refined as rigid groups with constrained Fe-C distances (SADI command).

Atomic coordinates (x 10^4) and equivalent isotropic displacement parameters ($Å^2$x 10^3) for **(3)**. U(eq) is defined as one third of the trace of the orthogonalized U^{ij} tensor.

	x	y	z	U(eq)
Cu(11)	-1966(1)	-3263(1)	2035(1)	38(1)
Cu(21)	-732(1)	-3366(1)	3318(1)	34(1)
Cu(31)	-2427(1)	-4198(1)	2776(1)	44(1)
Fe(11)	-2074(1)	-687(1)	3110(1)	37(1)
Fe(21)	883(1)	-4626(1)	1999(1)	53(1)
Fe(31)	-5794(2)	-4042(1)	991(1)	62(1)
Fe(3A)	-5874(8)	-3817(5)	1385(5)	68(3)
S(11)	-1666(2)	-2765(1)	2931(1)	36(1)
S(21)	-1081(2)	-4407(1)	2995(1)	42(1)
S(31)	-2897(2)	-4116(1)	1887(1)	41(1)
P(11)	-1823(2)	-3033(1)	1277(1)	40(1)
P(21)	444(2)	-2986(1)	4041(1)	36(1)
P(31)	-3007(2)	-4098(1)	3449(1)	40(1)
C(11)	-1216(7)	-1954(4)	3094(4)	37(3)
C(21)	-1863(8)	-1576(4)	2805(4)	29(3)
C(31)	-2712(8)	-1551(4)	2813(5)	36(3)
C(41)	-3103(8)	-1152(5)	2478(5)	42(3)
C(51)	-2516(8)	-944(5)	2263(5)	41(4)
C(61)	-1734(8)	-1207(5)	2456(5)	38(3)
C(71)	-1286(8)	-380(5)	3920(5)	37(3)
C(81)	-2139(9)	-364(5)	3903(5)	47(4)
C(91)	-2502(9)	43(5)	3559(5)	50(4)
C(101)	-1855(9)	261(5)	3368(5)	46(4)
C(111)	-1088(8)	1(5)	3602(5)	44(3)
C(121)	-801(8)	-4569(5)	2341(5)	41(3)
C(131)	97(8)	-4412(6)	2475(5)	43(3)
C(141)	493(11)	-3890(6)	2416(6)	71(5)
C(151)	1429(11)	-3893(7)	2658(7)	76(5)
C(161)	1464(12)	-4419(9)	2822(7)	88(6)
C(171)	744(11)	-4749(8)	2750(7)	83(5)
C(181)	186(11)	-5188(8)	1249(6)	76(5)
C(191)	495(15)	-4623(10)	1188(7)	107(7)
C(201)	1354(16)	-4542(9)	1410(8)	104(7)
C(211)	1626(11)	-5066(10)	1579(7)	96(6)
C(221)	899(15)	-5471(7)	1505(7)	96(6)
C(231)	-3885(8)	-3761(5)	1750(5)	57(4)
C(241)	-4567(6)	-4203(5)	1297(5)	60(5)
C(251)	-5125(7)	-4676(5)	1337(5)	69(5)
C(261)	-5677(7)	-4959(4)	782(5)	70(5)
C(271)	-5461(7)	-4661(5)	399(4)	75(5)
C(281)	-4775(7)	-4194(5)	718(5)	64(5)
C(291)	-5925(9)	-3220(5)	1476(5)	70(5)
C(301)	-6481(8)	-3700(6)	1499(5)	86(6)
C(311)	-7023(6)	-3968(5)	942(6)	91(7)
C(321)	-6801(7)	-3654(5)	575(5)	69(5)
C(331)	-6122(9)	-3192(4)	905(5)	76(10)
C(24A)	-5770(30)	-4667(8)	970(15)	60(20)
C(25A)	-5050(30)	-4331(17)	1070(20)	52(18)
C(26A)	-4710(16)	-4131(19)	1620(20)	70(20)
C(27A)	-5220(30)	-4342(18)	1859(13)	70(20)
C(28A)	-5880(30)	-4673(12)	1457(17)	110(30)

C(29A)	-6320(40)	-3238(19)	883(18)	130(60)
C(30A)	-5760(30)	-2910(9)	1400(20)	25(13)
C(31A)	-6080(30)	-2994(13)	1818(16)	70(20)
C(32A)	-6840(30)	-3370(20)	1560(30)	130(40)
C(33A)	-6990(20)	-3530(20)	990(30)	80(20)
C(341)	-1624(8)	-3653(5)	732(5)	43(3)
C(351)	-1947(3)	-4222(2)	713(2)	59(4)
C(361)	-1876(3)	-4740(2)	265(2)	83(5)
C(371)	-1390(3)	-4624(2)	-52(2)	81(5)
C(381)	-1044(3)	-4006(2)	3(2)	59(4)
C(391)	-1174(3)	-3544(2)	396(2)	53(4)
C(401)	-1068(3)	-2400(2)	1345(2)	46(3)
C(411)	-1191(3)	-2006(2)	967(2)	49(4)
C(421)	-582(3)	-1539(2)	1046(2)	49(4)
C(431)	175(3)	-1431(2)	1509(2)	50(4)
C(441)	317(3)	-1813(2)	1885(2)	60(4)
C(451)	-312(8)	-2273(5)	1809(5)	45(3)
C(461)	-2821(8)	-2798(5)	904(5)	40(3)
C(471)	-3212(9)	-2397(5)	1226(5)	50(4)
C(481)	-3987(5)	-2175(4)	1015(5)	68(5)
C(491)	-4390(5)	-2418(4)	436(5)	73(5)
C(501)	-4040(5)	-2843(4)	86(5)	65(4)
C(511)	-3268(8)	-3024(6)	326(6)	53(4)
C(521)	1351(7)	-2772(5)	3849(5)	35(3)
C(531)	2150(9)	-2970(5)	4048(5)	45(4)
C(541)	2804(8)	-2782(5)	3880(5)	48(4)
C(551)	2695(8)	-2396(5)	3511(5)	47(4)
C(561)	1919(9)	-2189(5)	3325(5)	49(4)
C(571)	1257(8)	-2390(5)	3475(5)	46(4)
C(581)	874(6)	-3472(5)	4531(5)	27(3)
C(591)	1240(8)	-3230(5)	5095(5)	46(4)
C(601)	1555(8)	-3619(6)	5449(6)	55(4)
C(611)	1516(8)	-4239(6)	5209(7)	58(4)
C(621)	1146(8)	-4484(6)	4652(6)	58(4)
C(631)	830(8)	-4101(5)	4303(5)	50(4)
C(641)	336(8)	-2268(5)	4497(4)	30(3)
C(651)	-456(8)	-2118(5)	4492(5)	40(3)
C(661)	-601(8)	-1559(5)	4802(5)	38(3)
C(671)	86(9)	-1143(5)	5114(5)	39(3)
C(681)	895(8)	-1264(5)	5143(5)	37(3)
C(691)	1029(8)	-1823(5)	4828(5)	45(4)
C(701)	-3485(8)	-4834(5)	3480(6)	45(3)
C(711)	-3956(10)	-5229(6)	2994(6)	71(5)
C(721)	-4280(10)	-5806(7)	3002(7)	89(5)
C(731)	-4084(10)	-5965(6)	3539(8)	76(5)
C(741)	-3665(9)	-5562(6)	4013(7)	64(4)
C(751)	-3330(8)	-4985(6)	3992(6)	50(4)
C(761)	-3870(9)	-3617(5)	3398(5)	42(3)
C(771)	-4632(10)	-3763(6)	3483(6)	66(5)
C(781)	-5252(9)	-3379(7)	3408(7)	86(6)
C(791)	-5179(10)	-2863(7)	3236(6)	72(5)
C(801)	-4439(10)	-2707(6)	3152(6)	63(4)
C(811)	-3767(8)	-3074(5)	3225(5)	47(4)
C(821)	-2270(9)	-3812(5)	4157(5)	44(3)
C(831)	-2498(10)	-3412(5)	4584(6)	62(4)
C(841)	-1917(12)	-3257(6)	5143(6)	80(5)

C(851)	-1167(12)	-3520(6)	5252(7)	88(6)
C(861)	-960(9)	-3906(6)	4853(7)	60(4)
C(871)	-1509(8)	-4055(5)	4295(6)	50(4)
Cu(12)	2548(1)	1751(1)	2079(1)	39(1)
Cu(22)	4182(1)	1447(1)	3240(1)	35(1)
Cu(32)	2395(1)	800(1)	2837(1)	33(1)
Fe(12)	3095(1)	4245(1)	3526(1)	52(1)
Fe(22)	5023(1)	128(1)	1489(1)	43(1)
Fe(32)	-1218(1)	720(1)	1738(1)	36(1)
S(12)	3293(2)	2124(1)	2977(1)	39(1)
S(22)	3650(2)	442(1)	2878(1)	35(1)
S(32)	1737(2)	850(1)	1954(1)	34(1)
P(12)	2360(2)	2141(1)	1341(1)	42(1)
P(22)	5445(2)	1769(1)	3871(1)	35(1)
P(32)	2029(2)	1004(1)	3604(1)	32(1)
C(12)	3771(7)	2931(4)	3189(5)	43(4)
C(22)	3091(9)	3341(5)	3136(5)	47(4)
C(32)	2852(10)	3708(5)	2729(5)	77(5)
C(42)	2171(12)	4004(7)	2824(9)	114(9)
C(52)	1881(12)	3793(8)	3179(11)	123(10)
C(62)	2479(9)	3416(6)	3417(7)	67(4)
C(72)	4192(12)	4513(7)	4157(8)	87(6)
C(82)	4195(9)	4818(7)	3764(8)	82(5)
C(92)	3491(11)	5154(6)	3698(9)	109(8)
C(102)	3104(12)	5039(8)	4074(9)	100(8)
C(112)	3501(17)	4633(10)	4365(9)	134(10)
C(122)	3685(7)	253(5)	2155(5)	40(3)
C(132)	4540(8)	420(5)	2145(5)	38(3)
C(142)	4833(9)	924(5)	1968(5)	47(4)
C(152)	5710(9)	918(6)	2021(5)	54(4)
C(162)	5975(9)	413(6)	2229(5)	60(4)
C(172)	5292(8)	98(6)	2313(5)	48(4)
C(182)	4037(11)	-344(10)	847(7)	94(6)
C(192)	4432(14)	114(9)	673(7)	94(6)
C(202)	5263(11)	-9(8)	728(6)	80(5)
C(212)	5399(11)	-529(8)	950(6)	70(5)
C(222)	4664(14)	-732(7)	1033(7)	89(6)
C(232)	684(7)	1106(5)	1828(5)	38(3)
C(242)	51(7)	629(5)	1858(5)	32(3)
C(252)	-467(8)	145(5)	1429(5)	39(3)
C(262)	-952(7)	-170(5)	1672(5)	37(3)
C(272)	-784(7)	125(5)	2244(5)	38(3)
C(282)	-166(7)	635(5)	2366(5)	42(3)
C(292)	-1527(7)	1443(5)	1389(6)	40(3)
C(302)	-2128(7)	916(5)	1086(5)	32(3)
C(312)	-2501(8)	750(6)	1464(5)	47(4)
C(322)	-2141(8)	1162(6)	1991(6)	53(4)
C(332)	-1508(8)	1595(5)	1948(6)	46(4)
C(342)	1305(8)	2407(5)	1133(6)	47(4)
C(352)	988(11)	2636(6)	1566(7)	67(5)
C(362)	193(13)	2847(7)	1434(9)	91(6)
C(372)	-262(12)	2817(7)	880(11)	104(7)
C(382)	60(12)	2593(7)	452(8)	85(6)
C(392)	856(9)	2370(6)	576(7)	69(5)
C(402)	3063(9)	2806(5)	1394(5)	38(3)
C(412)	2743(9)	3316(6)	1213(5)	46(3)

C(422)	3335(10)	3804(7)	1262(6)	65(5)
C(432)	4179(11)	3768(6)	1439(6)	70(5)
C(442)	4493(9)	3244(6)	1611(6)	66(4)
C(452)	3911(10)	2787(6)	1589(5)	56(4)
C(462)	2425(7)	1616(5)	718(5)	35(3)
C(472)	2066(8)	1017(5)	593(5)	46(3)
C(482)	2100(9)	591(5)	115(6)	57(4)
C(492)	2512(8)	743(6)	-227(5)	50(4)
C(502)	2871(8)	1330(6)	-103(5)	49(4)
C(512)	2845(8)	1766(5)	366(5)	41(3)
C(522)	6239(8)	1946(5)	3554(5)	41(3)
C(532)	5963(8)	2279(5)	3143(5)	44(3)
C(542)	6539(10)	2462(6)	2894(6)	59(4)
C(552)	7338(9)	2291(6)	3032(6)	60(4)
C(562)	7580(9)	1938(6)	3423(6)	60(4)
C(572)	7029(9)	1766(5)	3682(5)	42(3)
C(582)	5938(7)	1264(5)	4326(5)	36(3)
C(592)	5730(7)	650(5)	4135(5)	45(3)
C(602)	6083(8)	270(5)	4474(6)	53(4)
C(612)	6631(8)	483(6)	4993(6)	54(4)
C(622)	6857(8)	1114(6)	5218(6)	56(4)
C(632)	6505(8)	1503(5)	4857(5)	46(3)
C(642)	5459(8)	2489(5)	4366(4)	30(3)
C(652)	4759(8)	2572(5)	4561(5)	42(3)
C(662)	4744(8)	3100(6)	4947(6)	50(4)
C(672)	5411(10)	3558(5)	5142(5)	51(4)
C(682)	6109(9)	3496(6)	4965(5)	49(4)
C(692)	6127(8)	2953(5)	4578(5)	36(3)
C(702)	1250(8)	1564(5)	3619(5)	32(3)
C(712)	629(8)	1505(5)	3863(5)	43(4)
C(722)	11(8)	1908(5)	3828(5)	41(3)
C(732)	9(8)	2359(5)	3527(5)	46(4)
C(742)	638(8)	2404(5)	3290(5)	33(3)
C(752)	1261(7)	2018(5)	3333(4)	35(3)
C(762)	1552(7)	319(5)	3724(5)	34(3)
C(772)	1148(7)	-160(5)	3249(5)	38(3)
C(782)	773(7)	-694(5)	3320(5)	43(3)
C(792)	794(7)	-727(5)	3841(6)	42(3)
C(802)	1181(7)	-264(5)	4316(6)	45(4)
C(812)	1564(7)	263(5)	4246(5)	33(3)
C(822)	2852(7)	1274(4)	4274(4)	24(3)
C(832)	2791(8)	1723(5)	4727(5)	41(3)
C(842)	3419(8)	1875(5)	5240(5)	44(3)
C(852)	4125(9)	1565(6)	5318(5)	49(4)
C(862)	4214(8)	1133(5)	4889(5)	41(3)
C(872)	3599(8)	970(5)	4374(5)	38(3)
C(1S)	-1155(8)	-5939(5)	3027(6)	56(4)
C(2S)	-3209(9)	-5707(5)	1228(5)	62(4)
C(3S)	-7998(13)	-2731(9)	1284(7)	129(7)
C(4S)	-9007(8)	-1056(6)	361(6)	64(4)
C(5S)	-4234(11)	945(6)	6851(6)	89(6)
C(6S)	-3592(1)	1912(1)	943(1)	82(5)
Cl(1S)	-1106(1)	-6541(1)	2495(1)	134(2)
Cl(2S)	-285(1)	-5874(1)	3638(1)	106(2)
Cl(3S)	-2089(1)	-6024(1)	3186(1)	86(1)
Cl(4S)	-4107(1)	-6131(1)	696(1)	101(2)

Cl(5S)	-2289(1)	-5851(1)	1106(1)	99(2)
Cl(6)	-3212(1)	-5842(1)	1872(1)	96(2)
Cl(7S)	-7866(1)	-1966(1)	1247(1)	185(3)
Cl(8S)	-8970(1)	-3062(1)	864(1)	177(3)
Cl(9S)	-7917(1)	-2729(1)	1999(1)	132(2)
Cl(10)	-9789(1)	-848(1)	-165(1)	122(2)
Cl(11)	-8175(1)	-1307(1)	105(1)	95(1)
Cl(12)	-8618(1)	-431(1)	948(1)	67(1)
Cl(13)	-3595(1)	1483(1)	7395(1)	157(3)
Cl(14)	-5336(1)	1046(1)	6755(1)	108(2)
Cl(15)	-4021(1)	901(1)	6227(1)	87(1)
Cl(16)	-3373(1)	2021(1)	339(1)	109(3)
Cl(16)	-3874(1)	1475(1)	292(1)	88(3)
Cl(17)	-4682(1)	1794(1)	841(1)	89(3)
Cl(17)	-4362(1)	2207(1)	1178(1)	133(4)
Cl(18)	-3210(1)	2585(1)	1454(1)	80(2)
Cl(18)	-2909(1)	2564(1)	910(1)	174(5)

APPENDIX A.2.

Crystal data and structure refinement for $[Ag_{48}S_6(SCH_2Fc)_{36}]$ **(4)**

Empirical formula	$C_{403.50}\ H_{407}\ Ag_{48}\ Cl_{15}\ Fe_{36}\ S_{42}$	
Formula weight	14322.92	
Temperature	200(2) K	
Wavelength	0.71073 Å	
Crystal system	Monoclinic	
Space group	C2/c	
Unit cell dimensions	a = 27.646(6) Å	α= 90°.
	b = 44.274(9) Å	β= 108.01(3)°.
	c = 43.101(9) Å	γ= 90°.
Volume	50171(17) $Å^3$	
Z	4	
Density (calculated)	1.896 Mg/m^3	
Absorption coefficient	3.122 mm^{-1}	
F(000)	27788	
Crystal size	0.25 x 0.18 x 0.12 mm^3	
Theta range for data collection	1.73 to 25.00°.	
Index ranges	-32<=h<=31, -52<=k<=52, -48<=l<=51	
Reflections collected	172079	
Independent reflections	44118 [R(int) = 0.1095]	
Completeness to theta = 25.00°	99.8 %	
Refinement method	Full-matrix-block least-squares on F^2	
Data / restraints / parameters	44118 / 1770** / 1400	
Goodness-of-fit on F^2	1.051	
Final R indices [I>2sigma(I)]	R1 = 0.0981, wR2 = 0.2918	
R indices (all data)	R1 = 0.2075, wR2 = 0.3356	
Largest diff. peak and hole	2.223* and -1.354 e.$Å^{-3}$	

* Un-resolved solvent peak

** Disordered Cp rings were refined with common Fe-C distances and the AFIX command. The atomic coordinates of one solvent molecule were fixed after locating in the difference Fourier map (occupancy = 0.5).

Atomic coordinates (x 10^4) and equivalent isotropic displacement parameters ($Å^2$x 10^3) for **(4)**. U(eq) is defined as one third of the trace of the orthogonalized U^{ij} tensor.

	x	y	z	U(eq)
Ag(1)	1444(1)	2073(1)	6550(1)	80(1)
Ag(2)	1069(1)	1443(1)	6361(1)	77(1)
Ag(3)	1723(1)	2715(1)	6786(1)	85(1)
Ag(4)	754(1)	838(1)	6713(1)	83(1)
Ag(5)	-307(1)	1693(1)	6212(1)	73(1)
Ag(6)	1132(1)	1670(1)	7074(1)	79(1)
Ag(7)	637(1)	2469(1)	6768(1)	73(1)
Ag(8)	2003(1)	2452(1)	7657(1)	84(1)
Ag(10)	-354(1)	1226(1)	6703(1)	86(1)
Ag(11)	-208(1)	2067(1)	6829(1)	64(1)
Ag(12)	1051(1)	2066(1)	7616(1)	65(1)
Ag(13)	1248(1)	2918(1)	7711(1)	79(1)
Ag(14)	697(1)	3553(1)	7437(1)	87(1)
Ag(16)	-711(1)	1217(1)	7317(1)	71(1)
Ag(17)	-1236(1)	1708(1)	6507(1)	75(1)
Ag(18)	0	1735(1)	7500	62(1)
Ag(19)	0	2404(1)	7500	63(1)
Ag(20)	1541(1)	2419(1)	8252(1)	78(1)
Ag(21)	294(1)	2925(1)	7947(1)	76(1)
Ag(22)	955(1)	3497(1)	8163(1)	86(1)
Ag(24)	-60(1)	3462(1)	8283(1)	86(1)
Ag(25)	-1178(1)	3297(1)	8028(1)	91(1)
Ag(9)	-34(2)	606(2)	7013(2)	61(2)
Ag(15)	-1144(2)	679(1)	6834(1)	66(1)
Ag(23)	-1285(4)	704(2)	7522(3)	64(2)
Ag(9A)	176(2)	574(2)	7080(2)	62(2)
Ag(1A)	-952(2)	609(2)	6935(2)	67(1)
Ag(2A)	-1130(4)	652(3)	7595(3)	73(2)
Fe(1)	2744(2)	1481(1)	5627(1)	131(1)
Fe(3)	93(1)	-605(1)	6839(1)	111(1)
Fe(5)	296(1)	2176(1)	5227(1)	84(1)
Fe(7)	3188(2)	3481(1)	7019(1)	153(2)
Fe(8)	908(2)	3648(1)	5793(1)	166(2)
Fe(10)	-1399(2)	139(1)	5729(1)	122(1)
Fe(12)	-1808(1)	1296(1)	4993(1)	87(1)
Fe(13)	-2947(1)	1248(1)	6535(1)	105(1)
Fe(14)	1526(1)	2922(1)	9350(1)	81(1)
Fe(15)	3782(1)	2959(1)	8590(1)	141(2)
Fe(16)	2576(1)	4093(1)	8269(1)	108(1)
Fe(17)	1087(2)	4374(1)	9116(1)	164(2)
Fe(18)	812(2)	4782(1)	7184(2)	199(2)
Fe(2)	2720(3)	2738(1)	5670(2)	71(2)
Fe(4)	-2754(2)	572(1)	8120(2)	89(2)
Fe(6)	3482(3)	1870(2)	7259(2)	117(2)
Fe(9)	-2409(3)	-219(2)	6801(2)	119(3)
Fe(11)	725(2)	679(1)	5443(1)	58(2)
Fe(2A)	2977(4)	2637(2)	5773(2)	125(3)
Fe(4A)	-2382(3)	424(2)	8211(2)	113(2)
Fe(6A)	3581(2)	2041(2)	7321(2)	82(2)
Fe(9A)	-2639(2)	-140(1)	6736(1)	70(2)
Fe(11)	494(3)	691(1)	5363(2)	68(2)

S(1)	1920(2)	1598(1)	6437(1)	81(1)
S(2)	1575(2)	2549(1)	6244(1)	86(2)
S(3)	240(3)	369(1)	6587(2)	125(3)
S(4)	-1417(2)	1103(1)	7836(1)	77(1)
S(5)	423(2)	2084(1)	6342(1)	67(1)
S(6)	1799(2)	2051(1)	7200(1)	70(1)
S(7)	1907(2)	2936(1)	7317(1)	82(1)
S(8)	458(2)	3029(1)	6561(1)	80(1)
S(9)	-929(2)	269(1)	7296(2)	111(2)
S(10)	-1145(2)	978(1)	6443(2)	108(2)
S(11)	248(2)	1218(1)	6268(1)	70(1)
S(12)	-1198(2)	1847(1)	5979(1)	80(1)
S(13)	-1284(2)	1618(1)	7049(1)	62(1)
S(14)	716(2)	2516(1)	8304(1)	65(1)
S(15)	2364(2)	2301(1)	8230(1)	84(1)
S(16)	1662(2)	3177(1)	8215(1)	85(1)
S(17)	341(3)	3876(1)	8101(2)	112(2)
S(18)	1373(2)	3779(1)	7283(1)	98(2)
S(19)	0	3274(1)	7500	69(2)
S(20)	0	868(1)	7500	62(2)
S(21)	752(2)	2536(1)	7350(1)	66(1)
S(22)	-233(2)	1603(1)	7979(1)	65(1)
C(1)	1954(7)	1628(4)	6005(5)	78(5)
C(2)	2453(8)	1549(5)	6029(5)	96(6)
C(3)	2918(12)	1748(7)	6078(8)	166(11)
C(4)	3341(10)	1498(6)	6058(7)	129(8)
C(5)	3183(12)	1213(7)	6015(8)	158(10)
C(6)	2635(9)	1204(5)	6023(6)	125(8)
C(7)	2187(11)	1556(7)	5214(7)	153(10)
C(8)	2640(11)	1785(6)	5256(7)	151(10)
C(9)	3039(13)	1599(8)	5273(9)	174(12)
C(10)	2889(11)	1344(7)	5212(7)	144(10)
C(11)	2352(9)	1251(6)	5199(6)	123(8)
C(12)	2243(9)	2510(5)	6228(6)	116(7)
C(13)	2071(13)	2652(6)	5842(7)	110(20)
C(14)	2090(11)	2959(6)	5741(7)	65(9)
C(15)	2105(11)	2957(5)	5411(6)	87(11)
C(16)	2095(11)	2648(5)	5308(6)	68(9)
C(17)	2074(12)	2459(5)	5575(7)	62(9)
C(18)	3283(16)	2990(9)	5560(10)	131(18)
C(19)	3341(17)	3007(8)	5915(11)	130(18)
C(20)	3368(18)	2693(9)	6043(9)	134(19)
C(21)	3326(15)	2482(7)	5767(9)	83(11)
C(22)	3273(15)	2665(9)	5469(8)	128(18)
C(13A)	3490(20)	2860(11)	6016(13)	160(20)
C(14A)	3499(19)	2546(12)	6122(11)	150(20)
C(15A)	3504(17)	2351(9)	5850(12)	160(20)
C(16A)	3504(15)	2545(10)	5575(10)	113(15)
C(17A)	3498(19)	2859(10)	5678(12)	180(30)
C(18A)	2541(12)	2886(7)	5570(8)	73(10)
C(19A)	2403(13)	2886(6)	5837(7)	97(13)
C(20A)	2256(13)	2609(7)	5882(7)	66(10)
C(21A)	2304(15)	2438(7)	5641(9)	120(20)
C(22A)	2479(14)	2609(8)	5448(9)	125(16)
C(23)	496(10)	15(6)	6709(7)	145(10)
C(24)	3(9)	-180(6)	6681(7)	78(5)

C(25)	-224(10)	-233(6)	6942(6)	78(5)
C(26)	-638(10)	-452(6)	6823(6)	78(5)
C(27)	-667(11)	-535(7)	6488(7)	78(5)
C(28)	-271(11)	-367(7)	6400(7)	78(5)
C(29)	803(11)	-724(7)	6943(8)	107(13)
C(30)	619(13)	-744(7)	7226(8)	130(20)
C(31)	220(11)	-973(7)	7157(7)	82(10)
C(32)	157(10)	-1095(6)	6832(7)	97(13)
C(33)	517(10)	-941(6)	6699(6)	69(9)
C(24A)	725(15)	-206(8)	7018(10)	108(13)
C(25A)	1005(15)	-529(9)	7163(12)	190(30)
C(26A)	673(16)	-690(8)	7378(11)	135(19)
C(27A)	187(15)	-467(9)	7365(10)	129(16)
C(28A)	219(16)	-168(9)	7143(12)	230(30)
C(29A)	241(12)	-741(8)	6482(9)	97(12)
C(30A)	35(16)	-1007(8)	6651(11)	150(20)
C(31A)	-498(19)	-907(12)	6682(13)	200(30)
C(32A)	-620(20)	-580(13)	6532(15)	220(40)
C(33A)	-165(18)	-477(9)	6408(12)	150(20)
C(34)	-2048(6)	1027(4)	7891(4)	77(5)
C(35)	-3501(16)	503(9)	7917(9)	150(20)
C(36)	-3379(16)	811(9)	7937(9)	150(20)
C(37)	-3158(12)	886(7)	8267(9)	84(11)
C(38)	-3142(16)	623(9)	8452(8)	210(40)
C(39)	-3354(15)	386(7)	8236(11)	105(14)
C(40)	-2149(12)	775(6)	7972(7)	74(10)
C(41)	-2361(14)	501(7)	7763(7)	124(16)
C(42)	-2354(13)	237(6)	7989(6)	160(20)
C(43)	-2138(8)	348(4)	8337(5)	22(5)
C(44)	-2012(11)	680(5)	8327(6)	79(11)
C(35A)	-3240(20)	439(14)	8066(13)	280(50)
C(36A)	-3020(20)	661(10)	8324(16)	150(20)
C(37A)	-2705(19)	500(13)	8611(12)	210(30)
C(38A)	-2720(19)	178(11)	8530(14)	180(20)
C(39A)	-3050(20)	141(11)	8193(14)	160(20)
C(40A)	-1920(10)	701(5)	8072(6)	54(8)
C(41A)	-2019(12)	425(7)	7895(7)	114(15)
C(42A)	-1859(14)	184(7)	8123(9)	126(16)
C(43A)	-1662(13)	311(7)	8440(8)	133(17)
C(44A)	-1700(11)	631(6)	8409(6)	78(10)
C(45)	284(6)	2291(4)	5936(4)	71(5)
C(46)	351(6)	2063(3)	5692(4)	65(4)
C(47)	-99(7)	1914(4)	5463(5)	87(5)
C(48)	147(8)	1733(5)	5253(6)	106(7)
C(49)	644(7)	1773(4)	5355(5)	89(6)
C(50)	782(7)	2000(4)	5622(5)	89(6)
C(51)	188(9)	2657(5)	5193(6)	102(6)
C(52)	-148(10)	2518(6)	4962(7)	129(8)
C(53)	109(13)	2311(7)	4758(8)	162(11)
C(54)	572(10)	2378(6)	4882(7)	123(8)
C(55)	645(10)	2584(6)	5179(7)	133(9)
C(56)	2414(7)	1850(4)	7270(5)	85(5)
C(57)	2812(13)	2011(7)	7273(9)	91(15)
C(58)	3205(12)	2104(7)	7549(7)	88(11)
C(59)	3556(12)	2270(8)	7441(9)	115(15)
C(60)	3379(16)	2279(10)	7099(10)	130(20)

C(61)	2919(15)	2119(10)	6995(9)	90(20)
C(62)	4157(16)	1710(10)	7339(12)	170(20)
C(63)	3923(18)	1644(10)	6990(11)	170(20)
C(64)	3474(16)	1454(10)	6955(10)	134(17)
C(65)	3430(17)	1401(10)	7282(12)	220(30)
C(66)	3851(19)	1559(10)	7519(9)	133(18)
C(57A)	2818(11)	2125(7)	7262(7)	56(9)
C(58A)	3145(10)	2311(6)	7513(6)	82(11)
C(59A)	3463(10)	2484(6)	7372(6)	71(9)
C(60A)	3333(11)	2405(7)	7033(7)	69(10)
C(61A)	2935(13)	2183(8)	6965(7)	100(20)
C(62A)	4269(12)	1872(6)	7694(8)	175(13)
C(63A)	4351(12)	1938(6)	7391(8)	175(13)
C(64A)	3991(13)	1771(6)	7144(8)	175(13)
C(65A)	3687(13)	1602(6)	7293(8)	175(13)
C(66A)	3859(13)	1665(6)	7633(8)	175(13)
C(67)	2507(6)	3164(3)	7382(3)	94(6)
C(68)	2535(4)	3269(2)	7059(3)	96(6)
C(69)	2869(4)	3103(2)	6909(3)	155(10)
C(70)	2803(6)	3322(3)	6610(4)	134(9)
C(71)	2476(6)	3536(3)	6597(4)	153(10)
C(72)	2364(5)	3527(3)	6900(3)	185(13)
C(73)	3641(9)	3564(6)	7488(5)	163(11)
C(74)	3895(9)	3358(5)	7299(7)	185(13)
C(75)	3932(9)	3532(7)	7000(6)	195(14)
C(76)	3701(10)	3846(6)	7004(6)	213(15)
C(77)	3521(9)	3866(5)	7306(7)	181(12)
C(78)	525(6)	3128(4)	6168(4)	73(5)
C(79)	763(7)	3430(3)	6167(4)	97(6)
C(80)	495(6)	3707(4)	6106(4)	121(8)
C(81)	855(7)	3943(4)	6147(5)	130(8)
C(82)	1345(7)	3812(4)	6233(5)	142(9)
C(83)	1288(6)	3495(4)	6245(5)	149(10)
C(84)	461(10)	3476(7)	5352(7)	213(15)
C(85)	491(10)	3799(6)	5316(6)	182(12)
C(86)	1019(11)	3879(5)	5381(6)	180(12)
C(87)	1316(8)	3605(7)	5457(6)	208(15)
C(88)	971(12)	3356(5)	5439(7)	183(13)
C(89)	-1400(9)	-23(5)	7129(6)	111(7)
C(90)	-1808(12)	44(7)	7082(8)	85(12)
C(91)	-2169(15)	-1(10)	7263(9)	119(18)
C(92)	-2657(15)	124(11)	7070(10)	118(17)
C(93)	-2597(13)	246(9)	6770(9)	102(15)
C(94)	-2073(13)	197(8)	6778(8)	83(11)
C(95)	-2130(13)	-617(9)	6775(9)	180(30)
C(96)	-2503(16)	-639(8)	6878(8)	99(13)
C(97)	-2888(13)	-553(10)	6657(11)	110(16)
C(98)	-2753(14)	-479(10)	6417(9)	340(70)
C(99)	-2284(13)	-519(7)	6490(9)	75(10)
C(90A)	-2351(12)	55(8)	7172(8)	89(12)
C(91A)	-2031(9)	107(6)	6979(6)	46(7)
C(92A)	-2313(10)	264(6)	6697(6)	63(9)
C(93A)	-2808(11)	308(7)	6715(8)	82(12)
C(94A)	-2832(12)	179(10)	7008(9)	120(19)
C(95A)	-2419(12)	-583(8)	6639(8)	105(15)
C(96A)	-2796(13)	-591(8)	6815(8)	91(12)

C(97A)	-3247(11)	-423(7)	6622(8)	87(11)
C(98A)	-3148(10)	-311(7)	6327(7)	102(13)
C(99A)	-2637(11)	-410(6)	6337(7)	69(9)
C(100)	-1027(8)	751(5)	6111(5)	99(6)
C(101)	-1435(9)	488(5)	6047(6)	113(7)
C(102)	-1912(9)	421(5)	5852(6)	113(7)
C(103)	-2064(8)	114(5)	5885(6)	105(7)
C(104)	-1688(8)	-15(5)	6095(6)	103(6)
C(105)	-1246(8)	194(5)	6230(6)	106(7)
C(106)	-727(9)	94(6)	5617(6)	126(8)
C(107)	-1050(10)	323(6)	5414(7)	143(9)
C(108)	-1546(11)	143(6)	5224(7)	147(10)
C(109)	-1484(10)	-157(6)	5364(7)	133(9)
C(110)	-981(10)	-182(6)	5607(7)	132(8)
C(111)	100(6)	1015(4)	5859(4)	73(5)
C(112)	438(12)	898(8)	5785(9)	80(12)
C(113)	902(14)	1096(8)	5646(11)	130(20)
C(114)	1448(14)	854(9)	5710(11)	110(17)
C(115)	1322(15)	506(9)	5888(11)	127(19)
C(116)	698(15)	533(8)	5934(11)	150(20)
C(117)	41(10)	689(5)	5137(7)	59(9)
C(118)	349(10)	855(5)	5011(6)	59(8)
C(119)	704(9)	667(5)	4957(6)	58(8)
C(120)	615(10)	384(5)	5050(7)	64(9)
C(121)	205(10)	398(5)	5161(7)	71(10)
C(112)	1151(10)	543(6)	5761(7)	64(9)
C(113)	1276(10)	809(6)	5665(7)	65(10)
C(114)	964(10)	1016(5)	5719(7)	55(9)
C(115)	645(9)	878(5)	5848(6)	41(7)
C(116)	760(9)	586(5)	5874(6)	43(8)
C(117)	-217(10)	693(5)	5084(7)	60(9)
C(118)	73(11)	864(5)	4945(7)	70(10)
C(119)	420(10)	678(6)	4875(8)	78(11)
C(120)	345(11)	392(6)	4970(8)	108(15)
C(121)	-49(11)	401(5)	5099(7)	74(11)
C(122)	-1541(7)	1537(4)	5724(5)	89(6)
C(123)	-1411(7)	1517(4)	5406(5)	78(5)
C(124)	-1606(8)	1720(5)	5119(6)	106(7)
C(125)	-1323(8)	1623(5)	4913(6)	104(7)
C(126)	-1041(8)	1357(5)	5015(5)	97(6)
C(127)	-1066(7)	1305(4)	5348(5)	92(6)
C(128)	-2492(9)	1158(5)	5015(6)	116(7)
C(129)	-2529(10)	1310(6)	4732(7)	137(9)
C(130)	-2296(11)	1160(7)	4555(7)	147(10)
C(131)	-2009(9)	917(5)	4710(6)	117(7)
C(132)	-2165(9)	906(5)	5047(6)	121(8)
C(133)	-1974(6)	1522(4)	7014(4)	67(4)
C(134)	-2207(7)	1361(4)	6706(5)	80(5)
C(135)	-2269(8)	1020(5)	6691(6)	104(7)
C(136)	-2523(8)	969(5)	6327(5)	98(6)
C(137)	-2622(8)	1268(5)	6154(5)	102(6)
C(138)	-2427(7)	1496(4)	6413(5)	92(6)
C(139)	-3296(9)	1377(6)	6882(6)	122(8)
C(140)	-3389(10)	1060(6)	6829(7)	136(9)
C(141)	-3635(10)	1013(6)	6511(7)	140(9)
C(142)	-3744(12)	1314(7)	6346(8)	165(11)

C(143)	-3485(11)	1564(7)	6584(8)	155(10)
C(144)	772(6)	2608(4)	8748(4)	68(4)
C(145)	1209(6)	2830(3)	8867(4)	62(4)
C(146)	1150(7)	3143(4)	8921(4)	76(5)
C(147)	1615(8)	3256(5)	9041(5)	98(6)
C(148)	2041(9)	3038(5)	9088(6)	117(7)
C(149)	1746(8)	2759(5)	8966(5)	104(6)
C(150)	1215(9)	2645(5)	9603(6)	112(7)
C(151)	1099(9)	2947(6)	9635(7)	127(8)
C(152)	1565(9)	3093(5)	9781(6)	109(7)
C(153)	1984(9)	2912(5)	9816(6)	119(8)
C(154)	1758(10)	2622(6)	9730(7)	133(9)
C(155)	2712(8)	2634(4)	8469(5)	95(6)
C(156)	3197(9)	2656(5)	8369(6)	113(7)
C(157)	3257(11)	2861(6)	8150(7)	146(10)
C(158)	3782(12)	2864(7)	8099(8)	159(11)
C(159)	4041(11)	2632(7)	8366(8)	156(10)
C(160)	3693(11)	2473(6)	8484(7)	147(10)
C(161)	3625(12)	3196(8)	8971(9)	180(12)
C(162)	3706(12)	3443(7)	8741(8)	161(11)
C(163)	4136(13)	3359(7)	8721(8)	165(11)
C(164)	4410(13)	3100(8)	8882(9)	191(13)
C(165)	4027(14)	2975(8)	9037(9)	191(13)
C(166)	2107(7)	3444(4)	8129(5)	90(6)
C(167)	2124(8)	3758(5)	8303(5)	97(6)
C(168)	2471(10)	3816(6)	8621(7)	127(8)
C(169)	2387(11)	4129(7)	8678(8)	151(10)
C(170)	1988(11)	4231(6)	8383(7)	142(9)
C(171)	1833(7)	4007(5)	8165(5)	92(6)
C(172)	3154(10)	3940(6)	8084(7)	129(8)
C(173)	3351(11)	4121(7)	8361(7)	147(10)
C(174)	3105(11)	4414(6)	8279(8)	145(10)
C(175)	2730(10)	4403(6)	7977(7)	132(8)
C(176)	2713(9)	4120(5)	7833(6)	112(7)
C(177)	564(9)	4179(5)	8348(6)	118(7)
C(178)	692(8)	4089(4)	8694(4)	133(8)
C(179)	375(7)	4151(5)	8910(6)	164(11)
C(180)	655(9)	4039(5)	9242(5)	158(10)
C(181)	1145(8)	3909(5)	9232(5)	177(12)
C(182)	1168(7)	3940(4)	8893(5)	128(8)
C(183)	1424(12)	4768(6)	8915(6)	209(15)
C(184)	1854(10)	4594(7)	9162(9)	300(20)
C(185)	1717(11)	4564(6)	9480(7)	214(15)
C(186)	1203(11)	4720(6)	9430(6)	192(13)
C(187)	1021(9)	4846(5)	9081(7)	169(11)
C(188)	1076(9)	4115(5)	7019(6)	119(8)
C(189)	1048(11)	4342(5)	7257(6)	165(11)
C(190)	703(8)	4415(6)	7428(7)	170(11)
C(191)	903(11)	4664(6)	7633(6)	183(13)
C(192)	1371(11)	4744(6)	7589(7)	237(18)
C(193)	1461(9)	4545(7)	7356(7)	198(14)
C(194)	428(10)	4845(5)	6667(5)	143(9)
C(195)	144(8)	4926(6)	6876(7)	185(13)
C(196)	418(12)	5150(6)	7092(6)	206(15)
C(197)	872(10)	5208(5)	7018(7)	203(14)
C(198)	878(9)	5019(6)	6755(7)	188(13)

C(1S)	4175(11)	4512(6)	9343(7)	162(10)
Cl(1S)	3647(4)	4692(3)	9415(3)	253(5)
Cl(2S)	4010(3)	4138(2)	9221(2)	169(3)
Cl(3S)	4270(3)	4727(2)	9021(2)	177(3)
C(2S)	3194(10)	2202(6)	9470(7)	152(9)
Cl(4S)	3632(4)	2066(2)	9256(3)	230(4)
Cl(5S)	3239(3)	2595(2)	9483(2)	157(3)
Cl(6S)	2600(3)	2078(2)	9269(2)	154(3)
C(3S)	2804	326	5433	180(20)
Cl(10)	3218	598	5687	450(20)
Cl(11)	2890	327	5096	275(11)
Cl(12)	2375(10)	362(6)	5530(6)	282(12)
C(4S)	5120(20)	2707(13)	7851(15)	170(20)
C(5S)	5320(20)	2961(13)	8256(16)	180(20)
C(6S)	5000	2746(16)	7500	140(30)

APPENDIX A.3.

Crystal data and structure refinement for $[Ag_{10}(SCH_2Fc)_{10}(PPh_3)_4]$ (**5**)

Empirical formula	$C_{184}\ H_{172}\ Ag_{10}\ Cl_6\ Fe_{10}\ P_4\ S_{10}$	
Formula weight	4677.60	
Temperature	150(2) K	
Wavelength	0.71073 Å	
Crystal system	Triclinic	
Space group	P-1	
Unit cell dimensions	a = 17.2487(7) Å	α = 90.543(2)°.
	b = 17.7664(8) Å	β = 113.253(2)°.
	c = 18.0354(9) Å	γ = 118.190(2)°.
Volume	4342.6(3) $Å^3$	
Z	1	
Density (calculated)	1.789 Mg/m^3	
Absorption coefficient	2.205 mm^{-1}	
F(000)	2328	
Crystal size	0.20 x 0.08 x 0.08 mm^3	
Theta range for data collection	2.12 to 27.67°.	
Index ranges	-22<=h<=22, -23<=k<=23, -16<=l<=23	
Reflections collected	44222	
Independent reflections	19899 [R(int) = 0.1159]	
Completeness to theta = 27.67°	98.0 %	
Absorption correction	Semi-empirical from equivalents	
Max. and min. transmission	0.8521 and 0.6668	
Refinement method	Full-matrix least-squares on F^2	
Data / restraints / parameters	19899 / 0 / 1009	
Goodness-of-fit on F^2	0.913	
Final R indices [I>2sigma(I)]	R1 = 0.0621, wR2 = 0.1154	
R indices (all data)	R1 = 0.1750, wR2 = 0.1531	
Largest diff. peak and hole	1.549 and -1.596 $e.Å^{-3}$	

Atomic coordinates (x 10^4) and equivalent isotropic displacement parameters ($Å^2$x 10^3) for **(5)**. U(eq) is defined as one third of the trace of the orthogonalized U^{ij} tensor.

	x	y	z	U(eq)
Ag(1)	382(1)	6085(1)	544(1)	27(1)
Ag(2)	2177(1)	7857(1)	751(1)	33(1)
Ag(3)	1983(1)	5996(1)	53(1)	32(1)
Ag(4)	1150(1)	5243(1)	2074(1)	31(1)
Ag(5)	-657(1)	3496(1)	1077(1)	31(1)
P(1)	2978(2)	9422(1)	1583(2)	35(1)
P(2)	2225(2)	5037(1)	3316(1)	30(1)
S(1)	1840(1)	6862(1)	1845(1)	25(1)
S(2)	3369(1)	7512(1)	528(1)	30(1)
S(3)	1192(1)	4750(1)	660(1)	26(1)
S(4)	-732(1)	4717(1)	1556(1)	26(1)
S(5)	-699(2)	2237(1)	560(1)	33(1)
Fe(1)	1464(1)	7782(1)	4105(1)	36(1)
Fe(2)	5625(1)	6701(1)	2256(1)	34(1)
Fe(3)	1973(1)	2870(1)	-411(1)	30(1)
Fe(4)	-3290(1)	3903(1)	2376(1)	31(1)
Fe(5)	-2218(1)	847(1)	2259(1)	41(1)
C(1)	1525(6)	7151(5)	3188(5)	30(2)
C(2)	2365(6)	7417(5)	3958(5)	31(2)
C(3)	2065(7)	7030(6)	4554(6)	46(2)
C(4)	1018(8)	6507(5)	4140(6)	49(3)
C(5)	671(6)	6576(5)	3302(5)	33(2)
C(6)	1185(7)	8722(6)	3645(6)	48(3)
C(7)	514(7)	8213(6)	3959(7)	55(3)
C(8)	1074(7)	8300(6)	4819(7)	52(3)
C(9)	2084(7)	8846(5)	5037(6)	44(2)
C(10)	2143(7)	9115(5)	4316(6)	46(3)
C(11)	1493(6)	7423(5)	2412(5)	31(2)
C(12)	4469(5)	6830(5)	1457(5)	29(2)
C(13)	4115(5)	6014(5)	1673(5)	35(2)
C(14)	4483(6)	5532(5)	1453(5)	40(2)
C(15)	5053(6)	6038(6)	1059(6)	45(2)
C(16)	5062(6)	6847(6)	1069(5)	41(2)
C(17)	6434(6)	7717(6)	3290(5)	43(2)
C(18)	6068(6)	6880(6)	3498(6)	47(2)
C(19)	6466(6)	6440(6)	3265(6)	48(3)
C(20)	7053(6)	6976(6)	2893(6)	46(2)
C(21)	7025(6)	7762(5)	2909(6)	45(2)
C(22)	4234(5)	7525(5)	1534(5)	32(2)
C(23)	1432(5)	3598(5)	-162(5)	29(2)
C(24)	655(6)	2712(5)	-582(5)	36(2)
C(25)	645(6)	2525(6)	-1376(5)	42(2)
C(26)	1406(7)	3289(6)	-1413(6)	47(3)
C(27)	1881(6)	3948(5)	-687(5)	34(2)
C(28)	3034(6)	2941(6)	695(6)	39(2)
C(29)	2246(6)	2064(5)	321(5)	36(2)
C(30)	2139(6)	1823(6)	-472(6)	45(3)
C(31)	2876(6)	2553(6)	-608(6)	44(2)
C(32)	3423(6)	3240(6)	118(6)	42(2)
C(33)	1709(5)	4042(5)	691(5)	26(2)
C(34)	-2229(6)	4376(5)	1960(5)	27(2)

C(35)	-3177(6)	3800(6)	1285(5)	36(2)
C(36)	-3789(7)	4147(7)	1227(6)	49(3)
C(37)	-3225(7)	4927(6)	1865(6)	49(3)
C(38)	-2263(6)	5067(5)	2312(5)	35(2)
C(39)	-2996(6)	3197(6)	3224(6)	39(2)
C(40)	-3949(6)	2668(6)	2563(6)	41(2)
C(41)	-4497(6)	3070(6)	2524(6)	44(2)
C(42)	-3883(7)	3857(6)	3165(6)	42(2)
C(43)	-2962(7)	3929(6)	3586(6)	43(2)
C(44)	-1357(5)	4272(5)	2224(5)	30(2)
C(45)	-1522(6)	1656(5)	1653(6)	32(2)
C(46)	-943(7)	1991(6)	2518(6)	53(3)
C(47)	-1535(7)	2143(5)	2828(6)	51(3)
C(48)	-2442(8)	1878(6)	2130(7)	55(3)
C(49)	-2429(7)	1597(5)	1420(6)	46(2)
C(50)	-1885(7)	-93(5)	2599(6)	44(2)
C(51)	-2226(7)	109(5)	3119(6)	47(3)
C(52)	-3190(7)	-77(5)	2625(6)	47(3)
C(53)	-3460(7)	-399(5)	1771(6)	43(2)
C(54)	-2646(7)	-394(5)	1763(6)	48(3)
C(55)	-1266(6)	1365(5)	1039(6)	46(3)
C(56)	3981(6)	9825(6)	2627(5)	38(2)
C(57)	4618(7)	10722(6)	2986(7)	62(3)
C(58)	5347(7)	11023(6)	3768(6)	60(3)
C(59)	5448(7)	10456(7)	4250(6)	57(3)
C(60)	4830(7)	9559(7)	3901(7)	60(3)
C(61)	4102(6)	9249(6)	3096(6)	46(2)
C(62)	2171(7)	9773(5)	1668(6)	42(2)
C(63)	1304(7)	9558(6)	991(7)	54(3)
C(64)	645(7)	9770(6)	1032(8)	68(3)
C(65)	839(9)	10225(7)	1760(9)	70(4)
C(66)	1691(11)	10452(8)	2453(9)	82(4)
C(67)	2368(8)	10224(7)	2428(7)	66(3)
C(68)	3624(5)	10198(5)	1081(5)	32(2)
C(69)	4300(6)	10075(5)	942(5)	37(2)
C(70)	4862(6)	10670(6)	618(6)	45(2)
C(71)	4771(6)	11370(5)	411(5)	39(2)
C(72)	4081(6)	11482(6)	520(5)	41(2)
C(73)	3520(6)	10896(5)	862(5)	35(2)
C(74)	3366(6)	6066(5)	3973(5)	32(2)
C(75)	3812(6)	6275(6)	4831(6)	44(2)
C(76)	4679(7)	7067(7)	5295(6)	60(3)
C(77)	5106(7)	7667(6)	4878(6)	49(3)
C(78)	4656(6)	7468(6)	4024(7)	48(3)
C(79)	3788(6)	6685(5)	3561(5)	33(2)
C(80)	2641(7)	4312(6)	3122(6)	39(2)
C(81)	1946(7)	3493(6)	2612(6)	47(2)
C(82)	2191(9)	2901(7)	2445(6)	61(3)
C(83)	3157(10)	3122(8)	2805(8)	73(4)
C(84)	3885(9)	3955(8)	3322(8)	69(4)
C(85)	3637(8)	4559(7)	3492(7)	66(3)
C(86)	1695(6)	4542(5)	4001(5)	31(2)
C(87)	889(6)	4593(5)	3943(5)	35(2)
C(88)	457(6)	4222(6)	4469(6)	44(2)
C(89)	831(6)	3831(5)	5028(5)	36(2)
C(90)	1605(6)	3757(5)	5082(5)	39(2)

C(91)	2045(6)	4114(5)	4577(5)	33(2)
C(1S)	1583(7)	1513(6)	4786(6)	55(3)
Cl(1S)	1683(3)	593(2)	4719(2)	86(1)
Cl(2S)	1789(4)	2046(2)	4029(2)	130(2)
Cl(3S)	475(2)	1264(2)	4753(3)	133(2)

APPENDIX A.4.

Crystal data and structure refinement for $[Ag_8(SeCH_2Fc)_8(PPh_3)_4]$ **(6)**

Empirical formula	$C_{169}\ H_{158}\ Ag_8\ Cl_{30}\ Fe_8\ P_4\ Se_8$	
Formula weight	5317.77	
Temperature	293(2) K	
Wavelength	0.71073 Å	
Crystal system	Monoclinic	
Space group	C2/c	
Unit cell dimensions	a = 29.8840(6) Å	α= 90°
	b = 44.2400(7) Å	β= 130.463(1)°.
	c = 22.0150(5) Å	γ = 90°.
Volume	22144.1(8) $Å^3$	
Z	4	
Density (calculated)	1.595 Mg/m^3	
Absorption coefficient	2.943 mm^{-1}	
F(000)	10392	
Theta range for data collection	2.08 to 27.49°.	
Index ranges	-38<=h<=38, -57<=k<=56, -28<=l<=17	
Reflections collected	83259	
Independent reflections	25385 [R(int) = 0.1081]	
Completeness to theta = 27.49°	99.8 %	
Absorption correction	Semi-empirical from equivalents	
Refinement method	Full-matrix least-squares on F^2	
Data / restraints / parameters	25385 / 196 / 956	
Goodness-of-fit on F^2	1.511	
Final R indices [I>2sigma(I)]	R1 = 0.0887, wR2 = 0.2539	
R indices (all data)	R1 = 0.1653, wR2 = 0.2891	
Largest diff. peak and hole	2.043 and -1.551 $e.Å^{-3}$	

Atomic coordinates (x 10^4) and equivalent isotropic displacement parameters ($Å^2$x 10^3) for **(6)**. U(eq) is defined as one third of the trace of the orthogonalized U^{ij} tensor.

	x	y	z	U(eq)
Ag(1)	6141(1)	753(1)	4411(1)	47(1)
Ag(2)	5134(1)	1131(1)	1802(1)	43(1)
Ag(3)	5937(1)	1717(1)	2258(1)	45(1)
Ag(4)	5877(1)	1346(1)	3436(1)	42(1)
Se(1)	5911(1)	784(1)	3032(1)	42(1)
Se(2)	4642(1)	855(1)	446(1)	47(1)
Se(3)	6766(1)	1650(1)	3786(1)	43(1)
Se(4)	5201(1)	1702(1)	3520(1)	40(1)
P(1)	7141(1)	569(1)	5518(2)	51(1)
P(2)	6141(1)	1876(1)	1375(2)	49(1)
Fe(1)	7453(1)	723(1)	2849(1)	53(1)
Fe(2)	5047(1)	-204(1)	1280(1)	46(1)
Fe(3)	6238(1)	2704(1)	3736(1)	46(1)
Fe(4)	6684(1)	1671(1)	6424(1)	54(1)
C(1)	6779(4)	655(2)	2854(6)	40(2)
C(2)	7201(6)	402(3)	3262(9)	72(4)
C(3)	7253(8)	275(3)	2726(12)	92(5)
C(4)	6819(8)	444(4)	1951(11)	107(7)
C(5)	6565(5)	679(3)	2071(7)	61(3)
C(6)	7890(6)	1098(3)	3533(9)	73(4)
C(7)	8274(6)	856(3)	3801(8)	74(4)
C(8)	8252(6)	756(3)	3168(10)	75(4)
C(9)	7863(7)	944(3)	2515(11)	86(5)
C(10)	7627(5)	1159(3)	2741(8)	61(3)
C(11)	6664(5)	868(3)	3247(7)	54(3)
C(12)	4724(5)	206(2)	764(7)	48(3)
C(13)	4585(5)	137(3)	1268(7)	57(3)
C(14)	4247(6)	-139(3)	952(9)	75(4)
C(15)	4178(5)	-220(3)	317(7)	54(3)
C(16)	4467(5)	-10(2)	185(6)	44(3)
C(17)	5907(5)	-207(3)	1806(7)	64(3)
C(18)	5855(5)	-200(3)	2386(7)	57(3)
C(19)	5558(5)	-458(3)	2301(7)	59(3)
C(20)	5434(5)	-623(3)	1664(7)	62(3)
C(21)	5647(5)	-460(3)	1353(8)	56(3)
C(22)	5094(5)	466(2)	897(7)	56(3)
C(23)	6495(5)	2295(2)	3627(6)	42(2)
C(24)	5922(5)	2364(2)	2935(7)	52(3)
C(25)	5950(5)	2642(2)	2624(7)	52(3)
C(26)	6535(6)	2728(2)	3127(7)	55(3)
C(27)	6870(5)	2526(2)	3733(7)	51(3)
C(28)	6408(5)	2704(2)	4795(8)	57(3)
C(29)	5804(5)	2678(3)	4153(8)	69(4)
C(30)	5613(5)	2937(2)	3649(7)	53(3)
C(31)	6107(5)	3115(2)	4016(8)	57(3)
C(32)	6596(5)	2976(2)	4703(7)	56(3)
C(33)	6665(5)	2031(2)	4163(7)	51(3)
C(34)	6155(4)	1746(2)	5220(6)	42(2)
C(35)	6631(5)	1532(3)	5502(7)	62(3)
C(36)	7178(6)	1663(3)	6074(8)	70(4)

C(37)	7062(6)	1983(3)	6184(8)	60(3)
C(38)	6430(5)	2017(2)	5640(7)	52(3)
C(39)	6520(7)	1299(3)	6805(9)	87(5)
C(40)	7098(7)	1388(3)	7402(8)	83(5)
C(41)	7110(9)	1687(4)	7623(10)	103(6)
C(42)	6513(11)	1755(4)	7130(12)	117(7)
C(43)	6144(8)	1535(3)	6629(9)	83(5)
C(44)	5528(4)	1683(2)	4647(6)	46(3)
C(45)	7732(5)	735(2)	5585(6)	49(3)
C(46)	8224(5)	579(3)	5844(8)	72(4)
C(47)	8661(6)	724(3)	5863(10)	76(4)
C(48)	8601(5)	1022(3)	5666(8)	66(4)
C(49)	8072(6)	1187(3)	5403(8)	71(4)
C(50)	7659(5)	1045(2)	5363(7)	55(3)
C(51)	7231(4)	168(2)	5444(7)	52(3)
C(52)	7054(5)	68(2)	4701(8)	59(3)
C(53)	7145(5)	-241(3)	4630(9)	71(4)
C(54)	7379(6)	-435(3)	5258(11)	88(5)
C(55)	7516(6)	-341(3)	5958(10)	77(4)
C(56)	7459(5)	-36(3)	6057(8)	67(4)
C(57)	7387(5)	606(3)	6533(8)	61(3)
C(58)	7002(5)	542(3)	6649(8)	57(3)
C(59)	7182(6)	547(3)	7406(8)	66(4)
C(60)	7781(6)	634(3)	8044(8)	86(5)
C(61)	8171(6)	714(4)	7945(9)	86(5)
C(62)	7990(6)	691(3)	7212(8)	83(5)
C(63)	6821(5)	2077(3)	1879(7)	53(3)
C(64)	7275(5)	2026(3)	2650(8)	62(3)
C(65)	7788(6)	2185(4)	3032(9)	86(5)
C(66)	7886(7)	2393(4)	2687(11)	87(5)
C(67)	7445(7)	2459(3)	1949(11)	93(5)
C(68)	6914(6)	2299(3)	1536(9)	73(4)
C(69)	5591(5)	2120(2)	530(7)	49(3)
C(70)	5376(6)	2360(3)	671(8)	62(3)
C(71)	4964(7)	2544(3)	59(10)	75(4)
C(72)	4751(5)	2501(3)	-678(9)	70(4)
C(73)	4971(7)	2266(3)	-849(9)	85(5)
C(74)	5367(6)	2070(3)	-248(7)	64(3)
C(75)	6206(5)	1565(2)	884(7)	49(3)
C(76)	6613(7)	1544(3)	800(9)	73(4)
C(77)	6631(7)	1305(3)	400(9)	76(4)
C(78)	6268(7)	1074(3)	151(8)	73(4)
C(79)	5829(7)	1084(3)	225(8)	75(4)
C(80)	5809(5)	1322(2)	598(7)	49(3)
C(1S)	8842(19)	1769(5)	9411(18)	300(20)
Cl(1)	8815(10)	1975(5)	10024(15)	530(13)
Cl(2)	8731(7)	1388(4)	9337(11)	401(9)
Cl(3)	8711(7)	1890(4)	8586(10)	375(8)
C(2S)	8999(14)	-80(7)	4700(20)	157(17)
Cl(4)	8810(20)	-30(11)	3810(20)	370(30)
Cl(5)	9309(8)	-431(4)	5125(11)	433(9)
Cl(6)	8505(6)	-52(3)	4843(8)	337(7)
C(3S)	7024(6)	-1273(3)	3761(11)	136(7)
Cl(7)	7688(5)	-1138(2)	4536(7)	270(5)
Cl(8)	6919(4)	-1589(2)	4083(7)	243(4)
Cl(9)	6542(3)	-1000(2)	3509(5)	191(3)

C(4S)	9151(7)	1424(3)	4101(9)	123(6)
Cl(10)	9354(5)	1656(3)	3731(7)	284(5)
Cl(11)	9161(3)	1619(1)	4774(4)	142(2)
Cl(12)	9696(4)	1154(2)	4560(6)	223(4)
C(5S)	4490(30)	1670(30)	-2480(100)	400(120)
Cl(13)	5089(5)	1458(3)	-1782(7)	255(4)
Cl(14)	4652(10)	1941(6)	-2859(16)	317(13)
C(6S)	9353(13)	1138(6)	7700(20)	156(18)
Cl(16)	8969(9)	1373(4)	7797(13)	243(8)
Cl(17)	9860(9)	1290(4)	7672(14)	243(9)
Cl(18)	9649(6)	836(3)	8306(9)	175(5)
C(6SA)	9820(30)	1057(13)	6260(30)	180(40)
Cl(1A)	10270(40)	1363(15)	6610(50)	610(70)
Cl(1B)	9610(30)	928(18)	5390(30)	500(50)
Cl(1C)	10000(20)	794(11)	6950(30)	320(20)

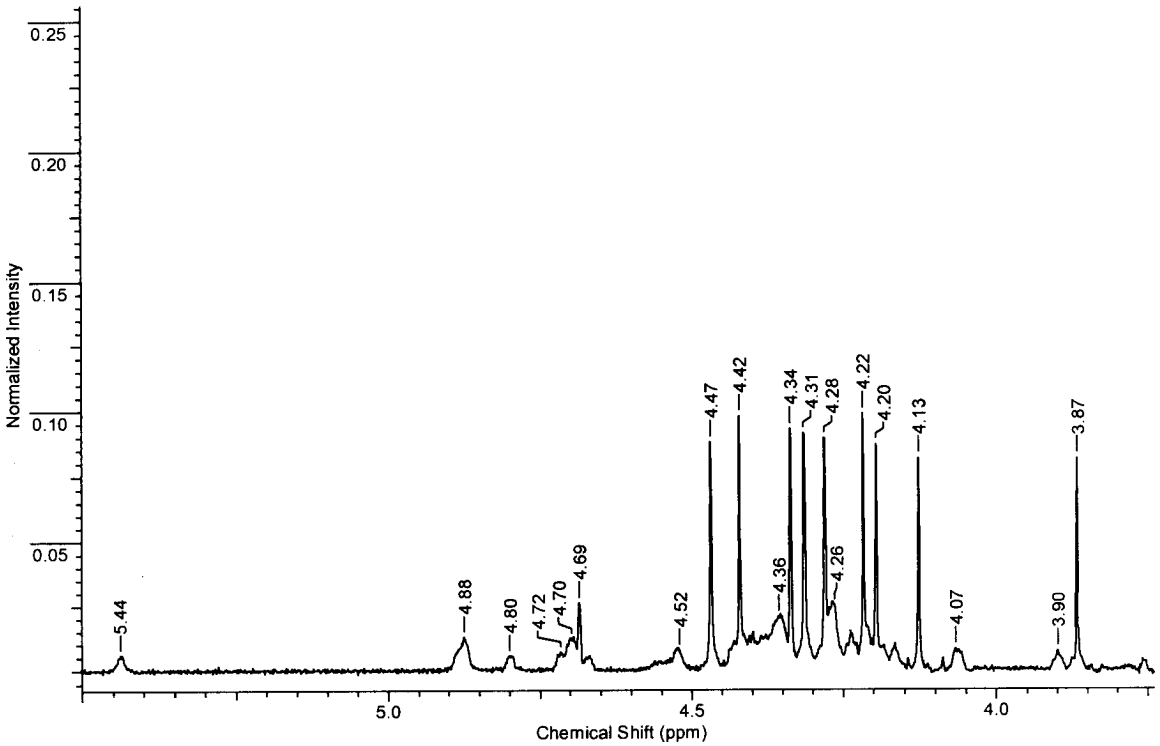

APPENDIX A5 ^{1}H-NMR Spectrum of $[Ag_{48}S_6(SCH_2Fc)_{36}]$ **(4)** in d_8-THF.

APPENDIX B:

Thermal Ellipsoid Diagrams Showing the Molecular Structure of the Internal Cores of **(3)**, **(5)** and **(6)**.

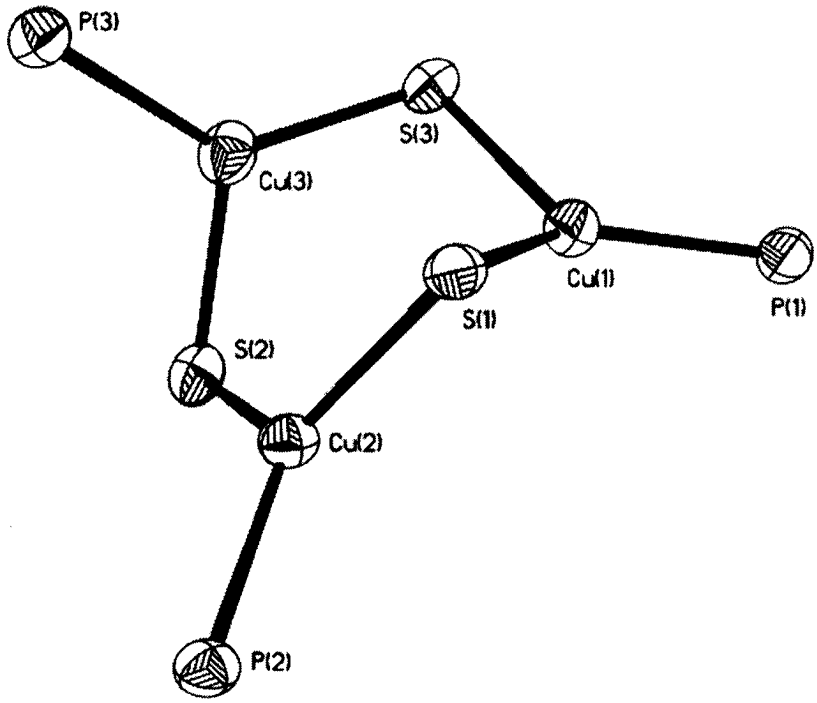

Appedix B.1. Molecular structure of complex (**3**) showing the disorder of the Cu_3S_3 core.

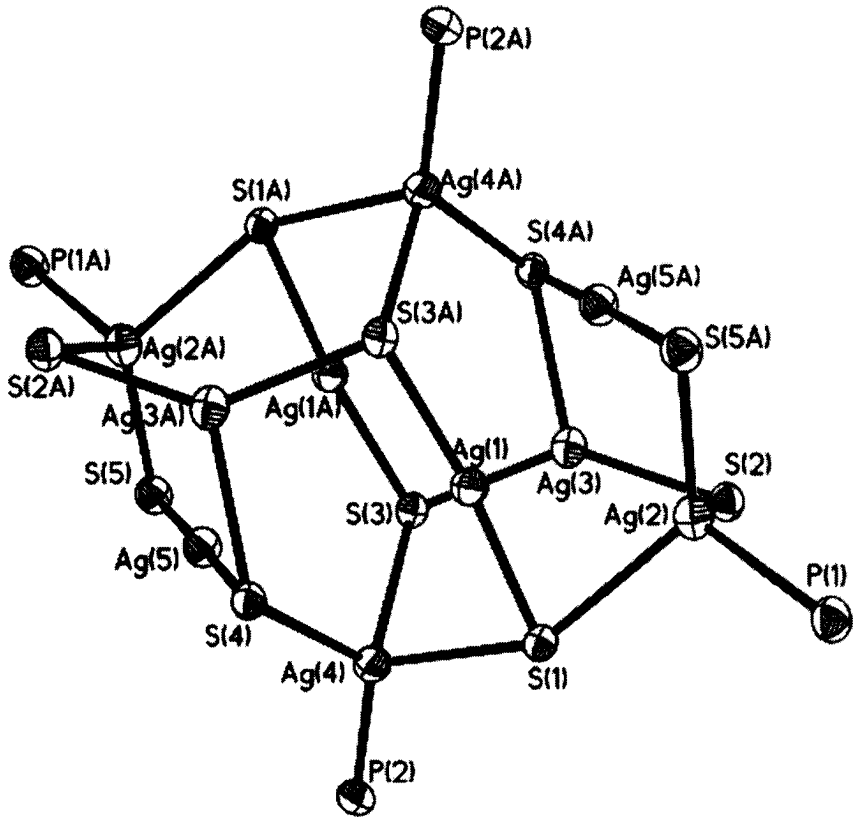

Appedix B.2. Molecular structure of complex (**5**) showing the disorder of the $Ag_{10}S_{10}$ core.

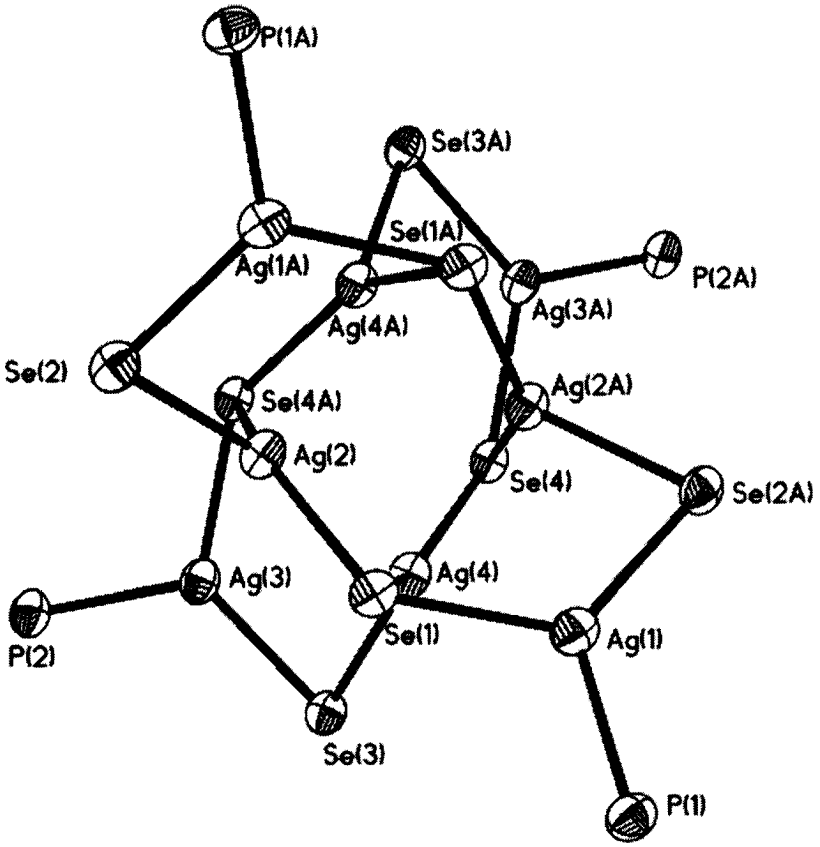

Appedix B.3. Molecular structure of complex (**6**) showing the disorder of the $Ag_{10}Se_8$ core.